

PERFORATION STRATEGIES FOR MULTI-LAYERED GAS CONDENSATE AND  
DRY GAS RESERVOIRS

Miss Pimsiri Sirikhuang

A Thesis Submitted in Partial Fulfillment of the Requirements  
for the Degree of Master of Engineering Program in Petroleum Engineering  
Department of Mining and Petroleum Engineering  
Faculty of Engineering  
Chulalongkorn University  
Academic Year 2012  
Copyright of Chulalongkorn University

บทคัดย่อและแฟ้มข้อมูลฉบับเต็มของวิทยานิพนธ์ตั้งแต่ปีการศึกษา 2554 ที่ให้บริการในคลังปัญญาจุฬาฯ (CUIR)  
เป็นแฟ้มข้อมูลของนิสิตเจ้าของวิทยานิพนธ์ที่ส่งผ่านทางบัณฑิตวิทยาลัย

The abstract and full text of theses from the academic year 2011 in Chulalongkorn University Intellectual Repository (CUIR)  
are the thesis authors' files submitted through the Graduate School.

กลยุทธ์การยิงต่อกรสำหรับแหล่งกักเก็บก๊าซธรรมชาติเหลวและก๊าซธรรมชาติแบบหลายชั้น

นางสาว พิมพ์ศิริ สิริช่วง

วิทยานิพนธ์นี้เป็นส่วนหนึ่งของการศึกษาตามหลักสูตรปริญญาวิศวกรรมศาสตรมหาบัณฑิต

สาขาวิชาวิศวกรรมปิโตรเลียม ภาควิชาวิศวกรรมเหมืองแร่และปิโตรเลียม

คณะวิศวกรรมศาสตร์ จุฬาลงกรณ์มหาวิทยาลัย

ปีการศึกษา 2555

ลิขสิทธิ์ของจุฬาลงกรณ์มหาวิทยาลัย

Thesis Title	PERFORATION STRATEGIES FOR MULTI-LAYERED GAS CONDENSATE AND DRY GAS RESERVOIRS
By	Miss Pimsiri Sirikhuang
Field of Study	Petroleum Engineering
Thesis Advisor	Assistant Professor Suwat Athichanagorn, Ph.D.

---

Accepted by the Faculty of Engineering, Chulalongkorn University in  
Partial Fulfillment of the Requirements for the Master's Degree

..... Dean of the Faculty of Engineering  
(Associate Professor Boonsom Lerdkhirunwong, Dr.Ing.)

#### THESIS COMMITTEE

.....Chairman  
(Associate Professor Sarithdej Pathanasethpong)

.....Thesis Advisor  
(Assistant Professor Suwat Athichanagorn, Ph.D.)

.....Examiner  
(Assistant Professor Jirawat Chewaroungroj, Ph.D.)

.....External Examiner  
(Witsarut Tungsunthornkhan, Ph.D.)

พิมพ์ศิริ ศิริช่วง: กลยุทธ์การยิงท่อกรูสำหรับแหล่งกักเก็บก๊าซธรรมชาติเหลวและก๊าซธรรมชาติแบบหลายชั้น (PERFORATION STRATEGIES FOR MULTI-LAYERED GAS CONDENSATE AND DRY GAS RESERVOIRS) อาจารย์ที่ปรึกษาวิทยานิพนธ์หลัก: ผศ. ดร. สุวัฒน์ อธิชนากร, 103 หน้า

ลักษณะของแหล่งผลิตก๊าซธรรมชาติและก๊าซธรรมชาติเหลวในอ่าวไทยเกิดจากการสะสมตัวของชั้นตะกอนแม่น้ำและปากแม่น้ำโบราณ ในขณะที่เดียวกันแหล่งกักเก็บดังกล่าวก็ได้ถูกรอยเลื่อนทางธรณีตัดเป็นโครงสร้างกักเก็บเล็กๆ กลวิธีการผลิตเพื่อให้ได้ผลผลิตก็คือการยิงผ่านชั้นกักเก็บตามลำดับที่เหมาะสม ในงานวิจัยนี้ระบบที่สนใจประกอบด้วยแหล่งกักเก็บก๊าซธรรมชาติและก๊าซธรรมชาติเหลว กลยุทธ์การยิงผ่านท่อกรูทั้งหมดจัดแบบได้ถูกนำมาวิเคราะห์เพื่อที่จะให้สามารถผลิตก๊าซธรรมชาติและก๊าซธรรมชาติเหลวได้สูงสุด

สำหรับแหล่งกักเก็บแบบสองชั้นที่มีชั้นบนเป็นแหล่งกักเก็บก๊าซธรรมชาติเหลวแบบใช้แรงผลักดันจากตัวเองและชั้นล่างเป็นก๊าซธรรมชาติ มีความสามารถในการซึมผ่านที่ 500 มิลลิดาร์ซี และความหนาที่ 100 ฟุต กลยุทธ์ในการยิงท่อกรูเพื่อให้ได้ผลผลิตก๊าซธรรมชาติเหลวและค่าเทียบเท่าเชิงปริมาณน้ำมันสูงสุดคือการยิงท่อกรูบริเวณแหล่งกักเก็บชั้นบนก่อนจนกระทั่งอัตราการผลิตของก๊าซธรรมชาติได้ครึ่งหนึ่งของอัตราการผลิตเบื้องต้น แล้วจึงยิงท่อกรูที่บริเวณแหล่งกักเก็บชั้นล่างโดยขณะที่แหล่งกักเก็บชั้นบนยังเปิดอยู่

เมื่อความหนาของแหล่งกักเก็บก๊าซธรรมชาติเหลวและก๊าซธรรมชาติลดลง เราควรจะชะลอการยิงชั้นล่างเพื่อที่จะสงวนปริมาณของก๊าซธรรมชาติในแหล่งกักเก็บชั้นล่างไว้ใช้เป็นแรงผลักดันให้ก๊าซธรรมชาติเหลวสามารถผลิตได้มากที่สุด อย่างไรก็ตามในส่วน of ค่าเทียบเท่าเชิงปริมาณน้ำมัน กลยุทธ์การผลิตแบบเดียวเป็นกลยุทธ์ที่ดีที่สุดสำหรับความหนาที่ 50 ฟุต ในกรณีที่ความสามารถในการซึมผ่านของชั้นผลิตก๊าซธรรมชาติเหลวและก๊าซธรรมชาติลดลง เราควรจะชะลอการยิงชั้นล่างเพื่อที่จะได้ผลผลิตก๊าซธรรมชาติเหลวและค่าเทียบเท่าเชิงปริมาณน้ำมันสูงสุดเช่นกัน

ภาควิชา วิศวกรรมเหมืองแร่และปิโตรเลียม

สาขาวิชา วิศวกรรมปิโตรเลียม

ปีการศึกษา 2555

ลายมือชื่อนิพนธ์.....

ลายมือชื่อ อาจารย์ที่ปรึกษา.....

## 5271611721: MAJOR PETROLEUM ENGINEERING

KEYWORDS: MULTILAYERED GAS CONDENSATE AND DRY GAS RESERVOIRS/ DRIVE MECHANISM/ RECOVERY FACTORS

PIMSIRI SIRIKHUANG: PERFORATION STRATEGIES FOR MULTILAYERED GAS CONDENSATE AND DRY RESERVOIRS. THESIS ADVISOR: ASST. PROF. SUWAT ATHICHANAGORN, Ph.D., 103 pp.

Multilayered gas and gas condensate reservoirs in the Gulf of Thailand are generally limited in extent and dissected by numerous faults. A single area may consist of a large number of individually distinguished reservoirs. The method to gain production is to perforate the layers in the right sequence. In this study, the system of interest consists of dry gas and gas condensate reservoirs. Seven different perforation strategies are analyzed in order to maximize condensate and gas production.

For two-layer reservoirs with depletion-drive gas-condensate reservoir on top and dry-gas reservoir at the bottom having permeability of 500 mD and thickness of 100 ft, the best perforation strategy to maximize condensate production and barrel of oil equivalent is to perforate the top reservoir first until gas production rate reaches half of initial production rate and then perforate the bottom layer while keeping the top zone open.

As the thickness of the gas condensate and dry gas reservoir decreases, we should delay the perforation of the lower zone in order to preserve the amount of gas in the lower reservoir to be used to lift condensate at late times in order to maximize condensate production. However, in term of barrel of oil equivalent, stand alone perforation is best for thickness of 50 ft. As the permeability of the gas condensate and dry gas zones decreases, we should also delay the perforation of the lower zone in order to maximize condensate production and barrel of oil equivalent.

Department: Mining and Petroleum Engineering.

Student's signature:.....

Field of Study: Petroleum Engineering.

Advisor's Signature:.....

Academic Year: 2012

## **Acknowledgements**

I would like to express the deepest appreciation to Assistant Professor Suwat Athichanagorn, who has the attitude and the substance of a genius: he continually and convincingly conveyed a spirit of adventure in regard to research and scholarship, and an excitement in regard to teaching. Without his guidance and persistent help this thesis would not have been possible.

I would like to thank all faculty members in the Department of Mining and Petroleum Engineering who have offered petroleum knowledge, technical advice, and invaluable consultation. I wish to thank the thesis committee members for their comments and recommendations that make this thesis formally complete.

I am extremely grateful to my workplace, Chevron Exploration and Production Thailand, for providing financial support for the study.

I would also like to thank Schlumberger for providing educational license of ECLIPSE 300 compositional reservoir simulator to Department of Mining and Petroleum Engineering, Chulalongkorn University.

# Contents

	Page
Abstract (in Thai).....	iv
Abstract (in English).....	v
Acknowledgements.....	vi
Contents .....	ii
List of Tables .....	ix
List of Figures .....	v
List of Abbreviations .....	viii
Nomenclature.....	x
<b>CHAPTER</b>	
<b>I INTRODUCTION .....</b>	<b>1</b>
1.1 Outline of Methodology .....	3
1.2 Thesis Outline .....	5
<b>II LITERATURE REVIEW .....</b>	<b>6</b>
<b>III THEORY AND CONCEPT .....</b>	<b>9</b>
3.1 General Definition of Multi-layered Reservoirs.....	10
3.2 Reservoir Simulation.....	11
3.3 Material Balance Concept .....	12
3.4 Material Balance in Gas Reservoir.....	12
3.5 Fluid Flow in Porous Medium.....	15
3.5.1 Darcy's Law.....	15
3.5.2 Radial Flow of Compressible Fluids .....	17
3.6 Gas Reservoir.....	19
3.6.1 Retrograde Gas Condensate Reservoir.....	19

<b>CHAPTER</b>	<b>Page</b>
3.6.2 Near Critical Gas-Condensate reservoir.....	20
3.6.3 Wet Gas Reservoir.....	21
3.6.4 Dry Gas Reservoir.....	22
3.7 Non-Darcy Flow.....	23
3.7.1 Non-Darcy Flow and Positive Coupling.....	24
3.8 Gas-Condensate Flow Behavior.....	25
3.8.1 Gas Condensate Flow Behavior .....	28
Fluid Composition Change.....	30
<b>IV RESERVOIR SIMULATION MODEL .....</b>	<b>31</b>
4.1 Grid Section.....	32
4.2 Fluid Section.....	34
4.3 SCAL (Special Core Analysis) Section.....	37
4.4 Wellbore Section.....	39
4.5 Vertical Flow Performance.....	40
<b>V RESULTS AND DISCUSSION .....</b>	<b>41</b>
5.1 Base Case.....	43
5.2 Effect of thickness .....	65
5.3 Effect of permeability .....	68
<b>VI CONCLUSION.....</b>	<b>71</b>
<b>REFERENCE.....</b>	<b>74</b>
<b>APPENDIX.....</b>	<b>76</b>
<b>VITAE.....</b>	<b>103</b>



## List of Tables

	Page
Table 3.1 Physical characteristics of condensate gas.....	26
Table 4.2 The initial composition of the reservoir fluid.....	34
Table 4.3 Physical properties of each component.....	35
Table 4.4 Binary interaction coefficient between components.....	35
Table 4.5 Gas and oil relative permeabilities.....	37
Table 4.6 Oil and water relative permeabilities.....	38
Table 5.1 Perforation strategy .....	42
Table 5.2 Summary of results for base case.....	63
Table 5.3 BOE for base case.....	63
Table 5.4 Summary of results for reservoir thickness 50 feet.....	65
Table 5.5 BOE for reservoir thickness 50 feet.....	65
Table 5.6 Summary of results for reservoir thickness 25 feet .....	66
Table 5.7 BOE for reservoir thickness 25 feet.....	66
Table 5.8 Summary of results for permeability of 100 mD for both top and bottom reservoirs.....	68
Table 5.9 BOE for permeability of 100 mD for both top and bottom reservoirs.....	68
Table 5.10 Summary of results for permeability of 20 mD for both top and bottom reservoirs.....	69
Table 5.11 BOE for permeability of 20 mD for both top and bottom reservoirs.....	69

## List of Figures

	Page
Figure 1.1 Shap & Patterns of Bar and Channel Sands.....	1
Figure 3.1 Multi-layered reservoirs with production tubing.....	10
Figure 3.2 p/z plot versus cumulative production.....	14
Figure 3.3 A typical phase diagram of a retrograde gas condensate.....	20
Figure 3.4 Phase diagram of wet gas.....	21
Figure 3.5 Phase diagram for dry gas.....	22
Figure 3.6 Pressure – Volume – Temperature diagram of condensate.....	25
Figure 3.7 Pressure – Volume – Temperature diagram of poor condensate content.....	27
Figure 3.8 Pressure – Volume – Temperature diagram of middle condensate content.....	27
Figure 3.9 Pressure – Volume – Temperature diagram of rich condensate content.....	28
Figure 3.10 Three regions of gas condensate fluid flow behavior.....	29
Figure 3.11 Three regions of gas condensate pressure profile.....	29
Figure 3.12 Shift of phase envelope with composition change.....	30
Figure 4.1 Top view of the reservoir model.....	32
Figure 4.2 Side view of the reservoir model.....	33
Figure 4.3 3D view of the reservoir model.....	33
Figure 4.4 Phase behavior of the gas-condensate reservoir fluid system.....	36
Figure 4.5 Gas and oil relative permeabilities.....	38
Figure 4.6 Oil and water relative permeabilities.....	39
Figure 4.7 Monobore well schematics.....	40
Figure 5.1 Grids representing well location in reservoir model.....	43
Figure 5.2 Gas production rate for Scenario 1.....	44
Figure 5.3 Condensate production rate for Scenario 1.....	45
Figure 5.4 Pressure vs time for Scenario 2.....	45
Figure 5.5 Phase behavior of the gas condensate reservoir fluid system.....	46
Figure 5.6 Gas production rate for Scenario 2.....	48

	Page
Figure 5.7 Condensate production rate for Scenario 2.....	48
Figure 5.8 Pressure vs time for Scenario 2.....	49
Figure 5.9 VLP of the gas-condensate reservoir fluid system.....	49
Figure 5.10 Gas production rate for Scenario 3.....	50
Figure 5.11 Condensate production rate for Scenario 3.....	51
Figure 5.12 Pressure vs time for Scenario 3.....	51
Figure 5.13 Gas production rate for Scenario 4.....	53
Figure 5.14 Condensate production rate for Scenario 4.....	53
Figure 5.15 Pressure vs time for Scenario 4.....	54
Figure 5.16 Gas production rate for Scenario 5.....	56
Figure 5.17 Condensate production rate for Scenario 5.....	56
Figure 5.18 Pressure vs time for Scenario 5.....	57
Figure 5.19 Gas production rate for Scenario 6.....	59
Figure 5.20 Condensate production rate for Scenario 6.....	59
Figure 5.21 Pressure vs time for Scenario 6.....	60
Figure 5.22 Gas production rate for Scenario 7.....	62
Figure 5.23 Condensate production rate for Scenario 7.....	62
Figure 5.24 Pressure vs time for Scenario 7.....	63
Figure B.1 Gas production rate for in case of thickness variation in Scenario 1.....	87
Figure B.2 Condensate production rate in case of thickness variation in Scenario 1.....	87
Figure B.3 Gas production rate in case of thickness variation in Scenario 2.....	88
Figure B.4 Condensate production rate in case of thickness variation in Scenario 2.....	88
Figure B.5 Gas production rate in case of thickness variation in Scenario 3.....	89
Figure B.6 Condensate production rate in case of thickness variation in Scenario 3.....	89
Figure B.7 Gas production rate in case of thickness variation in Scenario 4.....	90
Figure B.8 Condensate production rate in case of thickness variation in Scenario 4.....	90
Figure B.9 Gas production rate in case of thickness variation in Scenario 5.....	91
Figure B.10 Condensate production rate in case of thickness variation in Scenario 5.....	91

	Page
Figure B.11 Gas production rate in case of thickness variation in Scenario 6.....	92
Figure B.12 Condensate production rate in case of thickness variation in Scenario 6.....	92
Figure B.13 Gas production rate in case of thickness variation in Scenario 7.....	93
Figure B.14 Condensate production rate in case of thickness variation in Scenario 7.....	93
Figure B.15 Gas production rate in case of permeability variation in Scenario 1.....	94
Figure B.16 Condensate production rate in case of permeability variation in Scenario 1..	94
Figure B.17 Gas production rate in case of permeability variation in Scenario 2.....	95
Figure B.18 Condensate production rate in case of permeability variation in Scenario 2..	95
Figure B.19 Gas production rate in case of permeability variation in Scenario 3.....	96
Figure B.20 Condensate production rate in case of permeability variation in Scenario 3..	96
Figure B.21 Gas production rate in case of permeability variation in Scenario 4.....	97
Figure B.22 Condensate production rate in case of permeability variation in Scenario 4..	97
Figure B.23 Gas production rate in case of permeability variation in Scenario 5.....	98
Figure B.24 Condensate production rate in case of permeability variation in Scenario 5..	98
Figure B.25 Gas production rate in case of permeability variation in Scenario 6.....	99
Figure B.26 Condensate production rate in case of permeability variation in Scenario 6..	99
Figure B.27 Gas production rate in case of permeability variation in Scenario 7.....	100
Figure B.28 Condensate production rate in case of permeability variation in Scenario 7.....	100

## List of Abbreviations

API	degree (American Petroleum Institute)
bbbl	barrel (bbbl/d, bpd: barrel per day)
BHP	bottomhole pressure
CGR	condensate gas ratio
D	Darcy
GRV	Gross Rock Volume
GWC	Gas-Water Contact
K	kilo- (10 <sup>3</sup> or 1,000)
M	thousand (1,000 of petroleum unit),
MSCF/D	thousand standard cubic feet per day
NTG	Net-to-gross rock volume
OGIP	Original gas in-place
PVT	pressure-volume-temperature
PSIA	or psia pounds per square inch absolute
RF	Recovery factor
SCAL	special core analysis
SGAS	gas saturation
STB	or stb stock-tank barrel
STB/D	stock-tank barrels per day
SWAT	water saturation
THP	Tubing Head Pressure

## Nomenclature

$A$	cross-section area
$B_g$	gas Formation Volume Factor
$B_w$	water Formation Volume Factor
$C_f$	formation compressibility
$d$	differential operator
$G$	gas in place
$G_p$	cumulative gas production
$h$	height
$k$	permeability
$k_{rg}$	gas relative permeability
$k_{rw}$	water relative permeability
$M$	molecular weight
$p$	pressure
$q$	volumetric flow rate
$Q$	volumetric flow rate at standard conditions
$r$	radial direction
$R$	universal gas constant
$S$	saturation
$t$	time period
$T$	temperature
$V$	fluid volume
$W_p$	water production
$W_e$	water encroachment
$x$	1 distance in x direction, 2 x direction
$y$	direction
$z$	1 compressibility factor, 2 z direction

**GREEK LETTER**

$\square$	porosity
$\rho$	fluid density (mass/volume)
$\mu$	fluid viscosity
$\Delta$	difference operator
$\partial$	partial differential operator
$v$	flow velocity

**SUPERSCRIPTS**

$n$	current time level
$n+1$	new time level

**SUBSCRIPTS**

$A$	areal
$g$	gas
$i$	initial
$o$	oil
$r$	radial
$w$	water

# CHAPTER I

## INTRODUCTION

The Gulf of Thailand contains several structurally complex trans-tensional basins. These are made up of asymmetrical grabens filled with non-marine to marginal marine Tertiary sediments as old as Eocene. Underlying the graben sediments are a variety of Paleozoic marine carbonates, granitic intrusive rocks, and metasediments. Many of the basins contain thick sequence of gas-prone source rocks, but the limited lateral extent of these deposits, combined with variations in heat flow and depth of burial of the source rocks, causes the distribution of hydrocarbons to be complex and difficult to predict. In addition, the heat flow factor appears to have consequence in the discharge of significant CO<sub>2</sub> volume from the breakdown of basement carbonates. The content of CO<sub>2</sub> is related with most of Thailand's commercial gas production.

The hydrocarbon reserve exist in multi faulted sandstone reservoir are deposited in fluvio-deltic and coastal environments. Figure 1.1 represents the depositional environment distribution. The distributaries' channel originates the delta plain of field which potentially accumulates organic rich substances. In this area typically is found to have hydrocarbon reservoirs. All reservoirs developed to date have had a hydrostatic pressure regime.

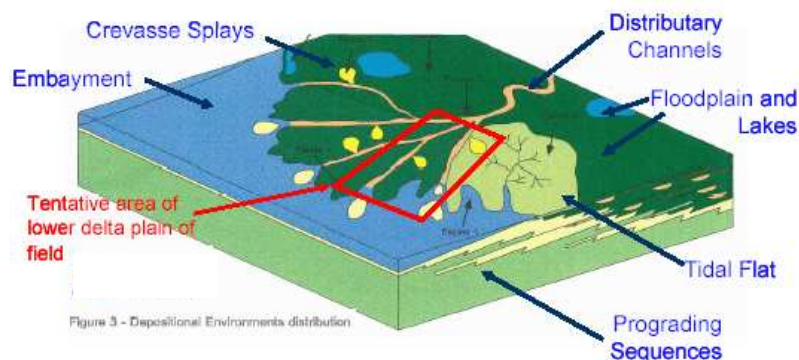


**Figure 1.1:** Shape & Patterns of Bar and Channel Sands



The reservoir drive mechanism for each sand layer in the Gulf of Thailand is found to be either depletion drive or water drive mechanism. This is according to the multiple deposition of the basin. Within a single compartment of the reservoirs, there can be numbers of reservoir sands. Finding 20 hydrocarbon-bearing sands in a single well is recurrent in the Gulf of Thailand. These reservoir sands are possible to be either channel or bar sands. The channel sands are typically thicker than bar sands. They are often supported by aquifer. The bar sands are thinner, with the shape of thin lens. They are found with or without aquifer support.

The channel sands encountered in the Gulf of Thailand multilayered gas reservoirs have porosity ranging from 8% to 30% and permeability ranging from 1 mD to 10 D. The channel sand thickness is in the range of 5 to 30 meters (16 to 100 feet). The channels are found as isolated channel, interconnected groups and even multiple interconnected groups.

In general, the bar sands have less porosity than the channel sands given the same depth. Their porosity lies in a range of 8% to 25% and permeability in the range of 1 mD to 10 D. The sand thickness is in the range of 1 to 20 meters (3 to 60 feet) in general.

Another complexity of the Gulf of Thailand multilayered gas reservoir is that channel sand can be either water drive or depletion drive, depending on the connection to an aquifer. The drive mechanism for specific sand layer will only be known once the sand is put into production. This complexity leads to the difficulty in selection of the sand to perforate.

In term of petroleum production, the two types of sands are not distinguished between each other. There are only thin or thick reservoirs, with either depletion or water drive mechanism. Yet the complexity encountered on both bar and channel reservoir's rock as well as fluid properties and with different drive mechanisms creates difficulties for engineers to find optimum production/perforation scenario, especially when these multiple reservoirs are to be produced through a common well.

In case of multi-layered gas condensate and dry gas reservoirs, the challenging to overcome liquid loading up in wellbore is generally known. This is due to the nature of gas condensate behavior. Initially, gas condensate is a single-phase fluid

presenting in gas phase. In the meantime once reservoir pressure drops to the dewpoint pressure then gas condensate forms to be liquid phase in the reservoir. The condensate liquid becomes static and has less mobility owing to capillary forces causing the effect of the inflow of fluid. In consequent, the production of gas condensate is found to be lost while in the reservoir. The declination of relative permeability near the wellbore demonstrates the condensate blockage effect. In that case with the aim of enhancing the gas condensate production, the use of in-situ dry gas reservoir is considered. The success to gain gas condensate production in the gulf of Thailand, one of the matters relies on perforation sequencing in multi-layered reservoir whether the in-situ dry gas is going to successfully boost up condensate production.

Currently, the Gulf of Thailand general practice is to produce from bottommost reservoirs upwards and shut any reservoirs with excessive water production. This method allows gas and gas condensate production to be produced from the deepest reservoir first, following by the next upper reservoirs consecutively. The benefit of this method is to allow the bottom reservoir to be produced then the shutting-off of the depleted reservoir can be done easily without missing the opportunity to produce upper commercial pay zones.

According to the complexity of the reservoir characteristics, the Gulf of Thailand dry gas and gas condensate reservoirs possess one of the most challenging reservoir management for petroleum engineers.

## **1.1 Objective**

The objectives of this study are as the follows:

1. To determine guideline for best perforation strategy in multi-layered gas condensate and dry gas reservoirs.
2. To understand the impact of production by the condensate blockage, liquid load up, and the effect of reservoir property variation and determine the best perforation strategy in each case.
3. To understand the impact of aquifer toward the gas condensate and dry gas production and determine the best perforation strategy in each case.

## 1.2 Outline of Methodology

In order to improve the multilayered dry gas and gas condensate reservoirs management, this thesis has been initiated to find the perforation strategy so that the well's production can be optimized. This includes study of optimal perforation sequencing and study of optimal perforation under production constraints.

The study is carried out in following steps:

### 1. Data collection

Prior to running the simulation, data have to be gathered and input into the program. These data include fluid composition from PVT analysis, reservoir fluid properties, rock properties, reservoir pressure, reservoir temperature, wellbore size, and tubing head pressure.

### 2. Set up of reservoir model

A compositional reservoir simulation program called ECLIPSE 300 is used to simulate the performance of condensate and gas production for two-layered reservoirs consisting of upper gas condensate reservoir and lower dry-gas reservoir. The PVT and SCAL data are based on available Gulf of Thailand reservoirs data. The resulting model is considered as representative model for multilayered dry gas and gas condensate reservoirs. In performing the model set up, the pre-assumption is that the drive mechanism associated with each sand layer is known.

### 3. Study various scenarios

Better understanding of the performance of the multilayered reservoir is expected through this step. After the model is set up to be a basis for the study, various perforation options are put into test through the model. This includes:

- (a) Concurrent perforation
- (b) Perforating the lower zone after the upper zone is depleted and shutting off the upper zone while producing the lower zone
- (c) Perforating the lower zone when the upper zone is depleted
- (d) Perforating the lower zone when the upper zone production is half
- (e) Perforating the lower zone when the upper zone production is declining

- (f) Perforating the upper zone when the lower zone is depleted
- (g) Perforating the upper zone when the lower zone production is half
- (h) Perforating the upper zone when the lower zone production is declining

In addition, the effects on production performance of the following variables are investigated:

1. Drive mechanism
2. Reservoir thickness
3. Reservoir permeability

#### **4. Result analysis**

After all steps are carried out, the results are analyzed and summarized

## **1.3 Thesis Outline**

This thesis consists of six chapters.

Chapter II outlines a list of related works/studies on multilayered gas condensate and dry gas reservoirs including perforation strategies.

Chapter III describes the setting of reservoir model, theory of gas reservoirs, and drive mechanisms.

Chapter IV discusses the principle of reservoir simulation, and model generation.

Chapter V discusses the case study and their results of reservoirs simulation obtained.

Chapter VI provides conclusion and recommendation

## CHAPTER II

### LITERATURE REVIEW

A number of literatures regarding behavior of multilayered reservoirs and perforation sequence have been reviewed as elaborated below. As a summary, only a small amount of the reviewed articles directly address the perforation sequence in multilayered dry gas and gas condensate reservoirs. This leaves the topics of interest becomes challenging.

Camacho et al. [1] examined the response of fractured wells in commingled reservoirs when the fracture length is assumed to vary from layer to layer. The analysis of multilayer reservoir extends from the finite-difference model developed by Bennett [2]. Some techniques to correlate the commingled reservoir solutions with existing single-layer solutions were used by redefining terms involving the fracture half-length and fracture conductivity in the definitions of dimensionless time and dimensionless fracture conductivity. In the study, the authors considered two modes of production which are constant-pressure and constant-rate conditions.

In conclusion, well response may be described by dimensionless pressure drop and dimensionless time based on thickness-averaged values of the layer permeability and the porosity-compressibility product of each layer. The analysis of buildup or drawdown data is possible to estimate the equivalent fracture half-length and the equivalent fracture conductivity. These data are useful to model a multilayer system with an equivalent single-layer system during the transient period.

Fetkovich et al. [3] presented the depletion performance of a two-layered gas reservoir producing without crossflow. They studied the field that has produced for more than 20 years at effectively a low constant wellbore pressure, thus giving continuous, declining rate/time data for analysis. Furthermore, a greater flexibility was then obtained with a conventional single-cell, pseudosteady-state, gas-forecasting program that combines gas material balance and a stabilized back-pressure curve for each layer.

In their results, for all combinations of properties examined, the rate/time and pressure/cumulative-production performance is not rate-sensitive at practical rates.

Also, different combinations of layer skins can demonstrate similar rate/time and pressure/cumulative-production differential-depletion response. They believe that all of the conclusions are applicable to the gas reservoir in their studies and most of them would be applicable to any no-crossflow layered reservoirs.

Jamiolahmady et al. [4] developed a number of finite-element-based simulators to study the flow of single-phase gas and gas-condensate in 1D openhole and 3D perforated-well completions. They evaluated the impact of perforation characteristics, fluid properties, rock characteristics, wellbore radius, fractional flow, and flow rate on well productivity using their in-house simulators. The model included the effect of changes in fluid properties, positive coupling, and negative inertia.

They expressed the results in the form of PR which is the ratio of the total flow rate of gas and condensate in the perforated completion to that of an openhole unperforated well at the same pressure drop and fractional flow at the wellbore conditions. At low velocity levels, the performance of a perforated completion for two-phase flow of gas and condensate is similar to that of single-phase gas. Furthermore, at low gas to total fractional flow rate values, the productivity of the perforated completion is improved but at high gas to total fractional flow rate values, negative inertial effect decreases the productivity.

Saleh and Stewart [5] considered well skin factor toward perforated completion. They analyzed the solution of skin factor both steady-state Darcy and non-Darcy flow including all interacting perforation parameters as well as formation anisotropy. Liquid drop out behavior and contribution to the skin which are necessary to understand gas condensate reservoirs are accounted for the extension from single phase results to two phase condensate gas flow.

In their conclusions, they found that the analytical skin model can easily be programmed and used for an accurate prediction of the perforation skin factor and well productivity ratio for any type of completion and perforation geometry. They constructed model in this study which requires input of perforation parameter, well data, and the perforation shooting pattern including formation and damaged zone parameters to calculate the perforation skin factor. Also, the interaction of non-Darcy flow and the liquid drop-out effect can be easily explained from this model.

Momin [6] studied the perforation strategies of multi-layered reservoirs in the determination of the optimum depletion scenario with different drive mechanisms. In this study, he used reservoir simulation to model the reservoirs and evaluate the effect of drive mechanism toward the recovery performance under various perforation strategies. In term of commingle production from both depletion drive and water drive reservoirs, separate production with early shutting-off of the water producing reservoirs would provide effective solution for recovery efficiency, crossflow, and recovery time.

The author clarifies that crossflow in the well is mainly from the difference between reservoir pressure, well bottomhole flowing pressure, and reservoir's rock and fluid properties. Permeability plays an important role in gas-water flows through reservoirs as it has direct effect on recovery efficiency once the reservoir permeability is above 200 mD. In combination drive reservoirs and water drive reservoirs, water shut off need to be performed where water production in the well becomes excessive.

Arianto et al. [7] presented completion solution for multilayered gas fields. The field of interest is Sanga-Sanga PSC, offshore Kalimantan which is fluvial gas field consisting of low permeability (1-100 mD), depletion drive reservoirs and higher permeability (100-1000 mD), water drive reservoirs. The classical way of perforation is to carry out a bottom-up perforation approach. However, this leads to low gas rate (as the bottom has low permeability), liquid loading, and/or poor well performance. Alternatively, production from shallow reservoirs can be chosen but the watered out perforation zone will be difficult to isolate. Their solution in the past was to use single selective completion. However, this solution is quite ineffective since their production tubing system has to be completed with various downhole equipment such as double tubing packer, sliding sleeve valve, etc, which increase the risk of system leakage and subsequent problems. In their study, they have decided to use dual completion, one for the shallow and one for the deep reservoirs which proves to be successful applications.

Al-Sheri et al. [8] tested commingled production from multilayered gas-carbonate reservoirs in Ghawar field, Saudi Arabia. They highlighted that the key successful factor for commingled production is to keep the flowing bottomhole pressure of the system below the lowest static reservoir pressure. They further

stressed that the best result would be obtained when similar static pressure zones are combined or when the lower static pressure zone exhibits higher productivity index. Along with several findings, they concluded from actual results that commingle production shows improvement both for production rate and recovery. This conclusion is made from comparing the commingled production vs. original selective zone production (i.e., to produce from only one reservoir zone at a time).



## CHAPTER III

### THEORY AND CONCEPT

In this chapter, we explain key concepts about multi-layered gas and gas condensate reservoirs and related theories involving flow behavior of the gas condensate system.

#### 3.1 General Definition of Multi-layered Reservoirs

A type of reservoir consists of an amount of layers which characteristics and properties are possible to be different in each layer. Communication across the layer is barely found therefore the communication occurs once the well is perforated through the production tubing. Figure 3.1 shows the configuration of multi-layered reservoirs in which the zones are isolated. The isolation of zones are created by cementing around production tubing which leads to sequencing zone opening in production method.

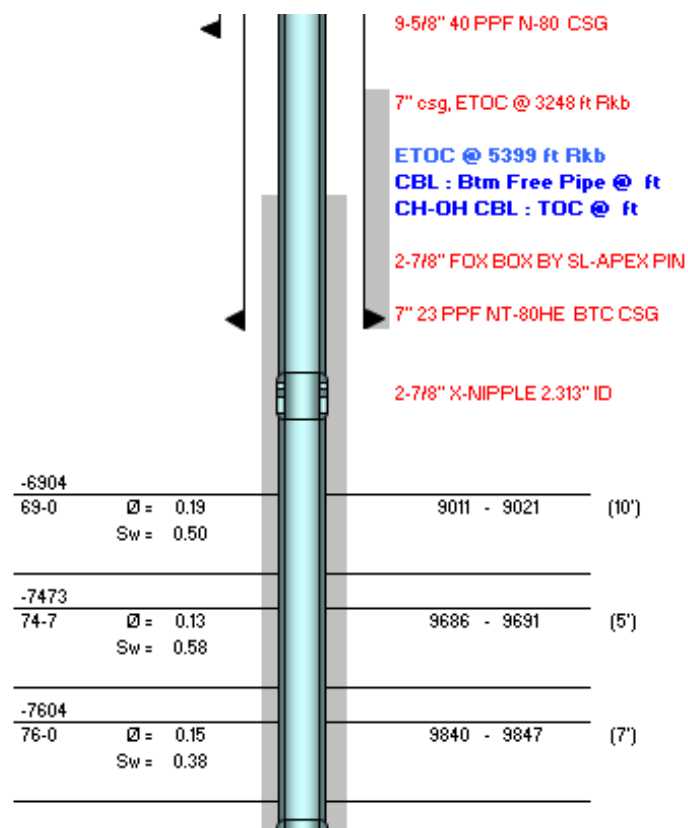


**Figure 3.1:** Multi-layered reservoirs with production tubing

### 3.2 Reservoir Simulation

The reservoir simulation technique is used in this study because it offers the advantage on capturing the flow of fluid in reservoirs, the interaction between each reservoir in the multilayered reservoirs through the common producing well, and the effect of different drive mechanisms on the producing characteristics of the multilayered reservoirs. These advantages are important in order to understand the behavior of multilayered reservoirs, and ultimately, to determine the application of the optimal production/perforation techniques.

The reservoir simulation software used in this study is the ECLIPSE 300 software. Compositional model is used in this study as the reservoirs of interest contain different hydrocarbon compositions of dry gas and gas-condensate. The data used to create reservoir model are field data of a well in Gulf of Thailand. To create the model, rock and fluid properties have to be known. The two important concepts that are used in reservoir simulations are the concept of material balance and the concept of fluid flow in porous medium.

### 3.3 Material Balance Concept

The law of conservation of mass is the basis of material balance calculations. Material balance is an accounting of material entering and leaving a system. The calculation treats the reservoir as a large tank of material and uses quantities that can be measured to determine the amount of a material that cannot be directly measured. In its simplest form, the equation can be written on volumetric basis as:

$$\text{Initial volume} = \text{volume remaining} + \text{volume removed}$$

Measurable quantities include cumulative fluid production volumes for oil, water, and gas phases, reservoir pressure, and fluid property data from samples of produced fluids. Material balance calculation may be used for several purposes. It provide an independent method of estimating the volume of oil, water, and gas in a reservoir for comparison with volumetric estimates. The magnitude of various factors in the material balance equation indicates the relative contribution of different drive

mechanisms at work in the reservoir. Material balance can be used to predict future reservoir performance and aid in estimating recovery efficiency.

### 3.4 Material Balance in Gas Reservoir

Reservoirs containing only free gas are termed gas reservoirs. Such a reservoir contains a mixture of hydrocarbons which exists wholly in the gaseous state. Gas reservoirs may have water influx from contiguous water-bearing portion of the formation or maybe volumetric (i.e., have no water influx). The general material balance equation applied to a gas reservoir is in the form of:

$$G(B_g - B_{gi}) + GB_{gi} \frac{(c_w S_{wi} + c_f)}{(1 - S_w)} \Delta \bar{p} + W_e = G_p B_g + B_w W_p \quad (3.1)$$

where

- G = initial gas in-place
- G<sub>p</sub> = cumulative gas production
- B<sub>g</sub> = gas formation volume factor
- B<sub>gi</sub> = initial gas formation volume factor
- c<sub>w</sub> = water compressibility
- S<sub>wi</sub> = initial water saturations
- c<sub>f</sub> = formation compressibility
- Δ $\bar{p}$  = difference in reservoir pressure compared to original reservoir pressure.
- W<sub>e</sub> = cumulative water encroached to reservoir
- B<sub>w</sub> = water formation volume factor
- W<sub>p</sub> = cumulative water production

Equation (3.1) is derived by applying the law of conservation of mass to the reservoir and associated production.

For gas reservoirs, the gas compressibility is much greater than the formation and water compressibility, and the second term on the left-hand side of Equation (3.1) becomes negligible. The new equation becomes

$$G(B_g - B_{gi}) + W_e = G_p B_g + B_w W_p \quad (3.2)$$

When there is neither water encroachment into the reservoir nor water production from the reservoir, the reservoir is said to be volumetric. In this case Equation (3.2) reduces to

$$G(B_g - B_{gi}) = G_p B_g \quad (3.3)$$

But

$$B_g = \frac{p_{sc} z T}{T_{sc} p} \quad (3.4)$$

Substituting  $B_g$  into Equation (3.4), we have

$$\frac{p}{z} = -\frac{p_i}{z_i G} G_p + \frac{p_i}{z_i} \quad (3.5)$$

Because  $p_i$ ,  $z_i$ , and  $G$  are constants for a given reservoir, Equation (3.5) suggests that a plot of  $p/z$  as the ordinate versus  $G_p$  would yield a straight line with:

$$\text{Slope} = -\frac{p_i}{z_i G}$$

$$y \text{ intercept} = \frac{p_i}{z_i}$$

The  $p/z$  plot versus cumulative production is shown in Figure 3.2.

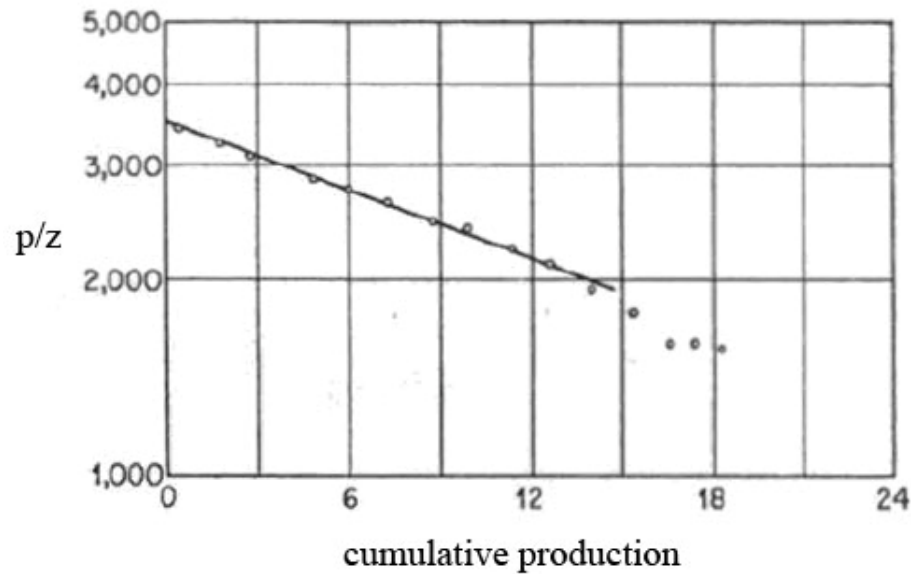


**Figure 3.2:**  $p/z$  plot versus cumulative production (Craft and Hawkins [9])

If  $p/z$  is set equal to zero, which would represent the production of all the gas from reservoir, then the corresponding  $G_p$  equals  $G$ , the initial gas in-place.

For gas-condensate reservoir, whether the pressure is above or below the dewpoint, two or three fluid phases may occur in a gas-condensate reservoir. The difference from dry gas reservoirs is that gas-condensate reservoirs are characteristically rich with intermediate and heavier hydrocarbon molecules. Hence, the requirement to correct concepts of this method is to consider the liquid volume remaining in the reservoir and any liquids produced at the surface.

### 3.5 Fluid Flow in Porous Medium

The fluid flow equations that are used to describe the flow behavior in a reservoir can take many forms depending upon the combination of variables presented previously (i.e., types of flow, types of fluids, etc.). By combining the conservation of mass equation with the transport equation (Darcy's equation) and various equations of state, the necessary flow equations can be developed. Since all flow equations to be considered depend on Darcy's law, it is important to consider this transport relationship first.

### 3.5.1 Darcy's Law

The fundamental law of fluid motion in porous media is Darcy's law. The mathematical expression developed by Darcy in 1756 states that the velocity of a homogeneous fluid in a porous medium is proportional to the head (or potential), and inversely proportional to the fluid viscosity. For a horizontal linear system, this relationship is:

$$v = \frac{q}{A} = \frac{-k}{\mu} \frac{dp}{dx} \quad (3.6)$$

where

- $v$  = apparent velocity in centimeters per second and is equal to  $q/A$ .
- $q$  = volumetric flow rate in cubic centimeters per second.
- $A$  = total cross-sectional area of the rock in square centimeters.  
other words,  $A$  includes the area of the rock material as well as the area of the pore channels.
- $\mu$  = fluid viscosity, centipoise.
- $\frac{dp}{dx}$  = pressure gradient, atmospheres per centimeter. Taken in the same direction as  $v$  and  $q$ .
- $K$  = permeability of the rock, Darcy.

The negative sign in Equation (3.6) is added because the pressure gradient  $\frac{dp}{dx}$  is negative in the direction of flow. For a horizontal-radial system, the pressure gradient is positive and Darcy's equation can be expressed in the following generalized radial form:

$$v = \frac{q_r}{A_r} = \frac{k}{\mu} \left( \frac{\partial p}{\partial r} \right)_r \quad (3.7)$$

where:

- $q_r$  = volumetric flow rate at radius  $r$
- $A_r$  = cross-sectional area to flow at radius  $r$
- $\left( \frac{\partial p}{\partial r} \right)_r$  = pressure gradient at radius  $r$

$v$  = apparent velocity at radius  $r$

The cross-sectional area at radius  $r$  is essentially the surface area of a cylinder.

For a fully penetrated well with a net thickness of  $h$ , the cross-sectional area  $A_r$  is given by:

$$A_r = 2\pi r h \quad (3.8)$$

Darcy's law applies only when the following conditions exist:

- Laminar (viscous) flow;
- Steady-State flow;
- Incompressible fluids;
- Homogeneous formation.

For turbulent flow, which occurs at higher velocities, the pressure gradient increases at a greater rate than does the flow rate and a special modification of Darcy's equation is needed. When turbulent flow exists, the application of Darcy's equation can result in serious errors.

### 3.5.2 Radial Flow of Compressible Fluids

For a viscous (laminar) gas flow in a homogeneous radial system, the real-gas equation of state can be applied to calculate the number of gas moles  $n$  at the pressure  $p$ , temperature  $T$ , and volume  $V$ :

$$n = \frac{pV}{zRT} \quad (3.9)$$

At standard conditions, the volume occupied by the above  $n$  moles is given by:

$$V_{sc} = \frac{nz_{sc}RT_{sc}}{p_{sc}} \quad (3.10)$$

Equivalently, the above relation can be expressed in terms of the reservoir condition flow rate  $q$ , in scf/day, and surface condition flow rate  $q_{sc}$ , in scf/day, as:

$$\frac{p \times q}{zT} = \frac{p_{sc}q_{sc}}{T_{sc}} \quad (3.12)$$

Rearranging:

$$\left(\frac{p_{sc}}{T_{sc}}\right) \left(\frac{zT}{p}\right) q_{sc} = q \quad (3.13)$$

where:

- $q$  = gas flow rate at pressure  $p$  in scf/day  
 $q_{sc}$  = gas flow rate at standard conditions, scf/day  
 $z$  = gas compressibility factor  
 $T_{sc}$  = standard temperature in °R and  
 $p_{sc}$  = standard pressure in psia

Dividing both sides of the above equation by the cross sectional area  $A$  and equating it with that of Darcy's law, i.e., Equation (3.6), gives:

$$\frac{q}{A} = \left(\frac{p_{sc}}{T_{sc}}\right) \left(\frac{zT}{p}\right) \left(\frac{1}{2\pi rh}\right) q_{sc} = -0.006328 \frac{k}{\mu} \frac{dp}{dr} \quad (3.14)$$

The constant 0.001127 is to convert Darcy's units to field units. Separating variables and arranging yields:

$$\left[ \frac{q_{sc} p_{sc} T z \mu}{(0.006328)(2\pi) T_{sc} k h} \right] \int_{r_1}^{r_2} \frac{dr}{r} = - \int_{p_1}^{p_2} p dp = \frac{1}{2} (p_1^2 - p_2^2) \quad (3.15)$$

Assuming that the product of  $z\mu_g$  is constant over the specified pressure range between  $p_1$  and  $p_2$ , and integrating, gives:

$$\frac{q_{sc} p_{sc} T z \mu}{0.01988 T_{sc} k h} \ln \left( \frac{r_2}{r_1} \right) = (p_1^2 - p_2^2) \quad (3.16)$$

Then,

$$q = \frac{0.703533 k h (p_1^2 - p_2^2)}{T (z \mu_g) \ln \left( \frac{r_2}{r_1} \right)} \quad (3.17)$$



where:

$q$	=	gas flow rate, scf/day
$k$	=	permeability, mD
$T$	=	temperature, °R
$\mu_g$	=	gas viscosity, cp
$h$	=	reservoir thickness, ft
$r$	=	total length of the radial system, ft

If one considers the drainage radius of the well, and adding skin factor into account, the final equation is,

$$q = \frac{0.703533kh(p_r^2 - p_{wf}^2)}{T(z\mu_g) \ln\left(\left(\frac{r_2}{r_1}\right) + S\right)} \quad (3.18)$$

It is essential to notice that those gas properties  $z$  and  $\mu_g$  are very strong functions of pressure, but they have been removed from the integral to simplify the final form of the gas flow equation. The above equation is valid for applications when the pressure is less than 2000 psi. The gas properties must be evaluated at the average pressure.

### 3.6 Gas Reservoir

To distinguish reservoir fluid type can only be confirmed by the observation from the laboratory. Notwithstanding, readily available production information usually will indicate the type of reservoir. The reservoir fluid can be categorized into five types; black oil, volatile oil, retrograde gas, wet gas, and dry gas.

Typically, if reservoir temperature is above the critical temperature of the hydrocarbon system, it is classified as a natural gas reservoir. On the basis of their phase diagrams and the prevailing reservoir conditions, natural gases can be classified into four categories;

- Retrograde gas-condensate

- Near-critical gas-condensate
- Wet gas
- Dry gas

### 3.6.1 Retrograde Gas Condensate Reservoir

In the event that the reservoir temperature ( $T$ ) lies between the critical temperature ( $T_c$ ) and cricondentherm ( $T_{ct}$ ) of the reservoir fluid, the reservoir is classified as a retrograde gas-condensate reservoir. This type of reservoir is a unique type of hydrocarbon accumulation in that the special thermodynamic behavior of the reservoir fluid is the controlling factor in the development and the depletion process of the reservoir. When the reservoir pressure is decreased on these mixtures, instead of expanding or vaporizing as might be expected, they vaporize instead of condensing as illustrate in Figure 3.3. The reason of this occurrence is because the reservoir pressure is above the upper dew-point pressure, the hydrocarbon system exists as a single phase in the reservoir. As the reservoir pressure declines isothermally from the initial pressure to the upper dew-point pressure, the attraction between the molecules of the light and heavy components cause them to move further apart. From this event, attraction between the heavy component molecules becomes more effective until liquid begins to condense. Further reduction in pressure permits the heavy molecules strike the liquid surface and causes more molecules to leave than enter the liquid phase. This means that all the liquid that formed must vaporize because the system is essentially all vapors at the lower dew point. It should be recognized that around the well bore where the pressure drop is high, and sufficient liquid drop out may accumulate to give two phase flow of gas and retrograde liquid.

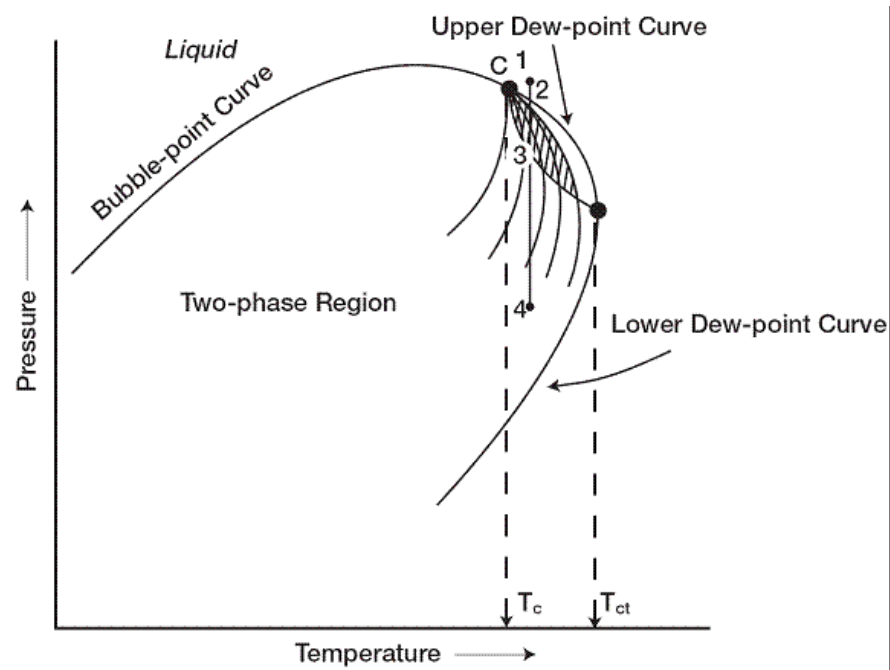


**Figure 3.3:** A typical phase diagram of a retrograde gas condensate (after Yisheng et. al. [10]).

### 3.6.2 Near Critical Gas-Condensate Reservoir

In case the reservoir temperature is near the critical temperature the hydrocarbon mixture is classified as a near-critical gas-condensate. The volumetric behavior of this category of natural gas is explained through the isothermal pressure declines and also by the corresponding liquid dropout curve. Because all the quality lines converge at the critical point, a rapid liquid buildup will immediately occur below the dew point as the pressure is reduced. This behavior can be justified by the fact that several quality lines are crossed very rapidly by the isothermal reduction in pressure. At the point where the liquid ceases to build up and begins to shrink again, the reservoir goes from the retrograde region to a normal vaporization region.

### 3.6.3 Wet Gas Reservoir

A typical phase diagram of a wet gas is shown in Figure 3.4 where reservoir temperature is above the cricondentherm of the hydrocarbon mixture. Because the reservoir temperature exceeds the cricondentherm of the hydrocarbon system, the reservoir fluid will always remain in the vapor phase region as the reservoir is depleted isothermally. As the produced gas flows to the surface, however, the pressure and temperature of the gas will decline. If the gas enters the two-phase region, a liquid phase will condense out of the gas and be produced from the surface separators. This is caused by a sufficient decrease in the kinetic energy of heavy molecules with temperature drop and their subsequent change to liquid through the attractive forces between molecules.

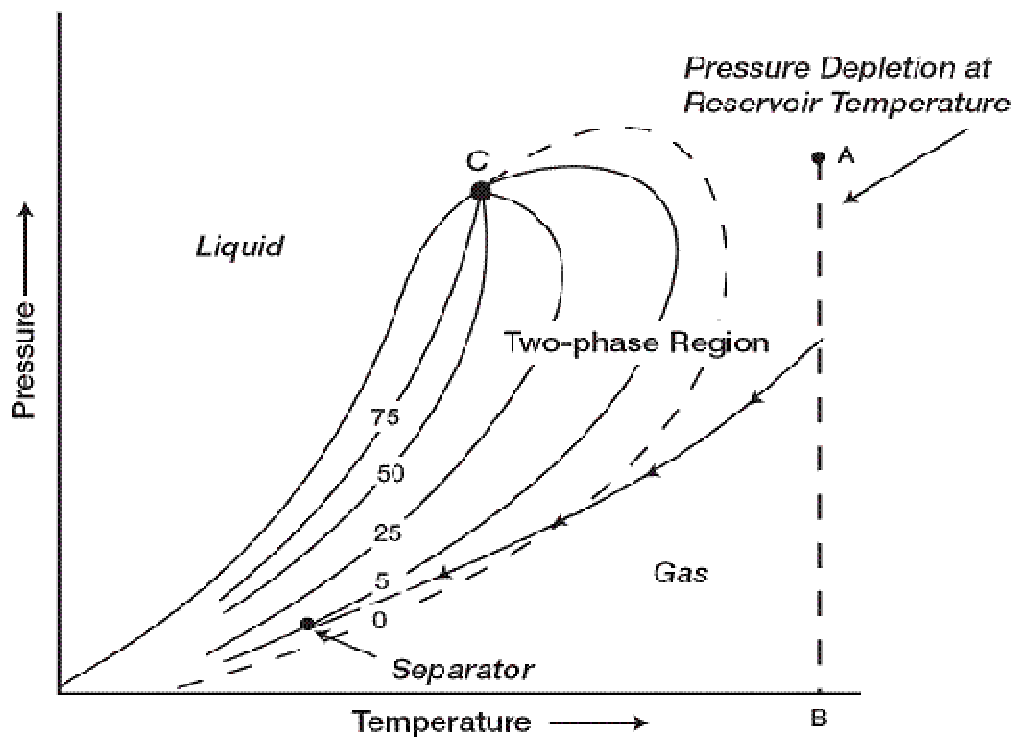


**Figure 3.4:** Phase diagram for a wet gas (after Yisheng et. al. [10]).

### 3.6.4 Dry Gas Reservoir

The hydrocarbon mixture exists as a gas both in the reservoir and in the surface facilities. The phase diagram as illustrated in Figure 3.5 showing dry gas reservoir is presenting only gas phase. The only liquid associated with the gas from a dry-gas reservoir is water. Usually a system having a gas-oil ratio greater than 100,000 scf/STB is considered to be a dry gas. Kinetic energy of the mixture is so high and attraction between molecules so small that none of them coalesce to a liquid at stock-tank conditions of temperature and pressure. It should be pointed out that the classification of hydrocarbon fluids might be also characterized by the initial composition of the system.

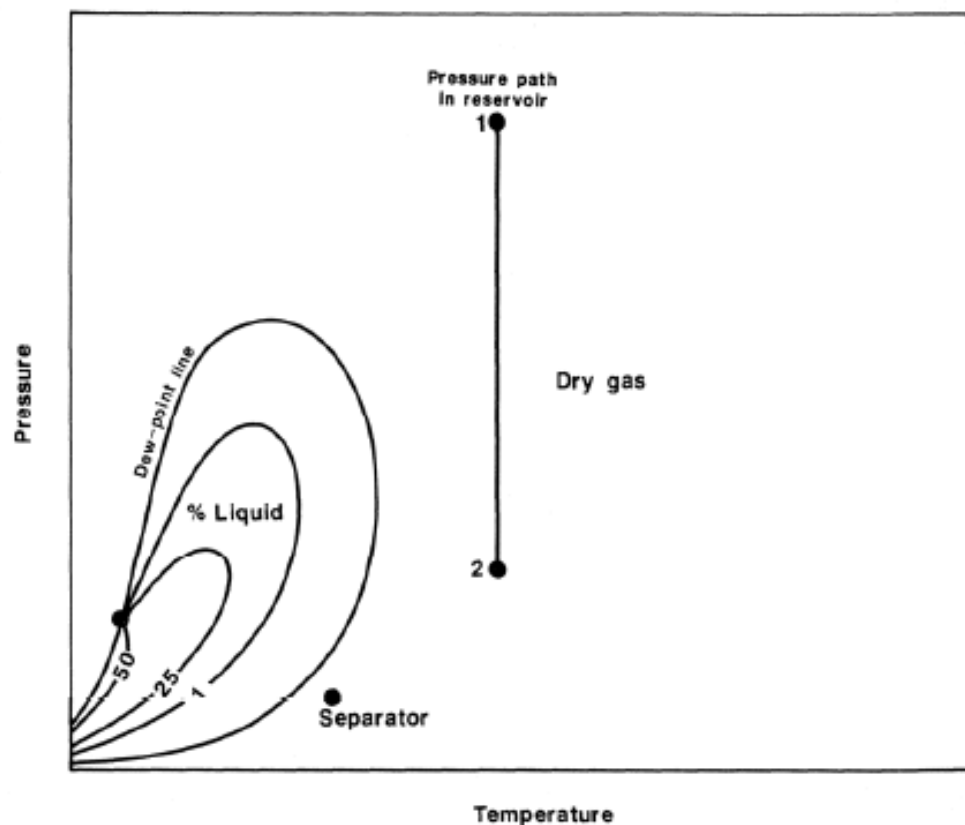


**Figure 3.5:** Phase diagram for dry gas (after McCain [11])

### 3.7 Non-Darcy Flow

For a certain pressure drawdown, the velocity of gas is at least an order of magnitude greater than for oil. The transient pressure response of a gas well might be affected by high velocity, not only the viscous force component represented by Darcy's equation, there is also an inertial force performing according to convective accelerations of the fluid particles in passing through the porous medium. Under this situation the proper flow equation is that of Forchheimer, which is (after Dake, [12])

$$\frac{dp}{dr} = \frac{\mu}{k}u + \beta\rho u^2 \quad (3.19)$$

where

$$\frac{dp}{dr} = \text{pressure gradient at radius } r$$

$$\beta = \text{velocity coefficient}$$

Regularly, unsteady-state flow equation for pressure drawdown analysis with constant-rate gas production is based on the solution for slightly compressible liquid flow with pressure replaced by pseudo pressure; (after Lee, [13])

$$P_p(P_{wf}) = P_p(P_i) - \frac{1.637q_g T}{kh} \left[ \log(t) + \log\left(\frac{k}{\phi \bar{\mu}_g \bar{c}_t r_w^2}\right) - 3.23 + 0.869s' \right] \quad (3.20)$$

In the case of normalized pseudopressure,  $P_a$ , the equation becomes

$$P_{a,wf} = P_{a,i} - \frac{162.6q_g \bar{B}_g \bar{\mu}_g}{kh} \left[ \log(t) + \log\left(\frac{k}{\phi \bar{\mu}_g \bar{c}_t r_w^2}\right) - 3.23 + 0.869s' \right] \quad (3.21)$$

Where  $s' = s + Dq_g$  is an effective skin factor including true formation damage and the effect of Non-Darcy flow.

From above equation, it can be rewritten in dimensionless form as;

$$t_D = \frac{0.0002637kt}{\phi \bar{\mu}_g \bar{c}_t r_w^2} \quad (3.22)$$

Conventionally, the non-Darcy flow effect can be indicated as a rate-dependent pseudoskin defined as  $Dq_g$ , where D is the non-Darcy flow coefficient.

### 3.7.1 Non-Darcy Flow and Positive Coupling

In near wellbore region of gas-condensate reservoirs, there are two phenomena that affect the well productivity and cannot be expressed by Darcy equation which are non-Darcy flow and positive coupling.

Non-Darcy flow is typically observed in high-rate gas wells when the flow converging to the wellbore reaches flow velocities exceeding the Reynolds number for laminar or Darcy flow, and results in turbulent flow. The effect of non-Darcy flow can be treated by the Forchheimer equation with an empirical correlation. Forchheimer [11] proposed the following quadratic equation to express the relationship between pressure drop and velocity in a porous medium:

$$\frac{dp}{dx} = \left( \frac{\mu}{kk_r A} \right) q + \beta \rho \left( \frac{q}{A} \right)^2 \quad (3.23)$$

where:

$q$	=	the volumetric flow rate
$k$	=	the rock permeability
$k_r$	=	the relative permeability
$A$	=	the area through which flow occurs
$\mu$	=	the fluid viscosity
$\rho$	=	the fluid density
$\beta$	=	the Forchheimer parameter
$\frac{dp}{dx}$	=	the pressure gradient normal to the area

Another phenomenon which is known as positive coupling occurs when the flow velocity is high and the interfacial tension between the flowing phases is low. In this case, capillary forces may no longer dominate the distribution of the phases on a pore scale. Subsequently, macroscopic flow properties become dependent on the ratio of viscous to capillary forces on a pore scale, denoted by the capillary number  $N_c$ .

$$N_c = \frac{k|\nabla P|}{\phi\sigma} \quad (3.24)$$

where:

$\sigma$  = interfacial tension

$\phi$  = porosity

### 3.8 Gas-Condensate Phase Behavior

Gas-condensate or retrograde gas is one of the various types of the reservoir fluid which has unique characteristics of phase diagram as illustrated in Figure 3.6. The region of retrograde condensate occurs at temperature between the critical temperature ( $T_c$ ) and the cricondentherm. The cricondentherm is the highest temperature on saturated envelope.

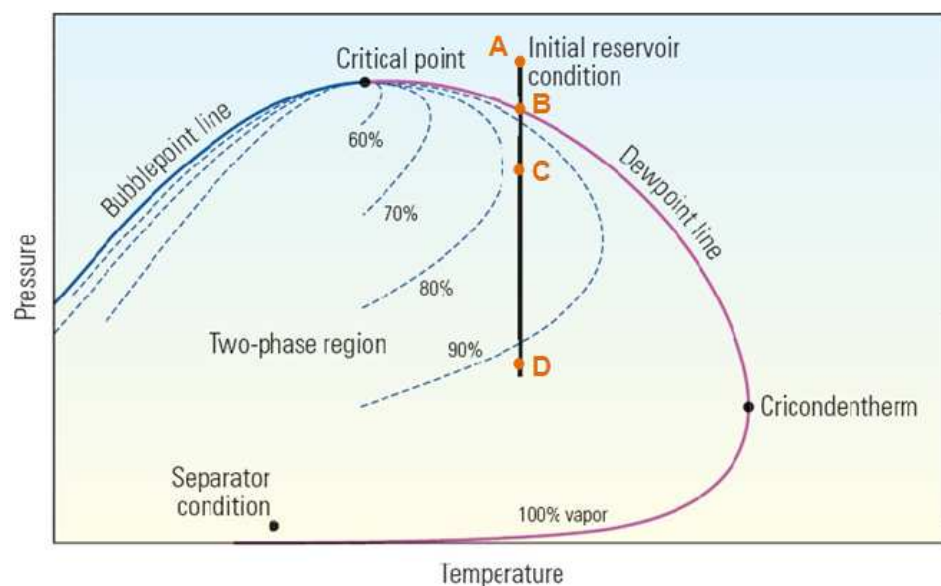


**Figure 3.6:** Pressure-Temperature diagram of condensate (after Fan et. al.

[9])



Gas-condensate is a single-phase gas at original reservoir condition (point A). At dewpoint pressure (point B), the fluid will start to separate into gas and liquid that is called a retrograde condensate. The liquid dropout in the pore space will lead to the formation of a liquid phase and a consequent reduction in the gas production of the well. This phenomenon continues until a point of maximum liquid volume is reached (point C). Lowering the pressure furthermore will cause the revaporization process (point D) but this process is typically below the economic life of the field, and this stage will not be reached.

The amount of liquid phase present depends not only on the pressure and temperature but also on the composition of the reservoir fluid. The condensate gas can be classified into three types; poor, middle and rich content condensate gas. The classifications and the physical characteristics are listed in Table 3.1.

**Table 3.1:** Physical characteristics of condensate gas (after Yisheng et. al. [10]).

Fluid type	Heavier hydrocarbon content $C_{7+}$	Reservoir fluid density ( $g/cm^3$ )	Production GOR ( $m^3/m^3$ )	Condensate content ( $g/m^3$ )
Poor	0.5 – 2.0	0.20 – 0.25	18000 - 5000	<150
Middle	2.0 – 4.0	0.25 – 0.30	5000 - 2000	150 - 350
Rich	4.0 – 9.0	0.30 – 0.45	2000 - 1000	250 - 600
Near critical	9.0 – 12.5	0.45 – 0.50	1000 - 700	600 - 800

A rich gas-condensate forms a higher percentage of liquid than a lean gas-condensate. The phase diagrams of poor, middle and rich content condensate gas are shown in Figures 3.7, 3.8 and 3.9, respectively.

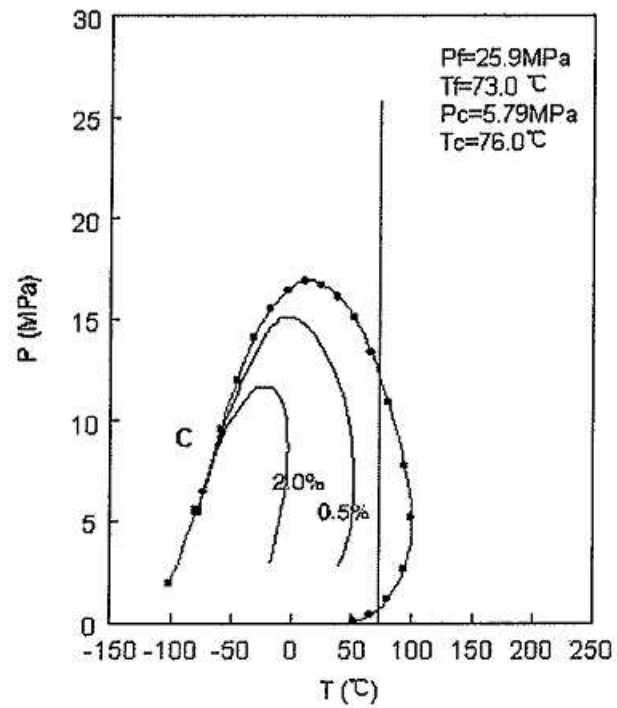


**Figure 3.7:** Pressure-Volume-Temperature diagram of poor condensate content (after Yisheng et. al. [10]).

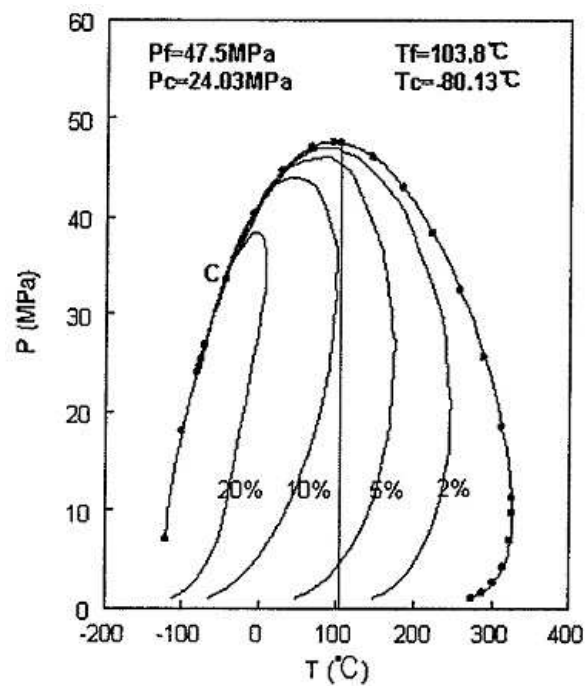


**Figure 3.8:** Pressure-Volume-Temperature diagram of middle condensate content (after Yisheng et. al. [10]).

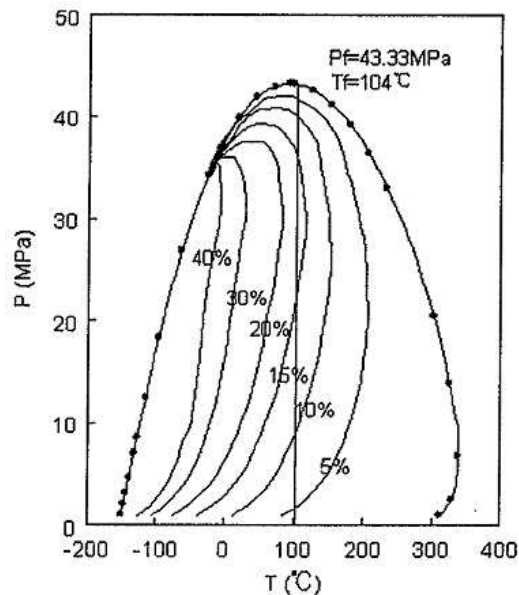


**Figure 3.9:** Pressure-Volume-Temperature diagram of rich condensate content (after Yisheng et. al. [10]).

### 3.8.1 Gas Condensate Flow Behavior

Fluid flow towards the well in a gas-condensate reservoir during depletion can be divided into three main flow regions. The two regions closest to the producing well exist when the pressure is below the dewpoint pressure and the third region exists when its pressure is above the dewpoint pressure as shown in Figures 3.10 and 3.11.

- Near-wellbore (Region 1): The condensate saturation of this region is greater than the critical condensate saturation. Both gas and condensate flow simultaneously at different velocities. The oil relative permeability increases with saturation while gas relative permeability decreases, illustrating the blockage effect.
- Condensate buildup (Region 2): Region where the condensate is dropping out of the gas. The condensate saturation of this region is less than the critical saturation. Only gas phase is flowing.
- Single phase gas (Region 3): This region is away from the producing well where only gas phase is present and flowing. Gas velocity in this region is

generally low because the cross sectional area is high. Composition in this region is equal to the original reservoir gas.

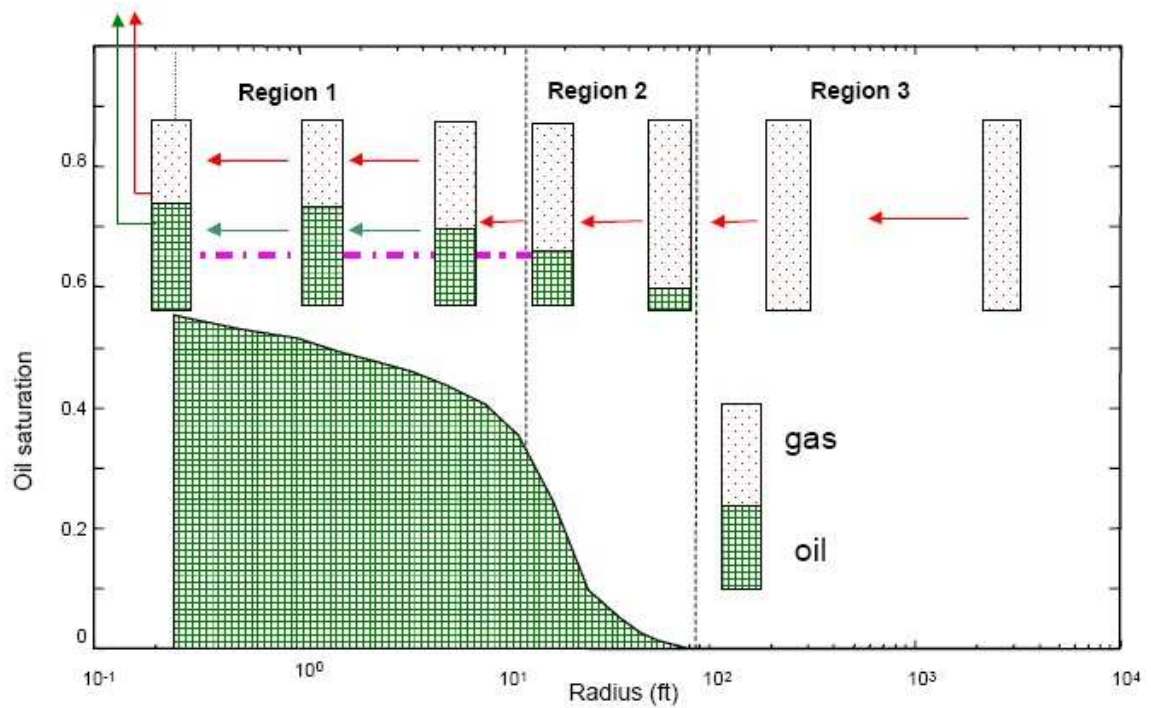


**Figure 3.10:** Three regions of gas-condensate fluid flow behavior (after Roussennac et. al. [13]).

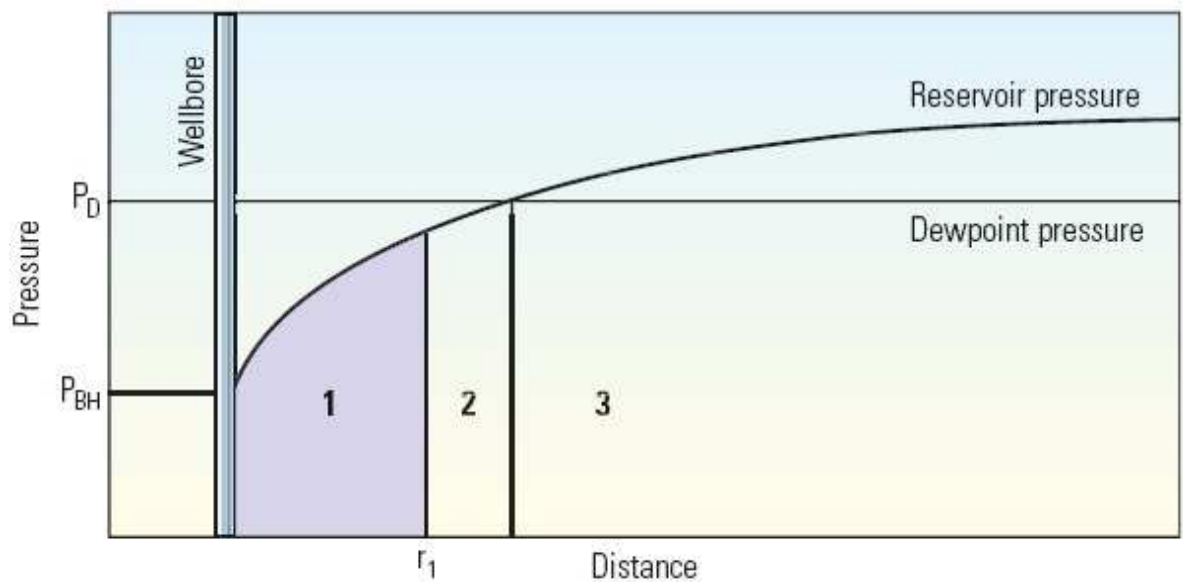


**Figure 3.11:** Three regions of gas-condensate pressure profile (after Fan et. al. [9]).

### 3.8.2 Fluid Composition Change

In gas-condensate system, the buildup of condensate is due to the pressure drop below the dewpoint pressure. The heavier components tend to drop out first and then become the condensate liquid. The phase diagram of the reservoir fluids is shifted clockwise to a system with higher critical temperature as shown in Figure 3.12.

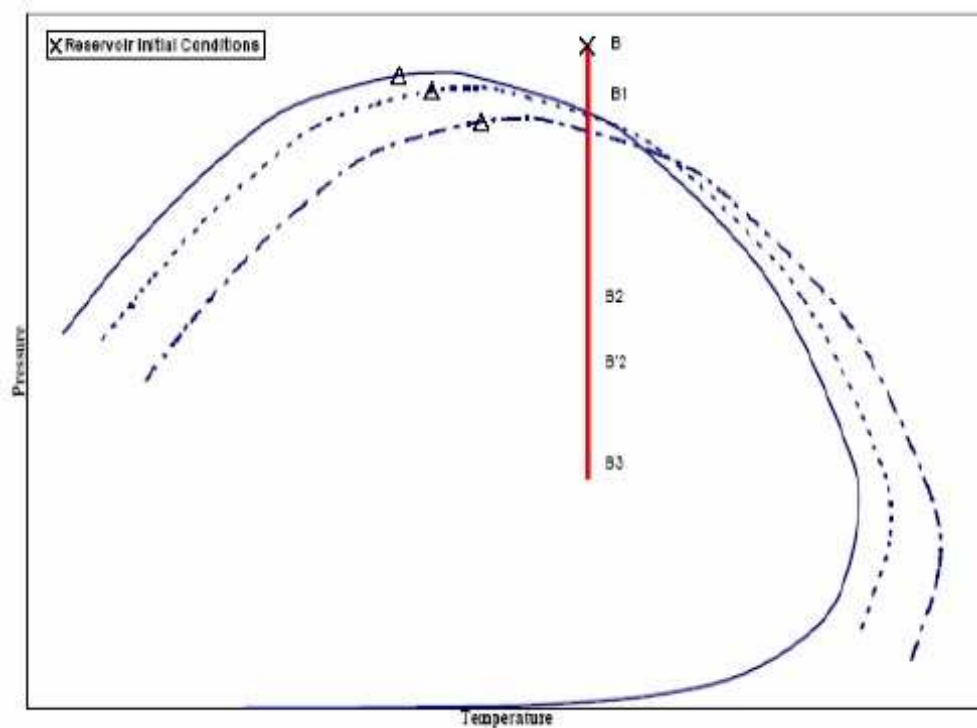


**Figure 3.12:** Shift of phase envelope with composition change (after Roussennac [13]).

## **CHAPTER IV**

### **RESERVOIR SIMULATION MODEL**

In order to determine optimal production for each perforation scenario in multilayered gas condensate and dry gas reservoirs, reservoir simulator was used as a tool to predict gas and condensate production under different strategies. As a result, the best strategy can be obtained.

The reservoir simulator ECLIPSE 300 specializing in compositional modeling was used in this study because it provides more accurate calculation of liquid dropout in porous media by using flash calculation. For the simulation method, the adaptive implicit (AIM) mode was selected. We can divide the reservoir simulation model in to four main sections as follows:

- 1. Grid section.** In this section, the geometry of the reservoir and its permeability and porosity were specified.
- 2. Fluid section.** The gas-condensate reservoir and source reservoir composition were specified in this section. The physical properties of each component and the EOS used in flash calculation were also specified. Initial reservoir condition was also included in this section.
- 3. SCAL section.** In special core analysis or SCAL section, oil relative permeability and gas relative permeability in gas at connate water as a function of gas saturation, oil relative permeability in water and water relative permeability as a function of water saturation were specified.
- 4. Wellbore section.** The wellbore model was constructed and used to calculate the vertical flow performance.

This chapter describes the selection of actual reservoir model for the study, their characteristics and resulting production profiles. Setting up of simplified model, assumptions used and matching results are also discussed. The detail of the simulation input is shown in Appendix A.

## 4.1 Grid Section

In this study, we generated two reservoirs which are dry gas reservoir and gas-condensate reservoir. Both reservoirs were constructed using Cartesian coordinate under plane geometry and homogeneous conditions. The dimension of each grid block is 80ft x 80ft x 20ft. The number of grid blocks of each reservoir is 25 x 25 x 5. The top of gas-condensate reservoir is located at a depth of 6,000 ft, and the top of dry gas reservoir is at 6,200 ft. The porosity of the reservoir was assumed to be 20.0%. The horizontal permeability was set at 500 mD, and the vertical permeability was 5 mD. The configuration of grids in reservoir model is shown in Figure 4.1-4.3.

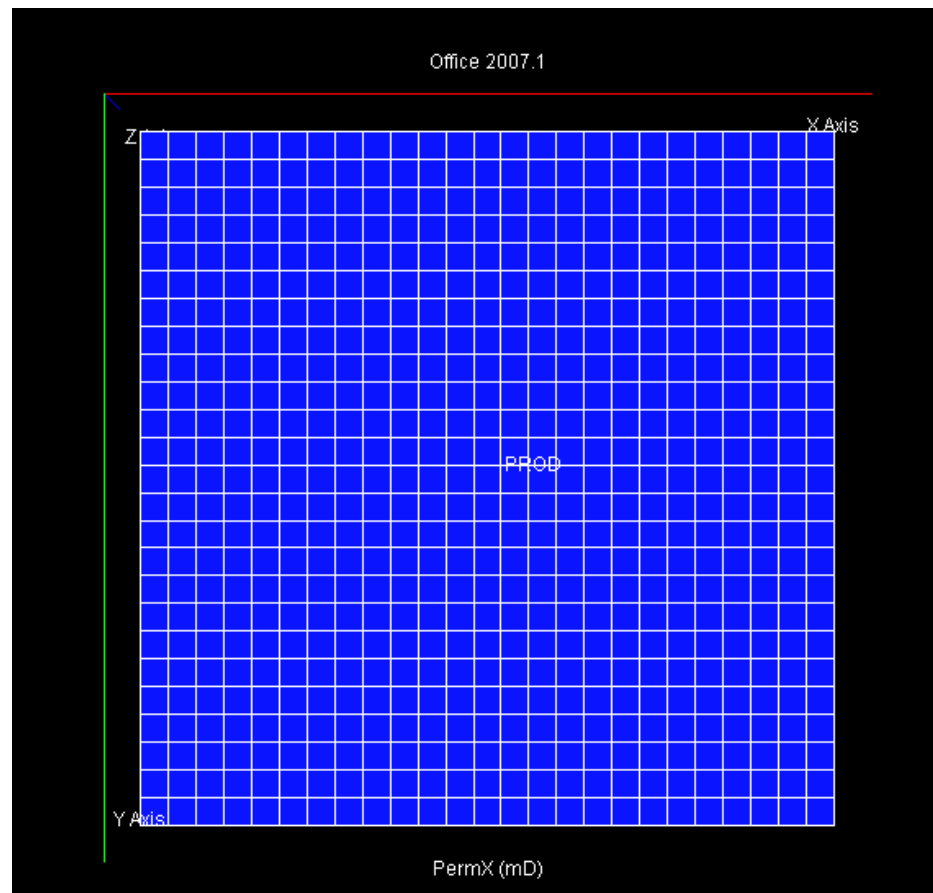


**Figure 4.1:** Top view of the reservoir model

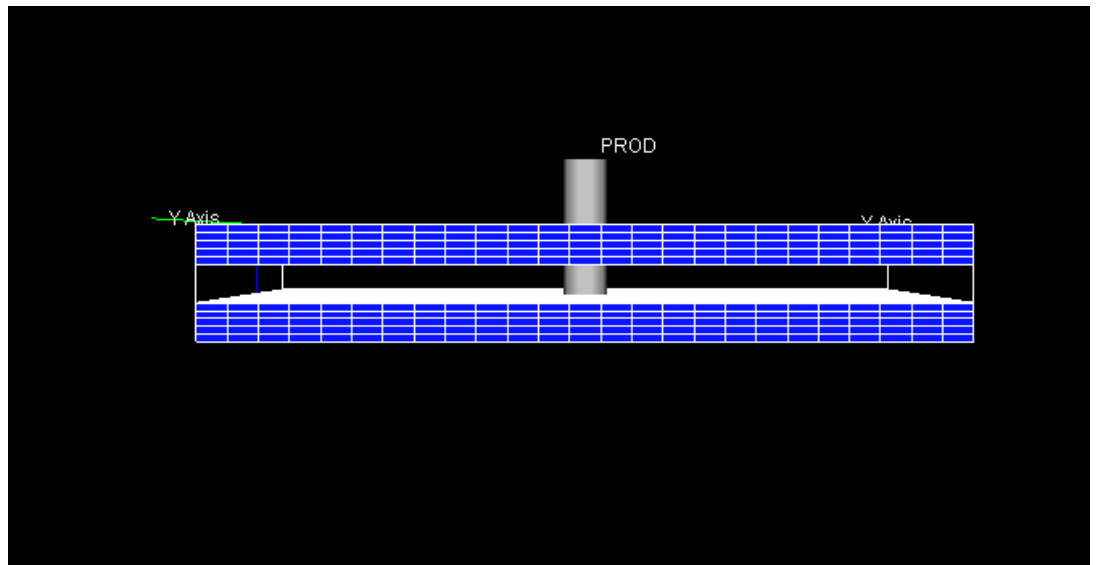


**Figure 4.2:** Side view of the reservoir model

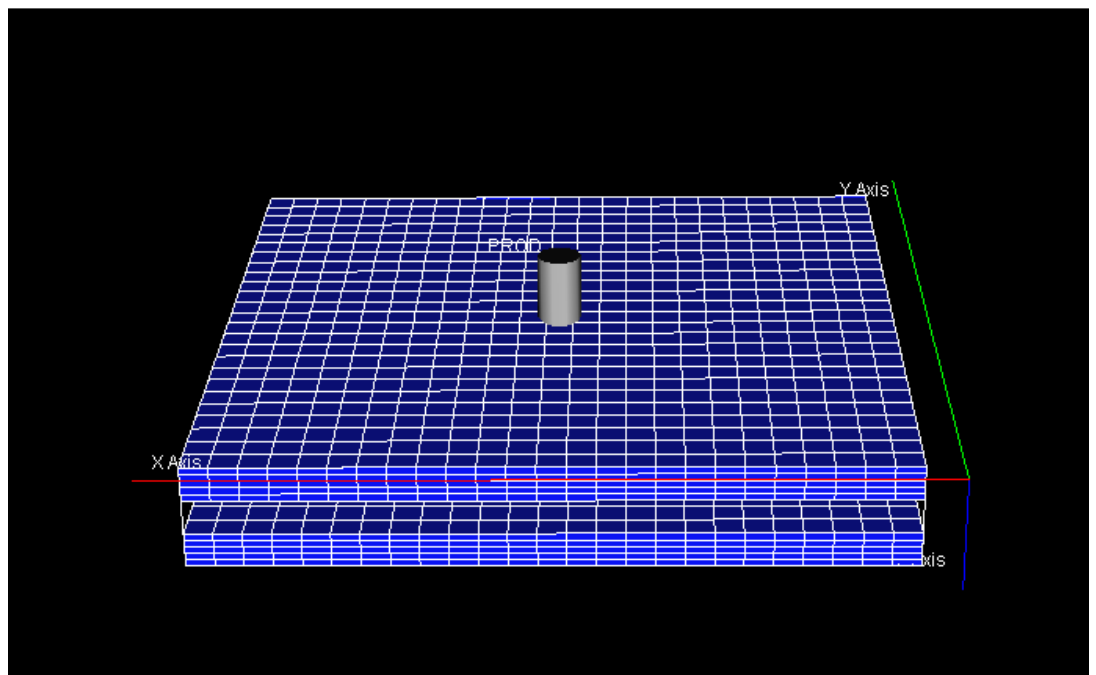


**Figure 4.3:** 3D view of the reservoir model



## 4.2 Fluid Section

The initial fluid conditions such as datum depth, pressure at datum depth, and water-oil contact depth was specified in Equilibration Data Specification (EQUIL) section which is used to generate consistent oil and gas compositions for each cell. The equation of state used in this study is Peng-Robinson. A typical composition of gas-condensate found in the Gulf of Thailand is used for the gas-condensate reservoir model. Table 4.2 illustrates the fluid composition in the gas-condensate reservoir.

**Table 4.2:** The initial composition of the reservoir fluid

Component	Mole fraction
Carbon dioxide	0.012302
Methane	0.599910
Ethane	0.084326
Propane	0.063988
Isobutane	0.034127
Normal butane	0.038989
Isopentane	0.014286
Normal pentane	0.013988
Hexane	0.072718
Hepthane plus	0.065366

The physical properties of each component and the binary interaction coefficients of this system are shown in Tables 4.3 and 4.4, respectively.

**Table 4.3:** Physical properties of each component

Component	Boiling points (°R)	Critical pressure (psia)	Critical temp. (°R)	Critical volume (ft <sup>3</sup> /lb-mole)	Molecular weight	Acentric factor
CO <sub>2</sub>	350.46	1071.3	548.46	1.5057	44.01	0.225
C <sub>1</sub>	200.88	667.78	343.08	1.5698	16.043	0.013
C <sub>2</sub>	332.28	708.34	549.77	2.3707	30.07	0.0986
C <sub>3</sub>	415.98	615.76	665.64	3.2037	44.097	0.1524
i-C <sub>4</sub>	470.34	529.05	734.58	4.2129	58.123	0.1848
n-C <sub>4</sub>	490.86	550.66	765.36	4.0847	58.123	0.201
i-C <sub>5</sub>	521.80	491.58	828.72	4.9337	72.15	0.227
n-C <sub>5</sub>	556.56	488.79	845.28	4.9817	72.15	0.251
C <sub>6</sub>	606.69	436.62	913.50	5.6225	86.177	0.299
C <sub>7+</sub>	734.08	403.29	1061.3	7.509	115	0.38056

**Table 4.4:** Binary interaction coefficient between components

	CO <sub>2</sub>	C <sub>1</sub>	C <sub>2</sub>	C <sub>3</sub>	i-C <sub>4</sub>	n-C <sub>4</sub>	i-C <sub>5</sub>	n-C <sub>5</sub>	C <sub>6</sub>	C <sub>7+</sub>
CO <sub>2</sub>	0.000	0.1000	0.100	0.100	0.100	0.100	0.100	0.100	0.1000	0.1000
C <sub>1</sub>	0.100	0.0000	0.000	0.000	0.000	0.000	0.000	0.000	0.0279	0.0378
C <sub>2</sub>	0.100	0.0000	0.000	0.000	0.000	0.000	0.000	0.000	0.0100	0.0100
C <sub>3</sub>	0.100	0.0000	0.000	0.000	0.000	0.000	0.000	0.000	0.0100	0.0100
i-C <sub>4</sub>	0.100	0.0000	0.000	0.000	0.000	0.000	0.000	0.000	0.0000	0.0000
n-C <sub>4</sub>	0.100	0.0000	0.000	0.000	0.000	0.000	0.000	0.000	0.0000	0.0000
i-C <sub>5</sub>	0.100	0.0000	0.000	0.000	0.000	0.000	0.000	0.000	0.0000	0.0000
n-C <sub>5</sub>	0.100	0.0000	0.000	0.000	0.000	0.000	0.000	0.000	0.0000	0.0000
C <sub>6</sub>	0.100	0.0279	0.010	0.010	0.000	0.000	0.000	0.000	0.0000	0.0000
C <sub>7+</sub>	0.100	0.0378	0.010	0.010	0.000	0.000	0.000	0.000	0.0000	0.0000

In this study, the reservoir temperature was assumed to be constant at 254 °F and the initial reservoir pressure of gas-condensate and dry gas reservoir was 2,600 and 2,685 psi respectively. With this reservoir pressure, reservoir temperature and fluid composition, the phase behavior of gas-condensate reservoir system is displayed in Figure 4.4.

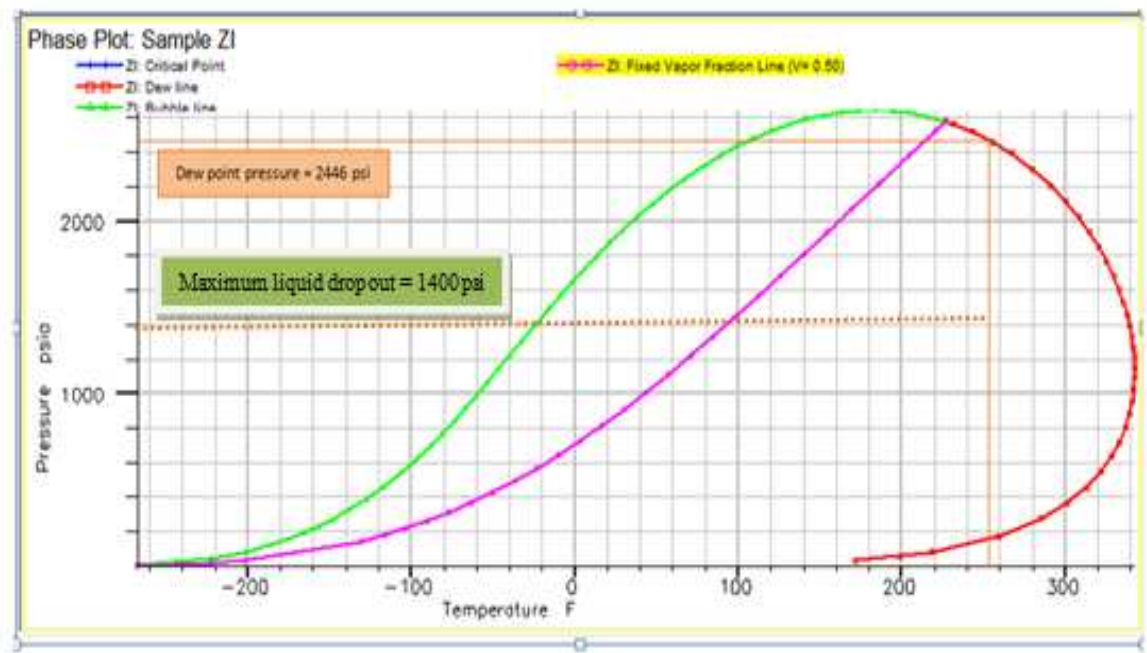


**Figure 4.4:** Phase behavior of the gas-condensate reservoir fluid system

This phase behavior was calculated by PVTi program in ECLIPSE simulator. The dew point pressure is 2,446 psi and the maximum liquid dropout of 12% occurs when the reservoir pressure drops to 1,400 psi.

### 4.3 SCAL (Special Core Analysis) Section

Two tables of relative permeabilities ( $k_r$ ) and capillary pressures ( $p_c$ ) as functions of saturation in ECLIPSE allow us to enter gas/oil relative permeabilities and gas/water relative permeabilities into the software as depicted in Tables 4.4 and 4.5, respectively. These functions are shown in Figures 4.5 and 4.6.

$k_{rg}$	is relative permeability to gas
$k_{ro}$	is relative permeability to oil
$k_{rw}$	is relative permeability to water
$S_w$	is saturation of water
$S_g$	is saturation of gas
$p_c$	is capillary pressure

**Table 4.5:** Gas and oil relative permeabilities

$S_g$	$k_{rg}$	$k_{ro}$
0	0	0.897
0.03515	7.63E-05	0.705923
0.0703	0.00061	0.544104
0.10545	0.002059	0.409125
0.1406	0.00488	0.298553
0.17575	0.009531	0.209941
0.2109	0.01647	0.140865
0.24605	0.026154	0.0889
0.2812	0.03904	0.051603
0.31635	0.055586	0.026534
0.3515	0.07625	0.011275
0.38665	0.101489	0.003398
0.4218	0.13176	0.000433
0.45695	0.167521	0
0.4921	0.20923	0
0.52725	0.257344	0
0.5624	0.31232	0
0.59755	0.374616	0
0.6327	0.44469	0
0.66785	0.522999	0
0.703	0.61	0

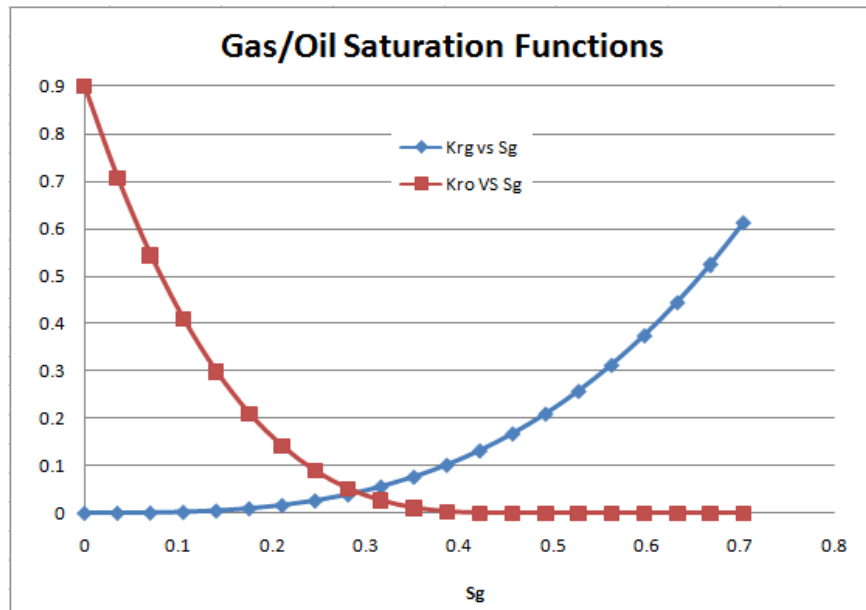


**Figure 4.5:** Gas and oil relative permeabilities.

**Table 4.6:** Oil and water relative permeabilities

$S_w$	$k_{rw}$	$k_{ro}$
0.297	0	0.897
0.319026	1.76E-05	0.769065
0.341051	0.000141	0.653913
0.363077	0.000476	0.55087
0.385102	0.001128	0.459264
0.407128	0.002203	0.378422
0.429154	0.003807	0.307671
0.451179	0.006045	0.246339
0.473205	0.009024	0.193752
0.49523	0.012849	0.149238
0.517256	0.017625	0.112125
0.539282	0.023459	0.081739
0.561307	0.030456	0.057408
0.583333	0.038722	0.038459
0.605358	0.048363	0.024219
0.627384	0.059484	0.014016
0.649410	0.072192	0.007176
0.671435	0.086592	0.003027
0.693461	0.102789	0.000897
0.715486	0.12089	0.000112
0.737512	0.141	0
1	1	0

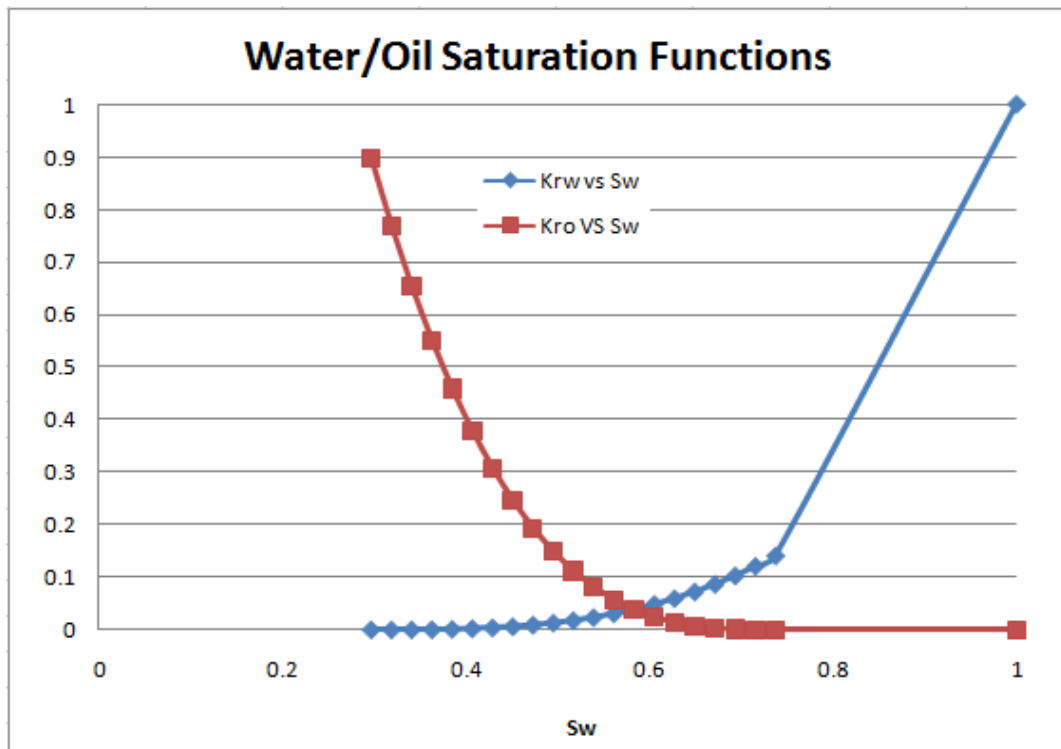


**Figure 4.6:** Oil and water relative permeabilities.

#### 4.4 Wellbore Section

In order to simulate the dynamic performance, the well model has been created using Prosper Software. The model is built based on monobore well design which is widely applied in the Gulf of Thailand. The well has a wellbore diameter of 6-1/8 inches with 3-1/2 inches production casing (inside diameter of 2.992 inches). The well is perforated from 6,000 ft to 6,280 ft, depending on the reservoir depth in each case. The schematic of wellbore and configuration is shown in Figure 4.7.

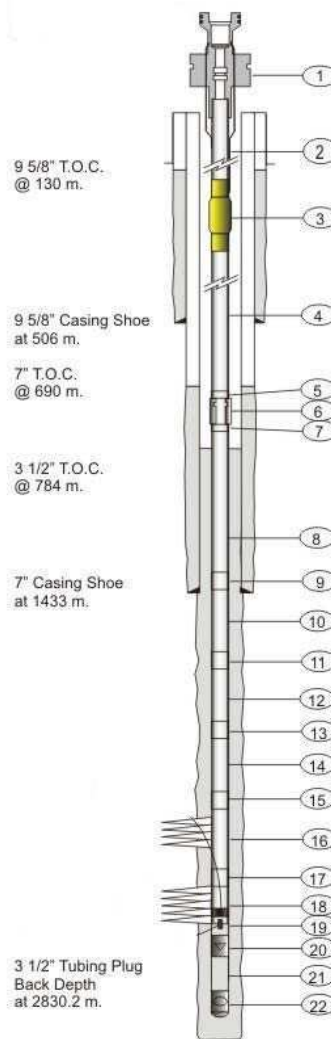


**Figure 4.7:** Monobore well schematics

## 4.5 Vertical Flow Performance

In this study, multiple sets of vertical flow performance (VFP) curves were generated by production and system performance analysis software (PROSPER) for the variety of composition in the source to target reservoirs. The chosen vertical flow correlation is Fancher Brown. The bottomhole flowing pressure is calculated based on the tubing head pressure, gas rate, and gas oil ratio of the producing well and source well for their respective section. The details of vertical flow performance curves used in this study are shown in Appendix B.

## CHAPTER V

### SIMULATION RESULTS AND DISCUSSIONS

This chapter present results and discussion of different perforation strategies for multi-layered gas and gas condensate reservoirs. To evaluate the effect of layer thickness, layer permeability, three sets of reservoir simulation were conducted and analyzed.

A target tubing head pressure of 100 psia with vertical flow performance is used for the production well. In dry gas and gas condensate reservoirs, there is no limitation on cross flow between the layers. The fluid is allowed to flow naturally from one to another once the zones are perforated. The economic limits are defined by assuming a typical daily operating cost at minimum gas rate of 500 MSCF/d. The top depth of the upper reservoir is 6,000 feet whereas the bottom layer is separated by 100 feet shale (inactive cells). The initial reservoir pressures are assumed to follow hydrostatic gradient.

The perforation/production scenarios under this study can be categorized into 7 scenarios. The first one is concurrent perforation. The rest are time lapse perforation. Time lapse perforation strategy allows a reservoir to be produced first, then with certain condition previously set, another reservoir will be perforated later. These scenarios are listed and described in Table 5.1.



**Table 5.1:** Perforation strategy

Scenario	Description	Explanation
1	Concurrent perforation	Perforate and produce all reservoirs until they are depleted.
2	Standalone perforation	Perforate the top zone first and produce until gas production reaches economic rate then shut off the top zone and perforate the bottom zone.
3	Commingle after top zone depletes	Perforate the top zone first and produce until gas production reaches economic limit then perforate the bottom zone.
4	Commingle after top zone rate half declines	Perforate the top zone first and produce until gas production decreases to half of the initial rate then perforate the bottom zone.
5	Commingle after top zone rate starts to decline	Perforate the top zone first and produce until gas production rate just drops below the initial rate then perforate the bottom zone.
6	Commingle after bottom zone rate half declines	Perforate the bottom zone first and produce until gas production decreases to half of initial production rate then perforate the top zone
7	Commingle after bottom zone rate starts to decline	Perforate the bottom zone first and produce until gas production rate just drops below the initial rate then perforate the top zone.

## 5.1 Base Case

The production well is placed at coordinate (13, 13) in the global grid representing the producer as shown in Figure 5.1. The maximum gas production rate which is set at 10,000 MSCF/D is used as the control variable. The gas production rate is kept constant as long as the reservoir pressure can sustain such rate with a tubing head pressure limit of 100 psia and vertical flow performance VFP NO.1 (see Appendix B).

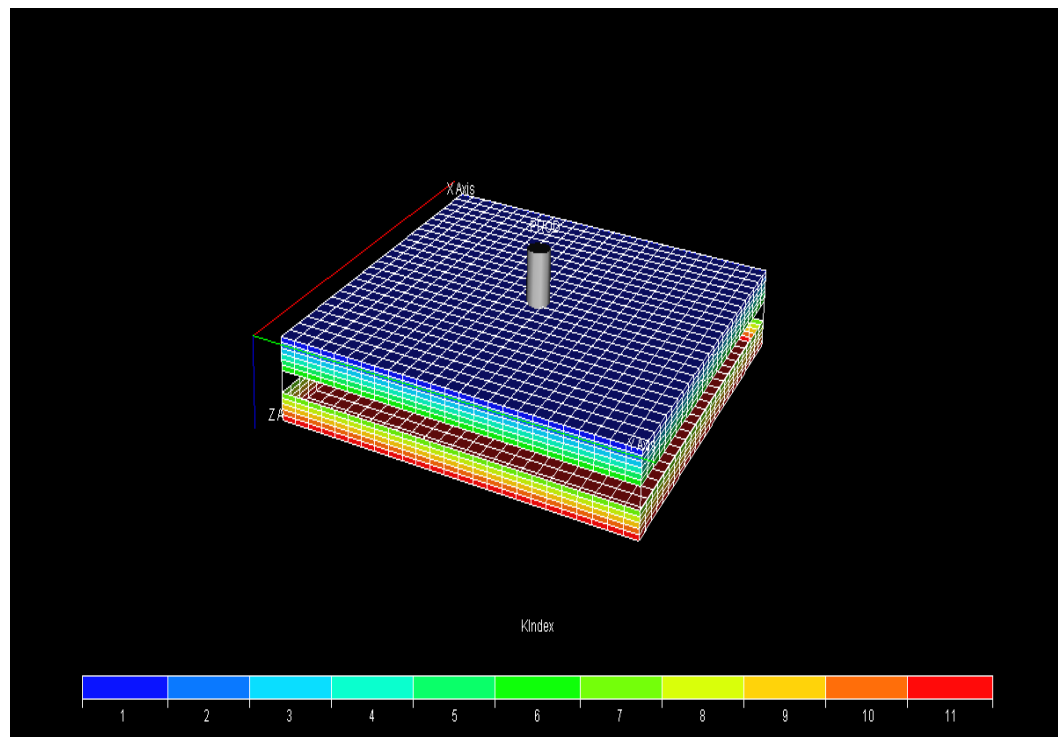


**Figure 5.1:** Grids representing well location in reservoir model

### Scenario 1:

In this case, both reservoirs are perforated at the same time and produced until the economic limit. Gas production rate and condensate production rate from the simulation is shown in Figures 5.2 and 5.3, respectively. At early times, gas production rate is constant while the bottom hole pressure declines (see Figure 5.4). After the bottom hole pressure drops below the dew point pressure of 2,446 psi, the condensate production rate declines since liquid starts to condense in the pore space. Once the liquid drops out in the reservoir, it is more difficult to move it out of the reservoir in comparison to moving the gas out.

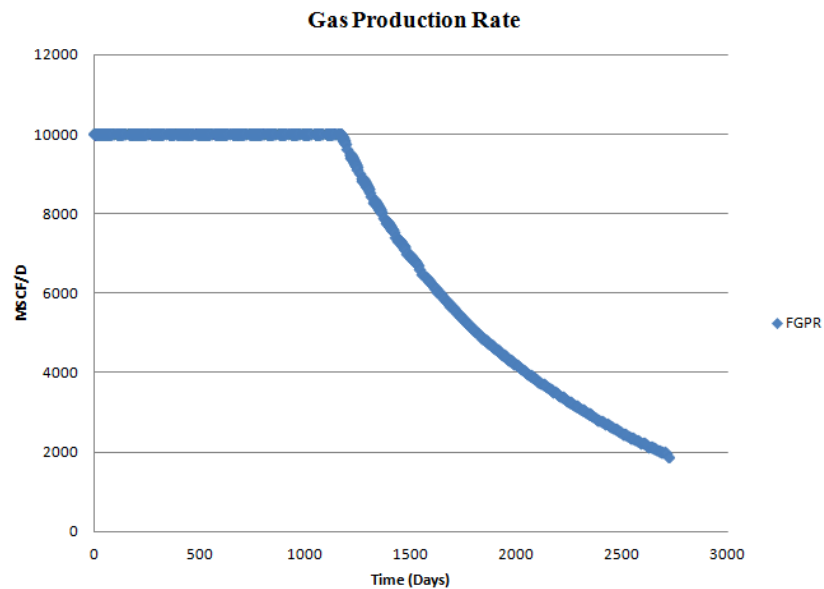


**Figure 5.2:** Gas production rate for Scenario 1.

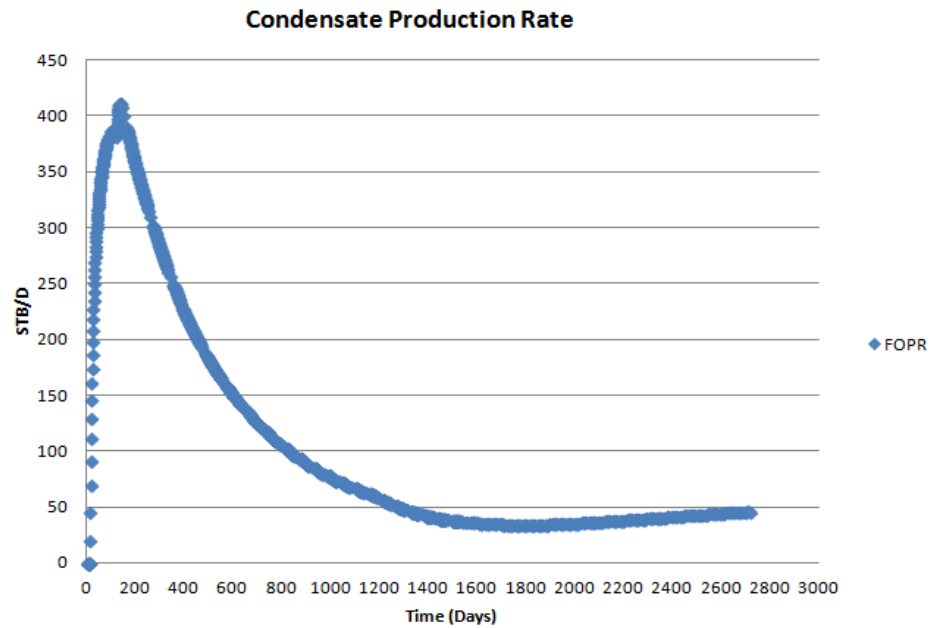


**Figure 5.3:** Condensate production rate for Scenario 1.

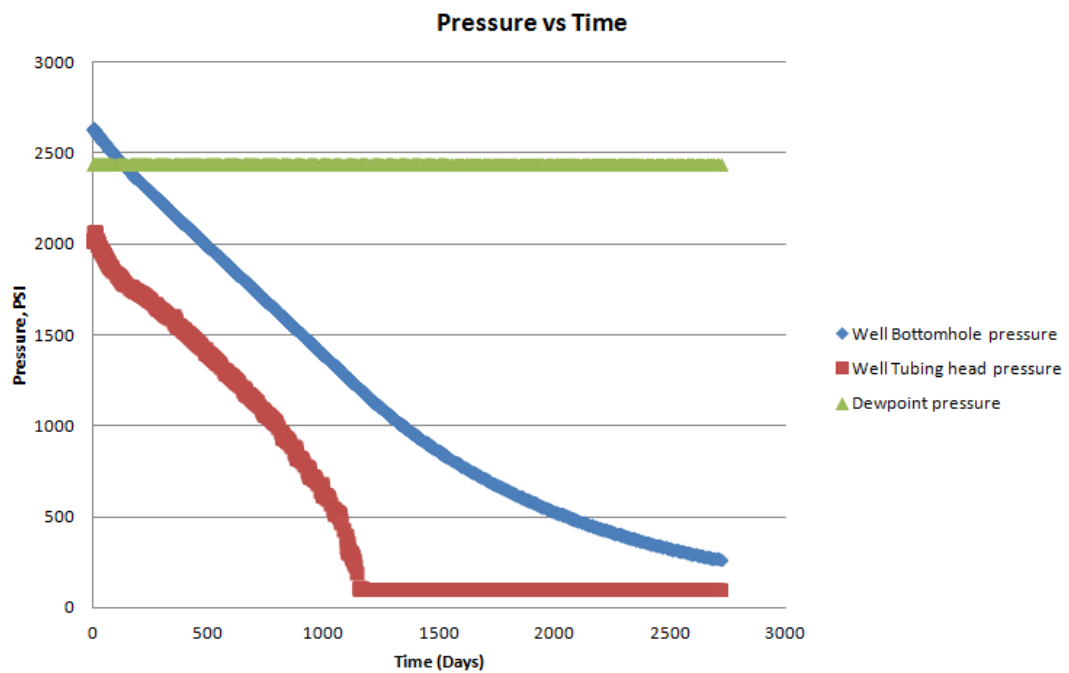


**Figure 5.4:** Pressure vs time for Scenario 1.

The condensate saturation around the wellbore increases as the pressure becomes lower. At early times of condensate accumulation, condensate cannot flow in the reservoir. This condensate accumulation around the wellbore are called

condensate blockage which causes the problem of gas flow performance. When the condensate saturation reaches the maximum, condensate starts to flow. The condensate saturation decreases at late time period because condensate revaporizes as the pressure drops to low values. Figure 5.5 is used to explain in details that when the pressure drops with constant reservoir temperature (254 °F), liquid is transformed to vapor. Since there is now a higher amount of gas in the reservoir and gas is less viscous than condensate, a higher volume of gas flows out of the reservoir, contributing to higher flow rates of gas and condensate (since revaporized gas will condense into condensate again at standard conditions). Finally, simulation run stops because of the liquid load up in the wellbore prevents the gas and condensate to flow.

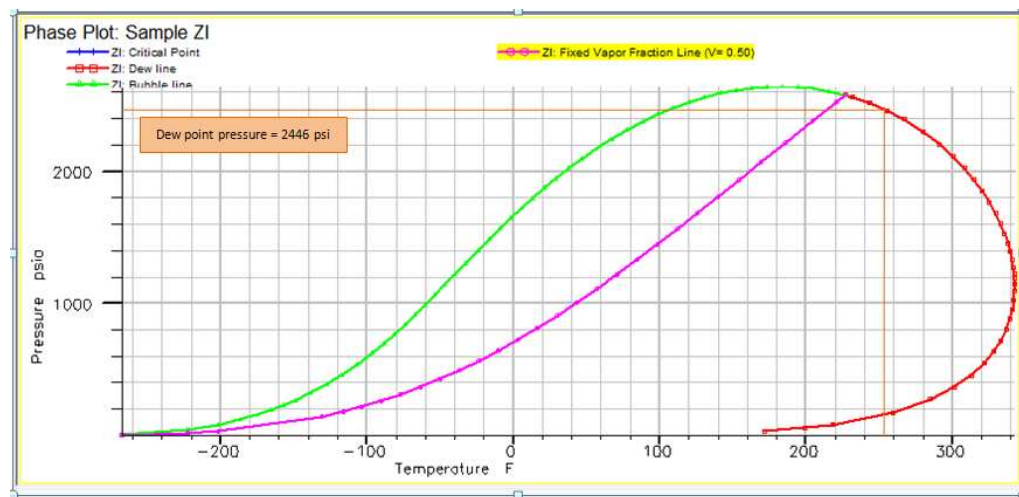


**Figure 5.5:** Phase behavior of the gas-condensate reservoir fluid system.

At the end of the production, the cumulative gas production is 19.22 Bscf, and cumulative condensate production is 278.02 MSTB. This means that only 20% of condensate and 91% of hydrocarbon gas is recovered. We can see that commingle production does not effectively recover condensate and gas from the reservoir.

### Scenario 2:

In this scenario, the top reservoir is set to produce until fully depleted and then shut off. After that, the bottom reservoir is opened in sequence. Therefore, in this scenario there is no cross flow. The gas and condensate production rate is shown in

Figures 5.6 and 5.7. At early times, gas production rate is constant while the bottom hole pressure declines (see Figure 5.8).

At the beginning, the maximum gas production rate is specified at 10 MMscf/d, the gas production rate maintains to produce at 10 MMscf/d until 639 days. Then, it declines dramatically to the gas production of 1004 Mscf/d and stops. The gas rate does not reach the economic limit of 500 Mscf/d because there is not enough bottomhole pressure to lift the fluid to the surface. At this point, the final bottomhole pressure is 259 psia as shown in Figure 5.8. Then, the top reservoir is shut, and the bottom reservoir is perforated. The bottom reservoir produces for another 518 days. After that, it starts to decline significantly. At 2764 days, the well dies even when the gas flow rate is higher than 2 MMscf/d due to the fact that production of water as a result of connate water expansion in the reservoir results in an increase in hydrostatic pressure. As shown in the vertical lift performance curve in Figure 5.9, the required bottomhole pressure at gas rate of 2.4 MMscf/d is more than 400 psia which is higher than the final bottomhole pressure shown in Figure 5.8. Thus, the well stops producing at this point. The cumulative production for gas and condensate are 18.96 Bcf and 453.55 MSTB, respectively.

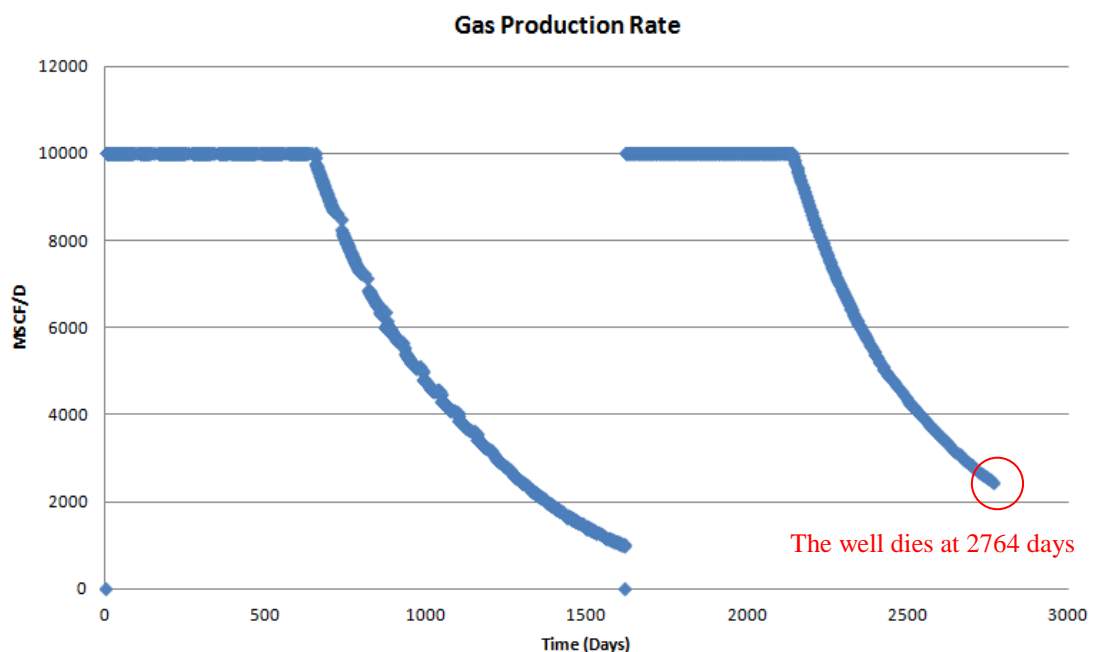


**Figure 5.6:** Gas production rate for Scenario 2

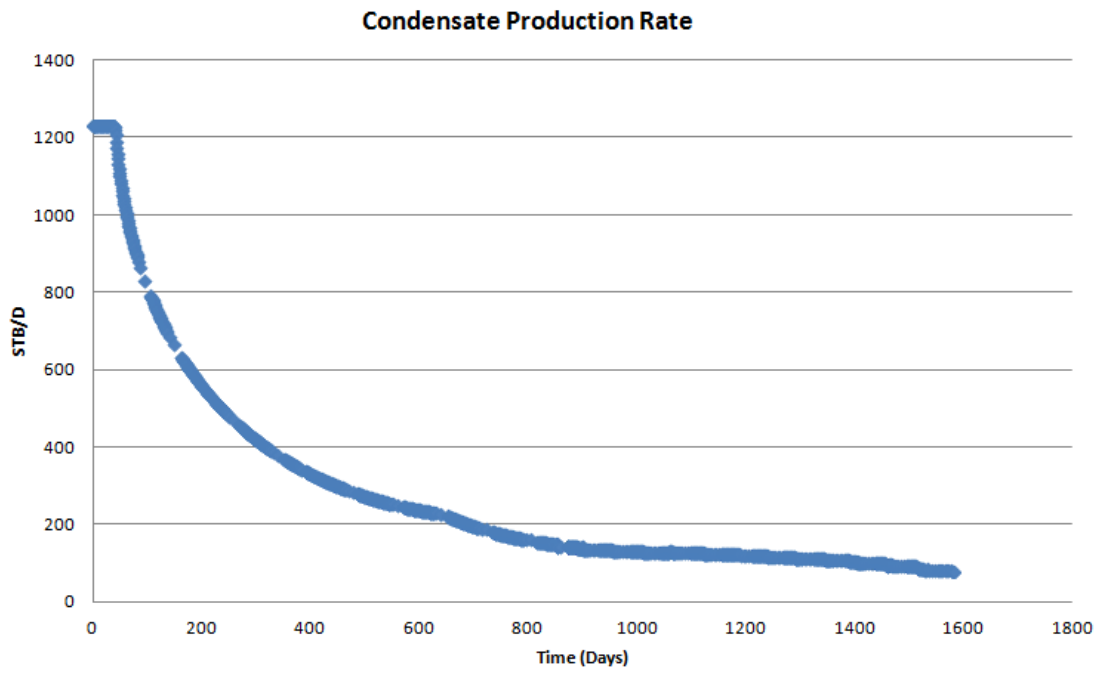


**Figure 5.7:** Condensate production rate for Scenario 2

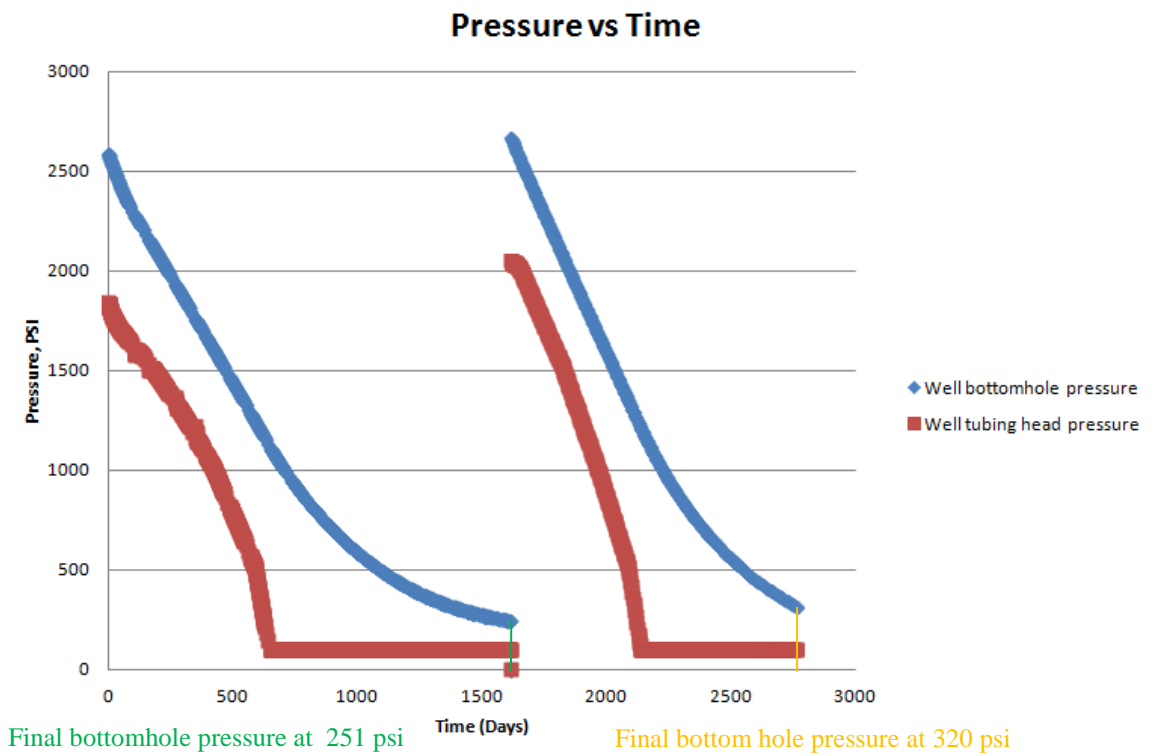


**Figure 5.8:** Pressure vs time for Scenario 2

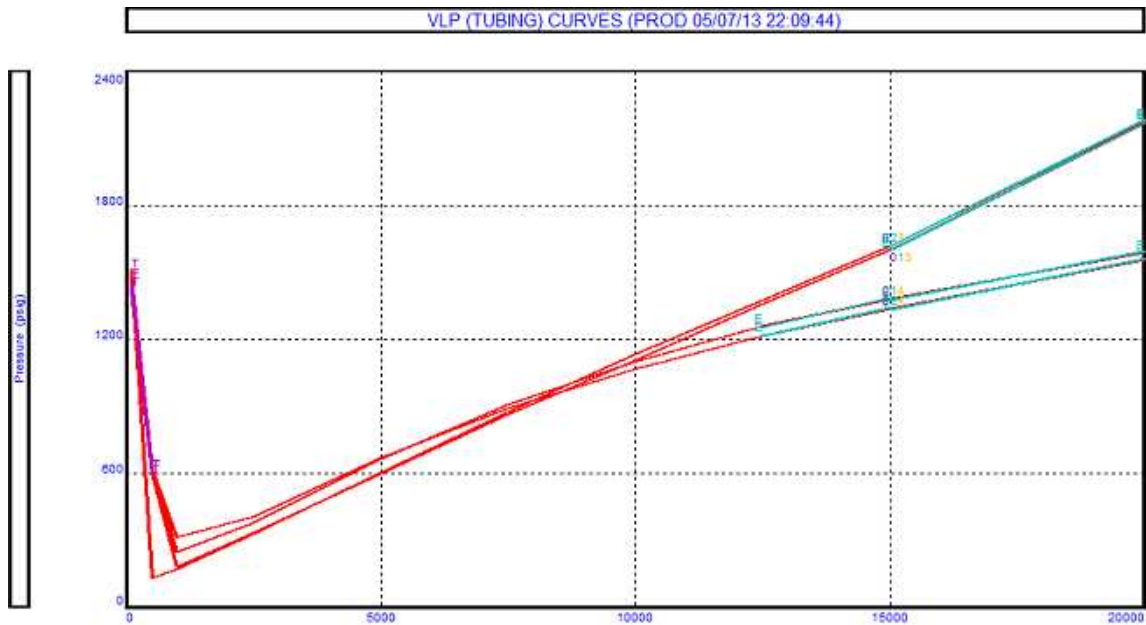


**Figure 5.9:** VLP of the gas-condensate reservoir fluid system.

### Scenario 3:

In this scenario, the top most reservoir is set to produce until the gas rate reaches the economic limit. Then, the bottom layer is perforated while the top layer is still open. The gas and condensate production rate is shown in Figures 5.10 and 5.11, respectively.

The gas production rate can be maintained at 10 MMscf/d until 639 days. Then, it declines dramatically to the gas production of 1009 Mscf/d and stops. The gas rate does not reach the economic limit of 500 Mscf/d because the bottomhole pressure as shown in Figure 5.12 is not sufficient to lift the fluid to the surface. Up until this time, the production and pressure profiles are the same as those in Scenario 2. Then, the bottom reservoir is perforated. The bottom reservoir produces for another 517 days. After that, the gas rate starts to decline significantly. At 2413 days, the well dies at bottom pressure of 688 psi which is not sufficient to lift the fluids to the surface. The cumulative production for gas and condensate are 17.7 Bcf and 453.35 MSTB, respectively.



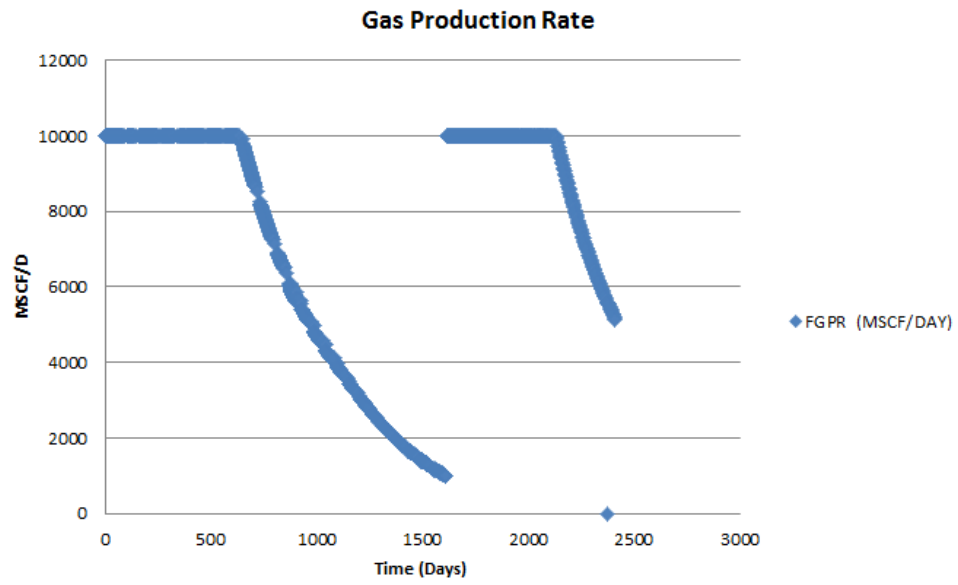


**Figure 5.10:** Gas production rate for Scenario 3

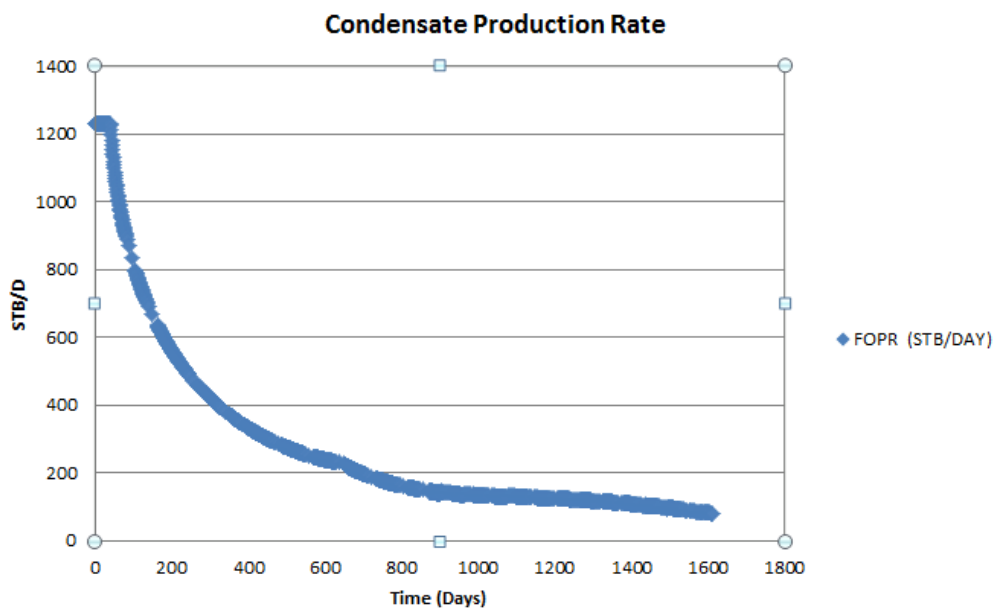


**Figure 5.11:** Condensate production rate for Scenario 3

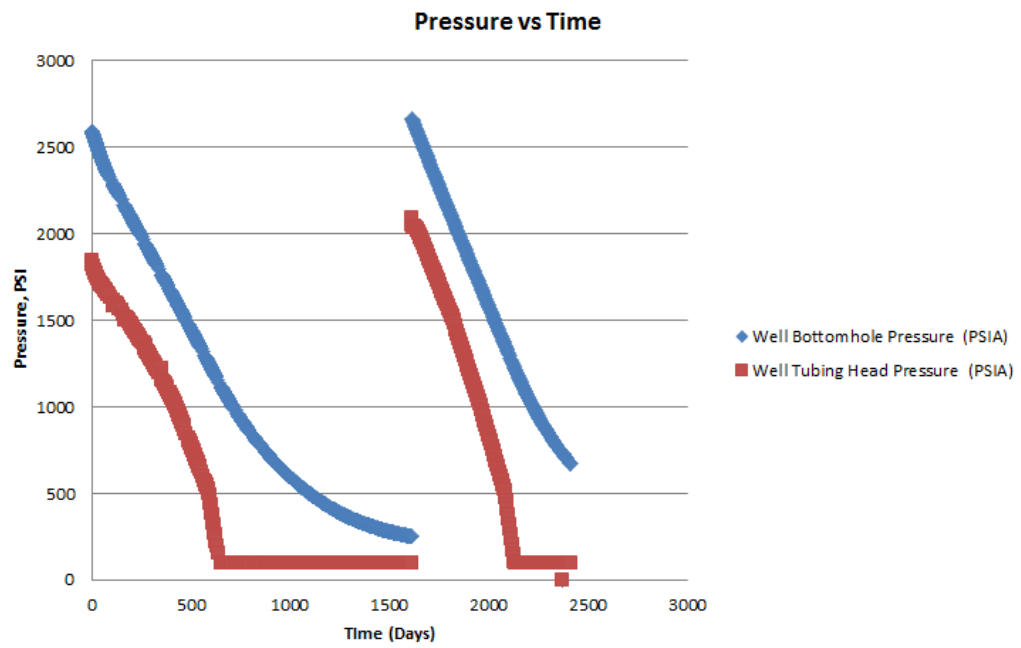


**Figure 5.12:** Pressure vs time for Scenario 3

**Scenario 4:**

In this scenario, the top most reservoir is set to produce until the gas rate reaches half of the initial gas production rate at 5000 Mscf/d. Then, the bottom layer is perforated while the top layer is still left open. The gas and condensate production rate is shown in Figures 5.13 and 5.14, respectively.

The gas production rate can be maintained at 10 MMscf/d until 639 days. Then, it declines dramatically to the gas production of 5,500 Mscf/d. Then, bottom reservoir is perforated before the rate falls below 5,000 Mscf/d in the next time step while the top reservoir is still opened. Up until this point, the production and pressure profiles are the same as those in Scenarios 2 and 3. Then, the bottom reservoir helps increase the gas production back to the plateau rate of 10 MMscf/d for another 341 days. After that, the gas rate starts to decline again. When the bottom reservoir starts to flow, condensate production stops for a while because gas from the lower reservoir flows into the upper reservoir as the lower reservoir has higher pressure than the upper reservoir. This crossflow stops at a later time as the pressures of the two reservoirs equalize. After that, condensate from the upper reservoir starts flowing again. However, the condensate production rate drops due to a change in composition of the fluids in the upper reservoir as dry gas from the lower reservoir mixes with gas condensate in the upper reservoir.

At 3105 days, gas production rate is still 1353 Mscf/d but stops flowing. It does not reach the gas production rate economic limit because the bottom pressure as shown in Figure 5.15 is not high enough to lift fluids consisting gas, condensate and some connate water production. The bottomhole pressure required for vertical lift performance is similar to the ones shown in Figure 5.9. The cumulative production for gas and condensate are 19.81 Bcf and 455.38 MSTB, respectively.

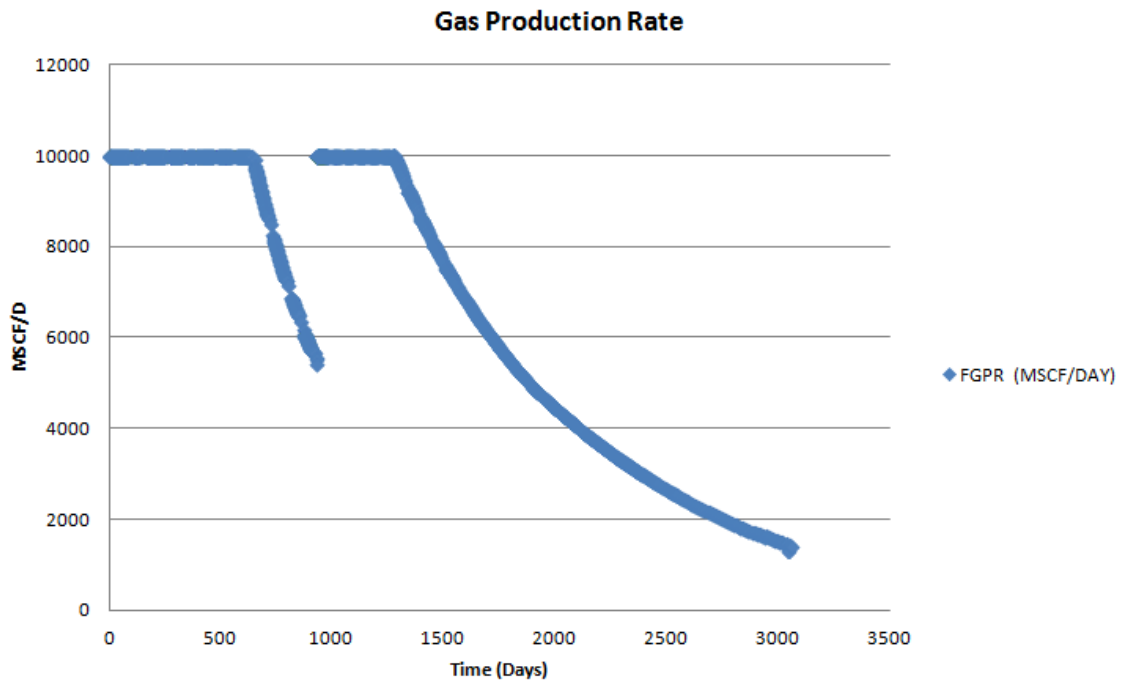


**Figure 5.13:** Gas production rate for Scenario 4

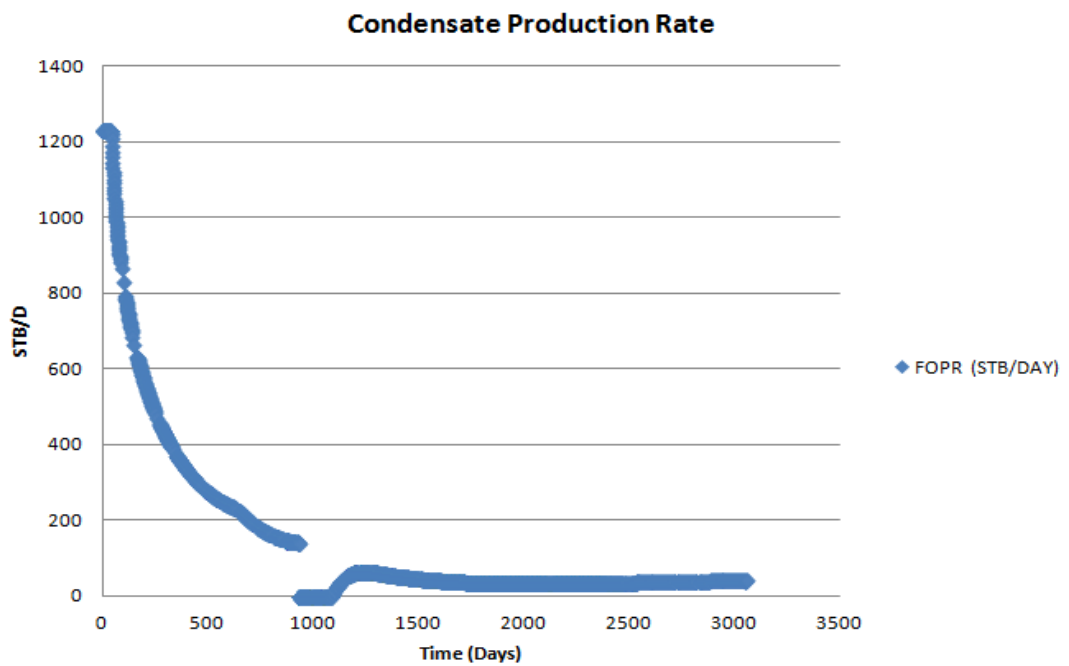


**Figure 5.14:** Condensate production rate for Scenario 4

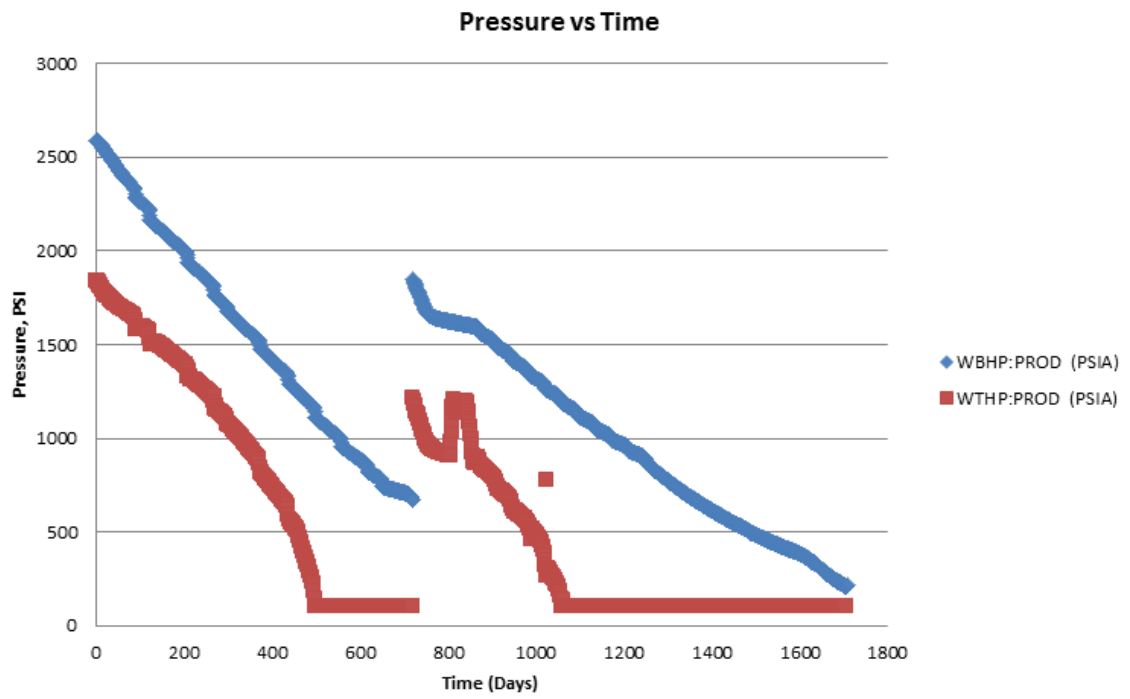


**Figure 5.15:** Pressure vs time for Scenario 4

**Scenario 5:**

In this scenario, the top reservoir is perforated first and set to produce until the gas rate starts to drop below the production plateau of 10 MMscf/d. Then, the bottom layer is perforated while the top layer is still open. The gas and condensate production rate is shown in Figures 5.16 and 5.17, respectively.

The gas production rate can be maintained at 10 MMscf/d until 639 days in the same manner as in Scenarios 2, 3, and 4. Then, it declines to the gas production of 9,789 Mscf/d. At this point, bottom reservoir is perforated while the top reservoir is still opened. The bottom reservoir produces at the plateau rate of 10 MMscf/d for another 528 days. After that, it starts to decline significantly. Similar to Scenario 4, when the bottom reservoir starts to flow, condensate production stops for a while because gas from the lower reservoir flows into the upper reservoir as the lower reservoir has higher pressure than the upper reservoir. This crossflow stops at a later time as the pressures of the two reservoirs equalize. After that, condensate from the upper reservoir starts flowing again. However, the condensate production rate drops due to a change in composition of the fluids in the upper reservoir as dry gas from the lower reservoir mixes with gas condensate in the upper reservoir.

At 3163 days, the well stops flowing and does not reach the economic limit of 500 Mscf/d because the bottom pressure is equal to as shown in Figure 5.18 is not sufficient to lift the fluids to the surface. At this point, gas production rate is 1038 Mscf/d while condensate production rate is 40.08 STB/d. The bottomhole pressure required for vertical lift performance is similar to the ones shown in Figure 5.9. The cumulative production for gas and condensate are 19.95 Bcf and 431.92 MSTB, respectively.

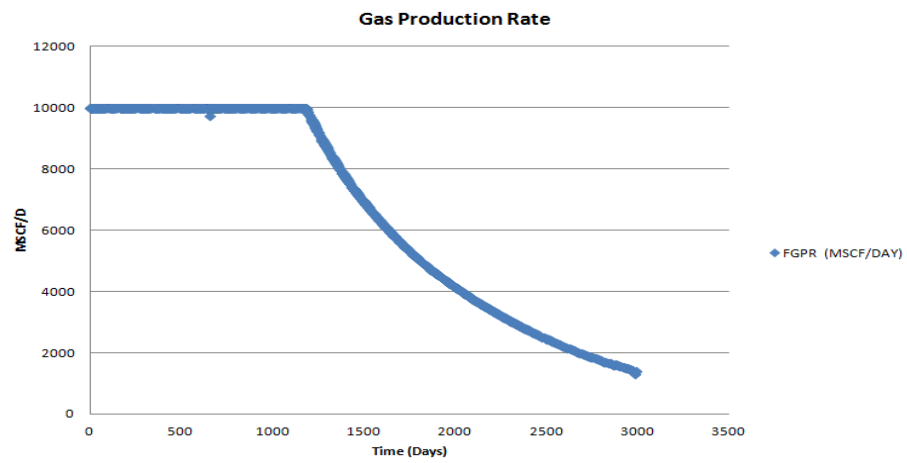


**Figure 5.16:** Gas production rate for Scenario 5

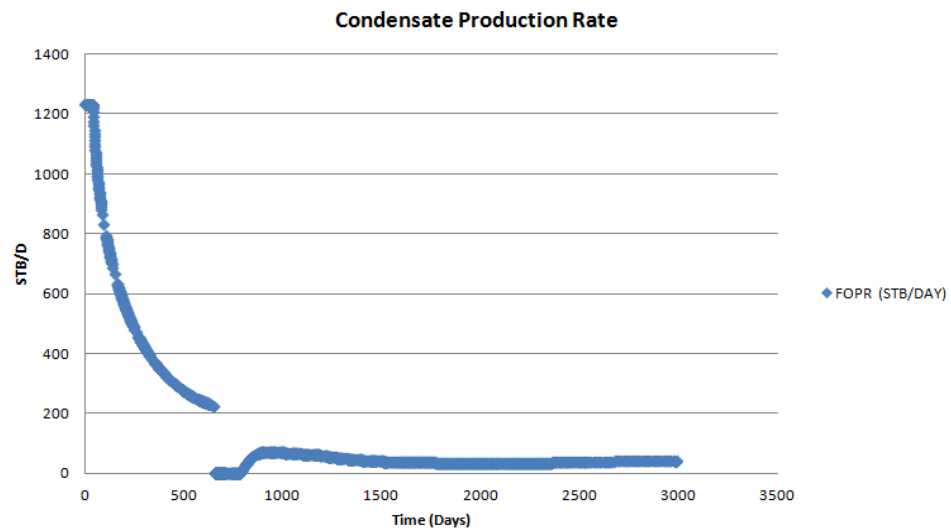


**Figure 5.17:** Condensate production rate for Scenario 5

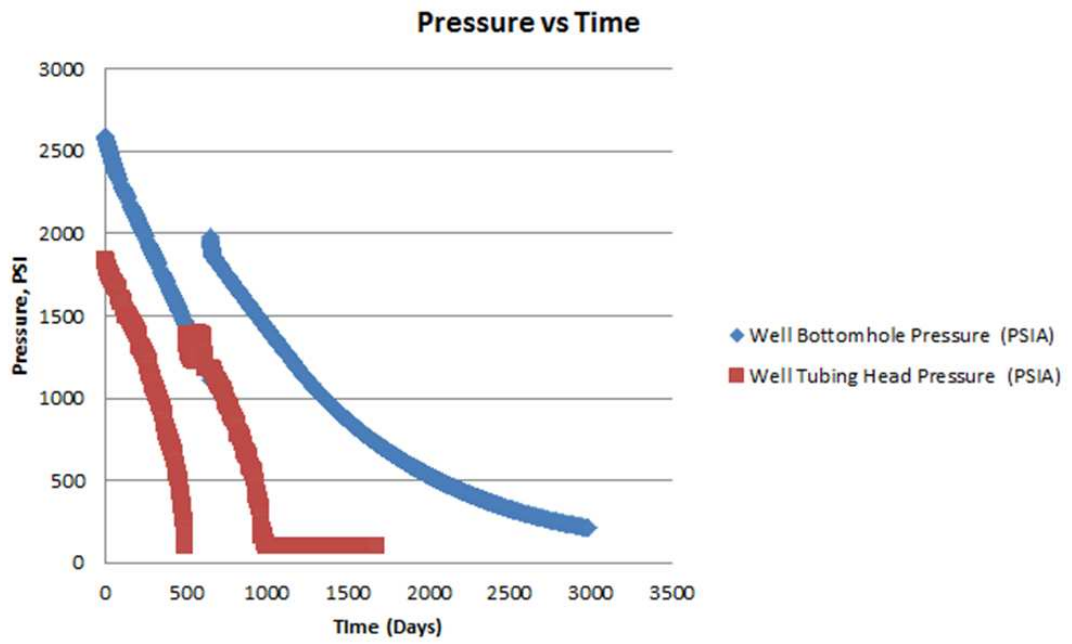


**Figure 5.18:** Pressure vs time for Scenario 5



**Scenario 6:**

In this scenario, the bottom reservoir is perforated first and is set to produce until the gas rate reaches half of the initial gas production rate at 5000 Mscf/d. Then, the top layer is perforated while the bottom layer is still opened. The gas and condensate production rate is shown in Figures 5.19 and 5.20.

The gas production rate maintains to produce at 10 MMscf/d until 520 days. Then, it declines dramatically to the gas production of 5,284 Mscf/d. Then, top reservoir is perforated while the bottom reservoir is still opened. The top reservoir produces for another 462 days. After that, gas rate starts to decline tremendously. As shown in Figure 5.21, condensate production is initially high and then drops rapidly. At 2720 days while gas production rate is 1646 Mscf/d and condensate production rate is 56.36 STB/d, the well stops flowing because the bottomhole pressure is not enough to lift the fluids to the surface. The bottomhole pressure required for vertical lift performance is similar to the ones shown in Figure 5.9. The cumulative production for gas and condensate is 19.05 Bcf and 366.8 MSTB, respectively. The cumulative condensate production is less than those in Scenarios 2 to 5 because the bottom reservoir is perforated first; thus, there is not enough gas to lift the condensate to surface at late times.

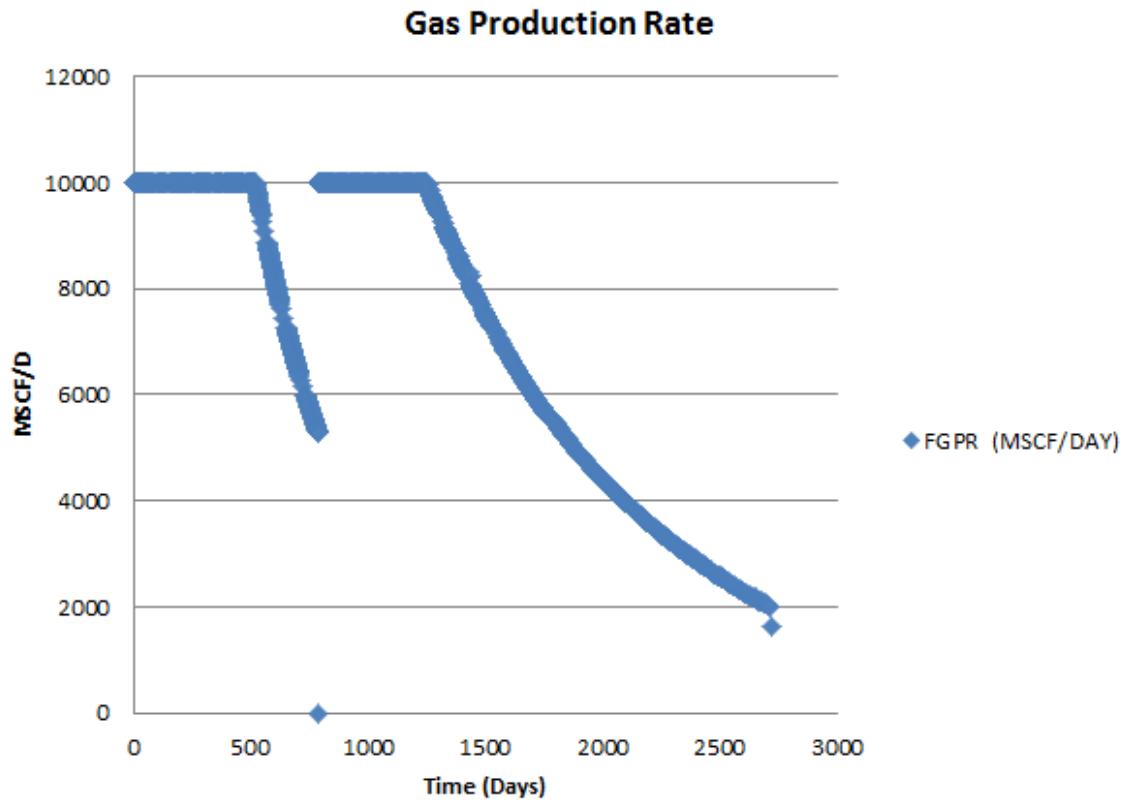


**Figure 5.19:** Gas production rate for Scenario 6

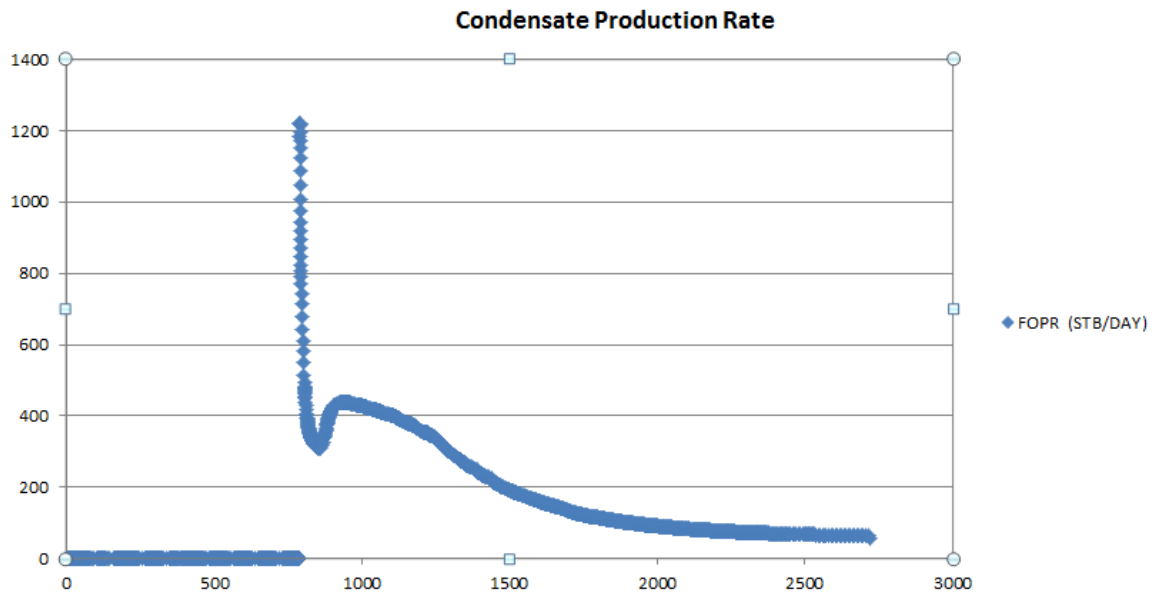


**Figure 5.20:** Condensate production rate for Scenario 6

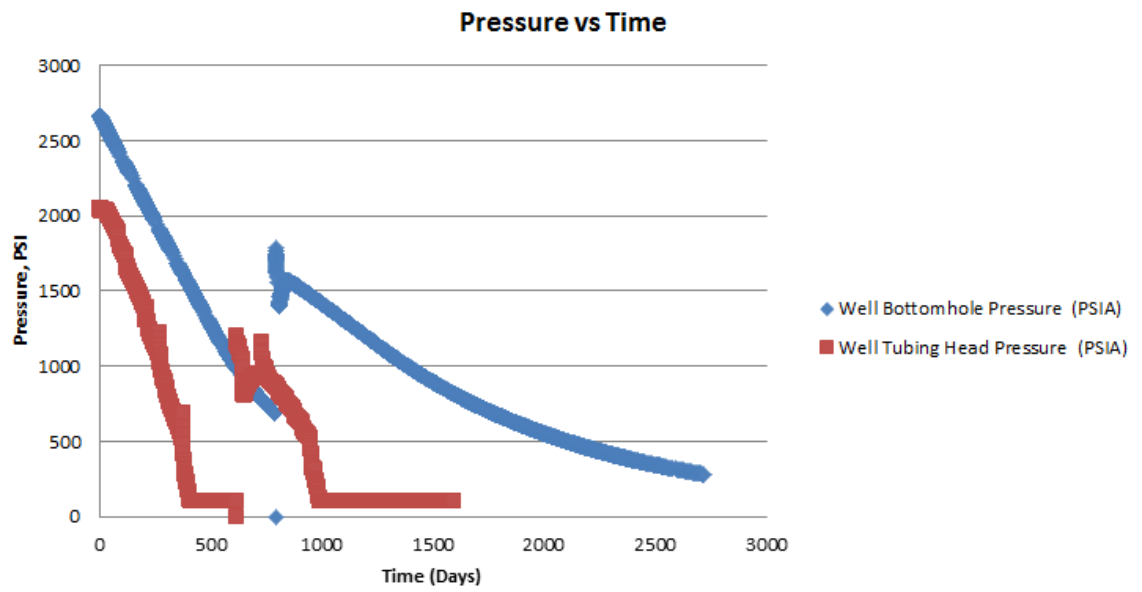


**Figure 5.21:** Pressure vs time for Scenario 6

**Scenario 7:**

In this scenario, the bottom reservoir is perforated first and set to produce until the gas rate starts to drop below the production plateau of 10 MMscf/d. Then, the top layer is perforated while the bottom layer is still open. The gas and condensate production rate is shown in Figures 5.22 and 5.23.

The gas production rate maintains to produce at 10 MMscf/d until 520 days. Up until this point, the production and pressure profiles are the same as those in Scenario 6. Then, top reservoir is perforated while the bottom reservoir is still opened. The top reservoir produces for another 671 days. After that, gas rate starts to decline dramatically. As shown in Figure 5.24, condensate production is initially high and then drops rapidly, similar to the Scenario 6. The well finally dies at 2676 days while gas production rate is 1500 Mscf/d and condensate production rate is 44.02 STB/d. At this point, it stops flowing because the bottomhole pressure as shown in Figure 5.24 is not enough to lift the fluids to the surface. The final pressure is 282 psi. The bottomhole pressure required for vertical lift performance is similar to the ones shown in Figure 5.9. The cumulative production for gas and condensate is 19.15 Bcf and 352.82 MSTB respectively. The cumulative condensate production is less than those in Scenarios 2 to 5 because the bottom reservoir is perforated first; thus, there is not enough gas to lift the condensate to surface at late times.

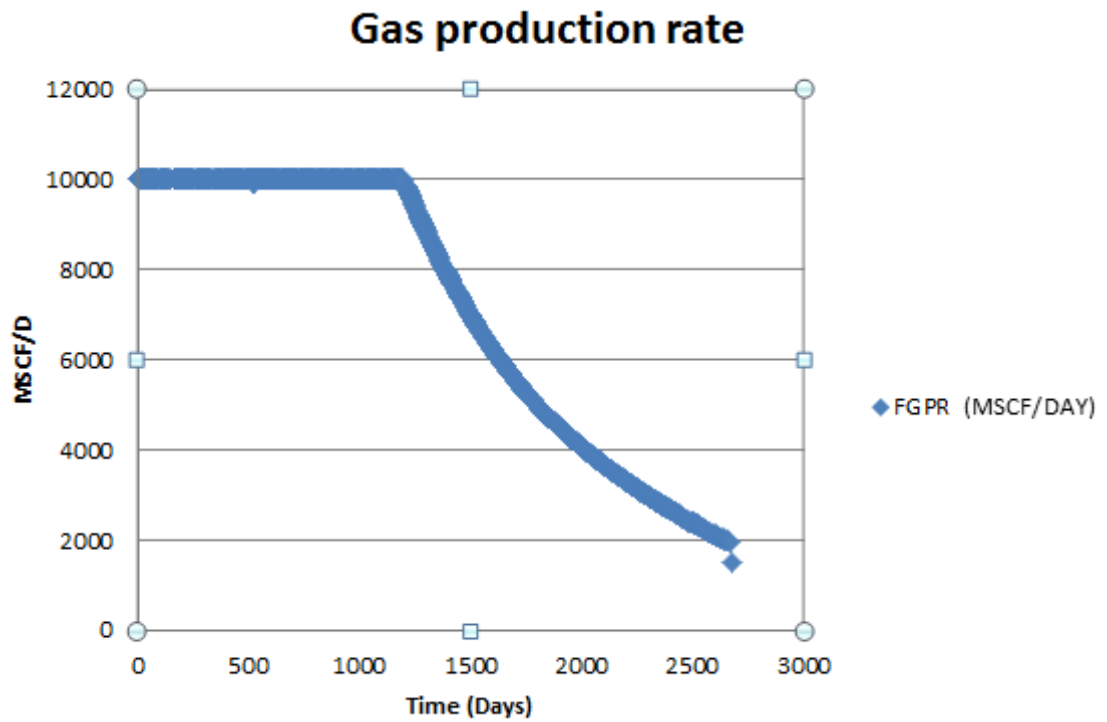


**Figure 5.22:** Gas production rate for Scenario 7

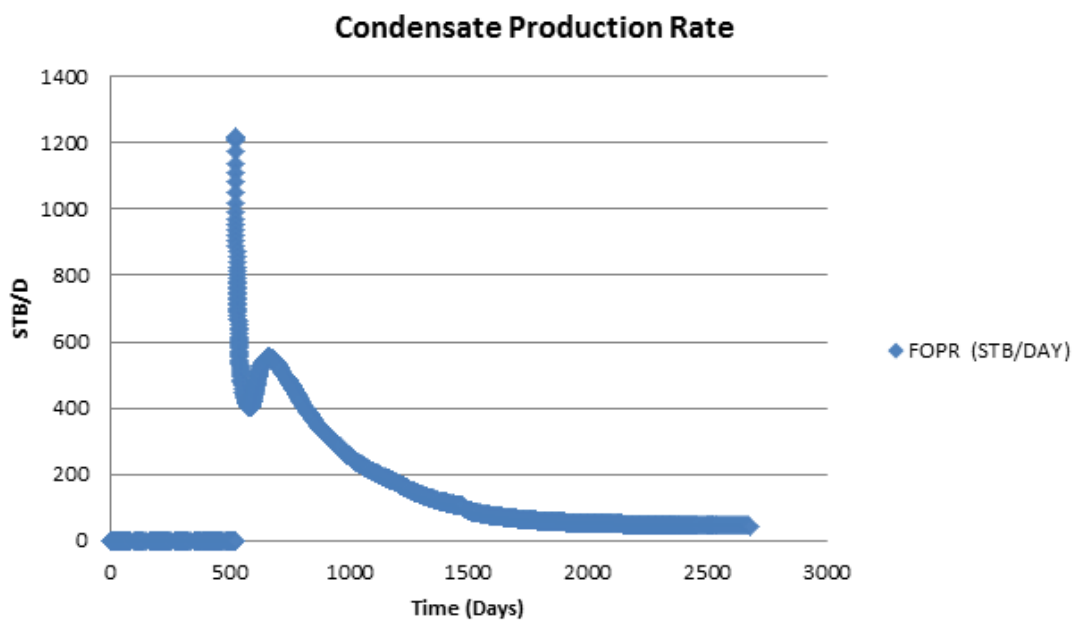


**Figure 5.23:** Condensate production rate for Scenario 7

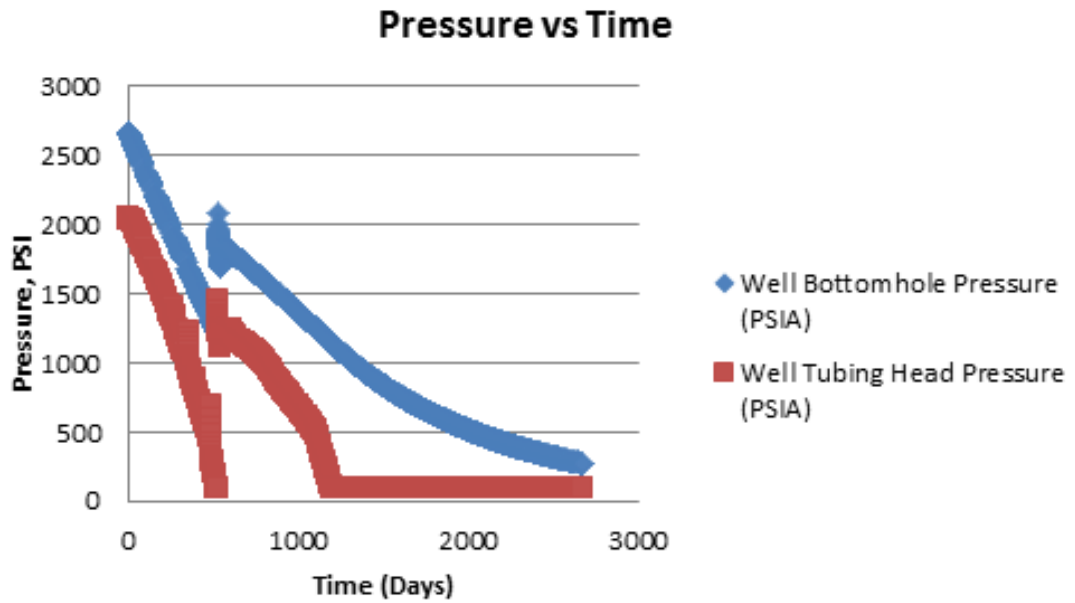


**Figure 5.24:** Pressure vs time for Scenario 7

**Table 5.2:** Summary of results for base case

Scenario	Production time in 1 <sup>st</sup> batch perforation (days)	Production time in 2 <sup>nd</sup> batch perforation (days)	Total Production Time	Cumulative gas production (BCF)	Cumulative condensate production (MSTB)	Gas RF (%)	Condensate RF (%)
1	2720	-	2720	19.25	278.49	91.10	19.72
2	1614	1147	2761	18.96	453.55	89.73	32.12
3	1612	800	2412	17.7	453.35	83.77	32.10
4	930	2175	3105	19.81	455.38	93.75	32.25
5	653	2519	3172	19.95	431.92	94.42	30.59
6	790	1931	2721	19.05	366.8	90.16	25.97
7	524	2153	2677	19.15	352.82	90.63	24.98

**Table 5.3:** BOE for base case

Scenario	BOE (MMSTB)
1	3.487
2	3.614
3	3.404
4	3.758
5	3.758
6	3.542
7	3.545

In summary, Table 5.2 indicates the cumulative gas production and cumulative condensate production, as well as recovery factor for gas and gas condensate. As observed from the table, the best perforation strategy is Scenario 4 since it yields the highest condensate recovery factor of 39%. Although the gas recovery factor of 93.75% in Scenario 4 is not the highest, it is only slightly lower than the highest one (94.42%) in Scenario 5. On the other hand, the condensate recovery factor of Scenario 5 is only slightly lower than that in Scenario 4. Scenario 4 is to perforate the top reservoir first until gas production rate reaches half of initial production rate and then perforate the bottom layer while keeping the top zone open while Scenario 5 is similar to Scenario 4 except that the lower zone is perforated when the gas production rate just drops below the plateau rate. The reason for these two scenarios to give the highest condensate recovery is because the gas from the bottom reservoir helps to lift the condensate fluid to the surface.

In terms of barrel of oil equivalent, Scenario 4 and 5 yields the same values as shown in Table 5.3. Thus, perforating the lower zone after the upper zone while the gas rate is still higher than half the original rate is recommended.

## 5.2 Effect of Thickness

In this section, the thickness of both reservoirs is varied to 50 feet and 25 feet, which is smaller than the original thickness of 100 feet. The results of simulation runs are shown in Tables 5.4 - 5.7.

**Table 5.4:** Summary of results for reservoir thickness 50 feet

Scenario	Production time in 1 <sup>st</sup> batch perforation (days)	Production time in 2 <sup>nd</sup> batch Perforation (days)	Total Time	Cumulative gas production (BCF)	Cumulative condensate production (MSTB)	Gas RF (%)	Condensate RF (%)
1	1,116	-	1,116	9.01	126.39	85.28	17.92
2	590	249	839	8.93	199.29	84.54	28.25
3	590	549	1139	6.82	205.06	64.56	29.07
4	480	250	730	6.73	194.90	64.75	27.62
5	337	332	669	6.63	178.37	62.75	25.28
6	276	306	582	5.81	103.85	54.99	14.72
7	276	306	582	5.80	103.80	54.90	14.71

**Table 5.5:** BOE for reservoir thickness 50 feet

Scenario	BOE(MMSTB)
1	1.628
2	1.688
3	1.342
4	1.317
5	1.283
6	1.072
7	1.071

**Table 5.6:** Summary of results for reservoir thickness 25 feet

Scenario	Production time in 1 <sup>st</sup> batch	Production time in 2 <sup>nd</sup> batch	Total Time	Cumulative gas production	Cumulative condensate production	Gas RF	Condensate RF
----------	--	--	------------	---------------------------	----------------------------------	--------	---------------



	(days)	(days)		(BCF)	(MSTB)	(%)	(%)
1	813		813	4.54	53.51	62.84	24.38
2	444	288	732	4.18	102.02	79.11	28.93
3	444	423	867	4.62	113.26	87.48	32.12
4	541	680	1221	4.63	111.24	87.82	31.55
5	333	488	821	4.58	102.42	86.79	29.05
6	359	473	832	4.50	87.54	85.26	24.82
7	242	570	812	4.54	64.10	88.36	18.43

**Table 5.7:** BOE for reservoir thickness 25 feet

Scenario	BOE (MMSTB)
1	0.809
2	0.798
3	0.883
4	0.884
5	0.866
6	0.838
7	0.822

The results in Table 5.4 indicate that the best perforation strategy in terms of maximizing condensate production for reservoir thickness of 50 feet is Scenario 3 which is to perforate the top reservoir first and produce until the gas production reaches the economic limit then perforate bottom reservoir later. This scenario gives the highest condensate production because the gas from bottom reservoir helps to lift the condensate fluid to be able to produce at the surface. The reason that the best strategy of condensate for reservoir thickness of 50 ft is Scenario 2, not Scenario 4 as in the case of 100-foot reservoir, is because thinner lower reservoir contains less amount of dry gas. If the lower reservoir is perforated early, there is not enough gas to lift fluids at late time. Thus, perforating the lower dry gas reservoir at the time when the production of the upper gas condensate reservoir is low is a good idea.

However, when BOE is used as a criterion, Scenario 2, which is to perforate each zone separately, is the best strategy as illustrated in Table 5.5 due to the fact that this strategy can recover more gas from the reservoir system. In Scenario 2, the lower gas reservoir does not stop short in the production of gas as there is no condensate to increase the hydrostatic pressure in the wellbore during the stand alone production from the lower reservoir.

Results of reservoir thickness of 25 feet in Table 5.6 show that the best perforation strategy to recover condensate is Scenario 3. The reason that this scenario gives the highest condensate production is the same as the one for reservoir thickness of 50 feet. Delaying the perforation of the lower dry gas reservoir helps preserve the amount of gas in the lower reservoir to lift condensate at late time when the energy from upper reservoir is low. When BOE is used as a criterion, Scenario 3 is still the best strategy as illustrated in Table 5.7.

### **5.3 Effect of permeability**

In this section, the permeability is lowered from 500mD in the base case to 100 mD and and 20 mD. The results of the study are shown in Tables 5.8-5.11.

**Table 5.8:** Summary of results for permeability of 100 mD for both top and bottom reservoirs

Scenario	Production time in 1 <sup>st</sup> batch (days)	Production time in 2 <sup>nd</sup> batch (days)	Total Time	Cumulative gas production (BCF)	Cumulative condensate production (MSTB)	Gas RF (%)	Condensate RF (%)
1	2,507	-	2,507	18.53	258.76	87.67	18.32
2	1,524	1,210	2,734	18.60	420.43	88.02	29.77
3	1,524	2,207	3,731	19.93	490.41	94.33	34.73
4	929	2,353	3,282	19.82	436.31	93.8	30.9
5	615	2,570	3,185	19.83	408.05	93.87	28.90
6	794	1,856	2,650	18.64	358.73	88.20	25.40
7	519	2,072	2,591	18.68	339.25	88.41	24.02

**Table 5.9:** BOE for permeability of 100 mD for both top and bottom reservoirs

Scenario	BOE (MMSTB)
1	3.347
2	3.521
3	3.813
4	3.741
5	3.715
6	3.466
7	3.453

**Table 5.10:** Summary of results for permeability of 20 mD for both top and bottom reservoirs

Scenario	Production time in 1 <sup>st</sup> batch (days)	Production time in 2 <sup>nd</sup> batch (days)	Total Time	Cumulative gas production (BCF)	Cumulative condensate production (MSTB)	Gas RF (%)	Condensate RF (%)
1	2,379	-	2,379	16.97	214.42	80.33	15.18

2	2,295	2,051	4,346	18.75	379.66	88.75	26.89
3	2,295	2,395	4,690	19.39	429.41	91.77	30.41
4	782	2,899	3,681	19.35	338.89	91.56	24.0
5	105	2,432	2,537	17.35	235.62	82.13	16.69
6	721	1,758	2,479	16.64	299.21	78.74	21.29
7	402	1,961	2,363	16.79	264.33	79.45	18.72

**Table 5.11:** BOE for permeability of 20 mD for both top and bottom reservoirs

<b>Scenario</b>	<b>BOE (MMSTB)</b>
1	3.044
2	3.506
3	3.662
4	3.564
5	3.129
6	3.073
7	3.063

The results in Table 5.8 indicates that the best perforation strategy for condensate production for reservoir permeability of 100 mD is Scenario 3 which is to perforate the top reservoir first and produce until the gas production reaches half of initial gas production rate then perforate bottom reservoir later. This scenario gives the highest condensate production because the gas from bottom reservoir helps to lift the condensate fluid to be able to produce at the surface. The reason that the best strategy for reservoir permeability of 100 mD is Scenario 3, not Scenario 4 as in the case of 500-mD reservoir, is because fluids flow more slowly in lower permeability reservoir. Thus, it takes time for gas condensate to flow out of the top reservoir. If the bottom reservoir is perforated too early, there is not enough gas to lift condensate at late time as condensate still flows out of the reservoir at late time. Thus, perforating the lower dry gas reservoir at the time when the production of the upper gas condensate reservoir is low is a good idea. When BOE is used as a criterion, Scenario 3 still gives the highest number as shown in Table 5.9.

Results of reservoir permeability of 20 mD in Table 5.10 show that the best perforation strategy to recover condensate is also Scenario 3, which is to perforate the top reservoir first until the gas rate reaches the economic limit and then perforate the bottom reservoir. The reason that this scenario gives the highest condensate production is the same as the one for reservoir permeability of 100 mD which is because delaying the perforation of the lower dry gas reservoir helps preserve the amount of gas in the lower reservoir to lift condensate at late time as condensate takes longer time to produce in low permeability reservoir. When BOE is used as a criterion, Scenario 3 still gives the highest number as shown in Table 5.11.

In summary, reservoir permeability has the effect on production strategy to optimize condensate production. As the permeability decreases, we should delay the perforation of the lower zone until the production of the upper zone reaches economic limit or until the upper zone cannot produce by itself anymore in order to preserve the amount of gas in the lower reservoir to be used to lift condensate at late times.

## **CHAPTER VI**

### **CONCLUSION**

This chapter summarizes results of reservoir simulation runs to determine the best perforation strategy for multi-layered gas condensate and dry gas reservoirs. The effects of formation thickness and layer permeability are also summarized.

The model consists of 2 sets of reservoirs which are top gas-condensate reservoir and bottom dry-gas reservoir having the same rock properties. The reservoir model is built using single well model. There are 4 major cases in this study. The first case is where two reservoirs in the model are under depletion drive mechanism. The second and third cases are when the thickness and permeability of the reservoir are varied homogenously in a reservoir. The last case of this study is the variation in term of size of the aquifer that drives the reservoir.

In total, 7 perforation strategies are investigated to determine which one is the best strategy for different reservoir systems. To summarize in short, we can group the seven approaches into 3 main ideas:

1. Concurrent perforation: This scenario is designed to perforate both reservoirs all at once and produce them together.
2. Standalone perforation: This criterion allows the top reservoir to be produced until fully depleted then shut off. Later the bottom reservoir is perforated.
3. Time lapse perforation: In case of top reservoir, the criteria to perforate the second zone can be classified into 3 cases as follows:
  1. Fully depleted. This criterion allows the gas production from the first producing layer to reach the economic limit before perforating the next layer.
  2. Half depleted. This criterion allows the next layer to be performed whenever the flow from the current layer drops to half of the initial flow rate.

3. Maintain production plateau: This criterion allows the next reservoir to be perforated once the production from the current layer drops just below the initial production rate.

In case of bottom reservoir, the criteria to perforate the second zone can be classified into 2 cases as follows:

1. Half depleted. This criterion allows the next layer to be performed whenever the flow from the current layer drops to half of the initial flow rate.
2. Maintain production plateau: This criterion allows the next reservoir to be perforated once the production from the current layer drops just below the initial production rate.

The results of the simulation are compared in term of cumulative gas and gas condensate production, time of production and recovery factor.

Based on the study results, the result can be summarized as follows:

1. For two-layer reservoirs with depletion-drive gas-condensate reservoir on top and dry-gas reservoir at the bottom having permeability of 500 mD and thickness of 100 ft, the best perforation strategy to maximize condensate production and barrel of oil equivalent is Scenario 4 which is to perforate the top reservoir first until gas production rate reaches half of initial production rate and then perforate the bottom layer while keeping the top zone open. The reason is because the gas from the bottom reservoir helps to lift the condensate fluid to the surface. Thus, perforating the lower zone after the upper zone while the gas rate is still higher than half the original rate is recommended.
2. Reservoir thickness has the effect on perforation strategy to optimize condensate production. As the thickness of the gas condensate and dry gas reservoir decreases, we should delay the perforation of the lower zone in order to preserve the amount of gas in the lower reservoir to be used to lift condensate at late times. In this case study, the best perforation strategy to optimize condensate production for reservoir thickness of 100 feet is Scenario

4 which is commingle after top zone production decreases by half while the best strategy for thickness of 50 and 25 feet is Scenario 3 which is commingle after top zone depletes.

However, in term of barrel of oil equivalent, Scenario 4 is best for thickness of 100 and 20 ft while Scenario 2 is best for thickness of 50 ft. For the thickness of 50 ft, the gas from the lower reservoir in Scenario 2 can be fully depleted whereas other scenarios do not allow full depletion of lower gas reservoir due to higher hydrostatic pressure in tubing as a result of condensate production.

3. Reservoir permeability has the effect on perforation strategy to optimize condensate production and barrel of oil equivalent. As the permeability of the gas condensate and dry gas zones decreases, we should delay the perforation of the lower zone in order to preserve the amount of gas in the lower reservoir to be used to lift condensate at late times as condensate takes longer time to produce in low permeability reservoir. In this case study, the best perforation strategy to maximize condensate recovery for reservoir permeability of 500 mD is Scenario 4 which is which is commingle after top zone production decreases by half while the best strategy for permeability of 100 and 20 mD is Scenario 3 which is to perforate the top reservoir first and produce until the gas production reaches half of initial gas production rate then perforate bottom reservoir later.



## REFERENCES

- [1] R.G. Camacho-V., R. Raghavan, A.C. Reynolds, SPE, U. of Tulsa, Response of Wells Producing Layered Reservoirs: Unequal Fracture Length. Paper SPE 12844 presented at the 1984 SPE/DOE/GRI Unconventional Gas Recovery Symposium held in Pittsburgh, May 13-15 1984.
- [2] Bennett, C.O.: Analysis of Fractured Wells, PhD dissertation, U. of Tulsa, Tulsa, OK 1982.
- [3] Michael J. Fetkovich, Mark D. Bradley, Adonna M. Works, Thomas S. Thrasher, SPE, Phillips Petroleum Co., Depletion Performance of Layered Reservoirs Without Crossflow. Paper SPE 18266 presented at the 1988 SPE Annual Technical Conference and Exhibition held in Houston, Oct 2-5 1988.
- [4] M. Jamiolahmady, A. Danesh, A. Razaei, R. Ataei, M. Sohrabi, Harriot-Watt U., Calculation of Productivity of Gas-Condensate Well: Application of Skin With Rate Dependent Pseudopressure. Paper SPE 94718 presented at the SPE European Formation Damage Conference held in Scheveningen, The Netherlands, 25-27 May 2005.
- [5] Amer M. Saleh, Schlumberger, George Stewart, Edinburgh Petroleum Services, New Approach Towards Understanding of Near Well Bore Behavior of Perforated Completions. Paper SPE 36866 presented at the 1996 SPE European Petroleum Conference held in Milan, Italy, 22-24 October 1996.
- [6] Ronasak Momin, Perforation Strategy for multilayered gas reservoir. 2009. Master's thesis, Chulalongkorn University.
- [7] Arianto, M.A., Susatyo, Y., Srisantoso B. and Sumaryanto, New Completion Solution for Multilayer Gas Fields – A Case History, SPE 10991 presented at the 2006 SPE Asia Pacific Oil & Gas Conference and Exhibition, Adelaide, Australia, 11-13 September 2006.
- [8] Al-Sheri D.A., Rabaa, A.S., Duenas, J.J. and Ramanathan, V, Commingled Production Experience of Multilayer Gas Carbonate Reservoirs in Saudi Arabia, SPE 97073 presented at the 2005 SPE Annual Technical Conference and Exhibition, Dallas, Texas, U.S.A., 9-12 October 2005.

- [9] Craft, B.C., Hawkins, M.F., *Applied Petroleum Reservoir Engineering*, New Jersey, U.S.A., Prentice-Hall, 1991.
- [10] F. Yisheng, L. Baozhu, H. Yongle, etc. *Condensate Gas Phase Behavior and Development. Paper SPE 50925 Presented at the 1998 SPE International Conference and Exhibition in China held in Beijing. 2-6 November 1998.*
- [12] L.P. Dake (1991), *Fundamental of Reservoir Engineering*. 12<sup>th</sup> Impression. Elsevier Science Publishing Company INC. New York. Pp 255-256.
- [13] John Lee and Robert A. Wattenbarger (1996), *Gas Reservoir Engineering*, SPE Textbook Series Vol.5. Society of Petroleum Engineers. Pp 116-117.
- [14] P. Forchheimer, "Wasserbewegung Durch Boden." *Zeitschrift des Vereines Deutscher Ingenieure*, vol. 49, p. 1736 and vol. 50, p. 1981, 1901.
- [15] Li Fan, Billy W. Harris, A. (Jamal) Jamaluddin, Jairam Kamath, Robert Mott, Gary A. Pope, Alexander Shandrygin, and Curtis Hays Whitson, *Understanding Gas-Condensate Reservoirs* 2006.
- [16] Bruno Roussennac, *Gas Condensate Well Test Analysis*. 2001. Master's thesis, Stanford University, Stanford, California. June, Pp. 11-15.

## APPENDICES

## APPENDIX A

### A-1) Reservoir model

Two reservoir models (dry gas reservoir and gas-condensate reservoir) are generated by entering required data into ECLIPSE 300 reservoir simulator. The reservoir model consists of 25x25x11 blocks in the x-, y-, and z- directions.

### A-2) Case Definition

Simulator:	Compositional	
Model Dimensions:	Number of cells in the x direction	25
	Number of cells in the y direction	25
	Number of cells in the z direction	11
Grid type:	Cartesian	
Geometry type:	Block Centered	
Oil-Gas-Water Options:	Water, gas condensate (ISGAS)	
Number of components:	10	
Pressure saturation options (solution type):	AIM	

### A-3) Reservoir properties

#### Grid

Properties: Active grid blocks:

Gas Condensate reservoir	X, Y, Z	=	25, 25, 1-5
Dry gas reservoir	X, Y, Z	=	25, 25, 7-11
Inactive grid blocks:	X, Y, Z	=	25, 25, 6
Porosity		=	0.20

Permeability	k-x	=	500	mD
	k-y	=	500	mD
	k-z	=	5	mD
	X Grid block sizes (All X = 1-25)	=	80	ft
	Y Grid block sizes (All Y = 1-25)	=	80	ft
	Z Grid block sizes (for Z = 1-5 and 7-11)	=	20	ft
	Z Grid block sizes (for Z = 6)	=	100	ft
	Depth of Top face (Top layer)	=	6,000	ft

## PVT Table

Fluid densities at surface conditions	Oil density	40	lb/ft <sup>3</sup>
	Water density	63	lb/ft <sup>3</sup>
	Gas density	0.001	lb/ft <sup>3</sup>
Rock properties	Reference pressure	3000	psia
	Rock compressibility	4.0E-6	/psi

**A-4) Miscellaneous**

Number of component	Number of component	10	
Standard condition	Standard temperature	60	°F
	Standard pressure	14.7	psia
Component names	Component 1	CO <sub>2</sub>	
	Component 2	C <sub>1</sub>	
	Component 3	C <sub>2</sub>	
	Component 4	C <sub>3</sub>	
	Component 5	i-C <sub>4</sub>	
	Component 6	n-C <sub>4</sub>	
	Component 7	i-C <sub>5</sub>	
	Component 8	n-C <sub>5</sub>	
	Component 9	C <sub>6</sub>	
	Component 10	C <sub>7+</sub>	
PROPS reporting options	Oil PVT tables	No output	
	Gas PVT tables	No output	
	Water PVT tables	No output	

## EoS Res Tables

Pure component boiling points (Reservoir EoS)	Component CO <sub>2</sub>	350.46	°R
	Component C <sub>1</sub>	200.88	°R
	Component C <sub>2</sub>	332.28	°R
	Component C <sub>3</sub>	415.98	°R
	Component IC <sub>4</sub>	470.34	°R
	Component NC <sub>4</sub>	490.86	°R
	Component IC <sub>5</sub>	541.80	°R
	Component NC <sub>5</sub>	556.56	°R
	Component C <sub>6</sub>	606.69	°R
	Component C <sub>7+</sub>	734.08	°R
Critical temperature (Reservoir EoS)	Component CO <sub>2</sub>	548.46	°R
	Component C <sub>1</sub>	343.08	°R
	Component C <sub>2</sub>	549.77	°R
	Component C <sub>3</sub>	665.64	°R
	Component IC <sub>4</sub>	734.58	°R
	Component NC <sub>4</sub>	765.36	°R
	Component IC <sub>5</sub>	828.72	°R
	Component NC <sub>5</sub>	845.28	°R
	Component C <sub>6</sub>	913.50	°R
	Component C <sub>7+</sub>	1061.3	°R
Constant reservoir temperature	Initial reservoir temperature	293	°F
Critical volume (Reservoir EoS)	Component CO <sub>2</sub>	1.5057	ft <sup>3</sup> /lb-mole
	Component C <sub>1</sub>	1.5698	ft <sup>3</sup> /lb-mole
	Component C <sub>2</sub>	2.3707	ft <sup>3</sup> /lb-mole
	Component C <sub>3</sub>	3.2037	ft <sup>3</sup> /lb-mole
	Component IC <sub>4</sub>	4.2129	ft <sup>3</sup> /lb-mole
	Component NC <sub>4</sub>	4.0847	ft <sup>3</sup> /lb-mole
	Component IC <sub>5</sub>	4.9337	ft <sup>3</sup> /lb-mole
	Component NC <sub>5</sub>	4.9817	ft <sup>3</sup> /lb-mole
	Component C <sub>6</sub>	5.6225	ft <sup>3</sup> /lb-mole
	Component C <sub>7+</sub>	7.509	ft <sup>3</sup> /lb-mole
Overall composition for region 1	Component CO <sub>2</sub>	1.2302	%
	Component C <sub>1</sub>	59.991	%
	Component C <sub>2</sub>	8.4326	%
	Component C <sub>3</sub>	6.3988	%
	Component IC <sub>4</sub>	3.4127	%
	Component NC <sub>4</sub>	3.8989	%
	Component IC <sub>5</sub>	1.4286	%
	Component NC <sub>5</sub>	1.3988	%
	Component C <sub>6</sub>	7.2718	%
	Component C <sub>7+</sub>	6.5366	%

Critical pressure (Reservoir EoS)	Component CO <sub>2</sub>	1071.3	psia
	Component C <sub>1</sub>	667.78	psia
	Component C <sub>2</sub>	708.34	psia
	Component C <sub>3</sub>	615.76	psia
	Component IC <sub>4</sub>	529.05	psia
	Component NC <sub>4</sub>	550.66	psia
	Component IC <sub>5</sub>	491.58	psia
	Component NC <sub>5</sub>	488.79	psia
	Component C <sub>6</sub>	436.62	psia
	Component C <sub>7+</sub>	403.29	Psia
Equation of State (Reservoir EoS)	Equation of State Method	PR (Peng-Robinson)	
Molecular weights (Reservoir EoS)	Component CO <sub>2</sub>	44.01	
	Component C <sub>1</sub>	16.043	
	Component C <sub>2</sub>	30.07	
	Component C <sub>3</sub>	44.097	
	Component IC <sub>4</sub>	58.124	
	Component NC <sub>4</sub>	58.124	
	Component IC <sub>5</sub>	72.151	
	Component NC <sub>5</sub>	72.151	
	Component C <sub>6</sub>	84	
	Component C <sub>7+</sub>	115	
Acentric factor (Reservoir EoS)	Component CO <sub>2</sub>	0.225	
	Component C <sub>1</sub>	0.013	
	Component C <sub>2</sub>	0.0986	
	Component C <sub>3</sub>	0.1524	
	Component IC <sub>4</sub>	0.1848	
	Component NC <sub>4</sub>	0.201	
	Component IC <sub>5</sub>	0.227	
	Component NC <sub>5</sub>	0.251	
	Component C <sub>6</sub>	0.299	
	Component C <sub>7+</sub>	0.38056	



## A-5) SCAL

## Gas/Oil relative permeabilities

where:

- $k_{rg}$  is relative permeability to gas  
 $k_{ro}$  is relative permeability to oil  
 $k_{rw}$  is relative permeability to water  
 $S_w$  is saturation of water  
 $S_g$  is saturation of gas  
 $p_c$  is capillary pressure

$S_g$	$k_{rg}$	$k_{ro}$
0	0	0.897
0.03515	7.63E-05	0.705923
0.0703	0.00061	0.544104
0.10545	0.002059	0.409125
0.1406	0.00488	0.298553
0.17575	0.009531	0.209941
0.2109	0.01647	0.140865
0.24605	0.026154	0.0889
0.2812	0.03904	0.051603
0.31635	0.055586	0.026534
0.3515	0.07625	0.011275
0.38665	0.101489	0.003398
0.4218	0.13176	0.000433
0.45695	0.167521	0
0.4921	0.20923	0
0.52725	0.257344	0
0.5624	0.31232	0
0.59755	0.374616	0
0.6327	0.44469	0
0.66785	0.522999	0
0.703	0.61	0

## Gas/Water relative permeabilities

$S_w$	$k_{rw}$	$k_{ro}$
0.297	0	0.897
0.319026	1.76E-05	0.769065
0.341051	0.000141	0.653913
0.363077	0.000476	0.55087
0.385102	0.001128	0.459264
0.407128	0.002203	0.378422
0.429154	0.003807	0.307671
0.451179	0.006045	0.246339
0.473205	0.009024	0.193752
0.49523	0.012849	0.149238
0.517256	0.017625	0.112125
0.539282	0.023459	0.081739
0.561307	0.030456	0.057408
0.583333	0.038722	0.038459
0.605358	0.048363	0.024219
0.627384	0.059484	0.014016
0.649410	0.072192	0.007176
0.671435	0.086592	0.003027
0.693461	0.102789	0.000897
0.715486	0.12089	0.000112
0.737512	0.141	0
1	1	0

**A-6) Initialization Equilibration**

Equilibration Region	Keywords	EQUIL(Equilibrium Data Specification)		
EquilReg 1	Equilibrium Data Specification	Datum Depth	6,000	ft
		Pressure at Datum Depth	2,600	psia
		Oil-Water Contact	9,000	ft
EquilReg 2	Equilibrium Data Specification	Datum Depth	6,200	ft
		Pressure at Datum Depth	2,685	psia
		Oil-Water Contact	9,000	ft

**Region/Array**

Initial Water Saturation (SWAT)	:	0.297
Initial Gas Saturation (SGAS)	:	0.703
Initial Pressure	:	2,600 psia
Dewpoint Pressure	:	2,448 psia

**A-7) Region**

Keywords	Region	Cell		
		X	Y	Z
Equilibration Region Numbers	1	1-25	1-25	1-5
	2	1-25	1-25	7-11
EOS Region Numbers	1	1-25	1-25	1-5
	2	1-25	1-25	7-11
FIP Region Numbers	1	1-25	1-25	1-5
	2	1-25	1-25	7-11

**A-8) Schedule****Production Well***Well Specification (PROD) [WELSPEC]*

Well	PROD
Group	-
I Location	13
J Location	13
Datum depth	6,000 ft
Preferred Phase	Gas
Inflow Equation	STD
Automatic Shut-In instruction	Shut
Cross Flow	Yes
Density calculation	SEG
Type of Well Model	STD

*Well Comp Data (PROD) [COMPDAT] (Top Reservoir)*

Well	PROD
K Upper	1
K Lower	5
Open/Shut Flag	Open
Well bore ID	0.5520833 ft.
Direction	Z

*Well Comp Data (PROD) [COMPDAT] (Bottom Reservoir)*

Well	PROD
K Upper	7
K Lower	11
Open/Shut Flag	Open
Well bore ID	0.5520833 ft.
Direction	Z

*Production Well Control (PROD) [WCONPROD]*

Well	PROD
Open/Shut Flag	Open
Control	GRAT
Gas rate	10000 MSCF/D
THP target	100 psia
VFP Pressure Table	1

*Production Well Economics Limits [WECON]*

Well	PROD
Minimum oil rate	-
Minimum gas rate	500 MSCF/D
Workover procedure	None
End run	YES

## APPENDIX B

### B-1) Effect of Thickness

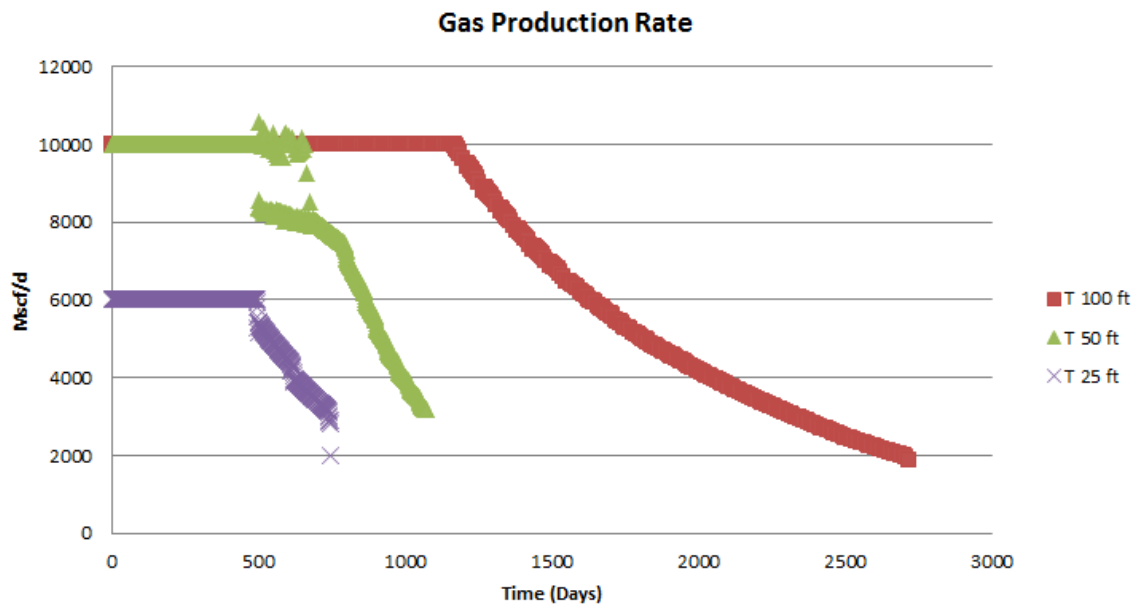


**Figure B.1:** Gas production rate in case of thickness variation in Scenario 1

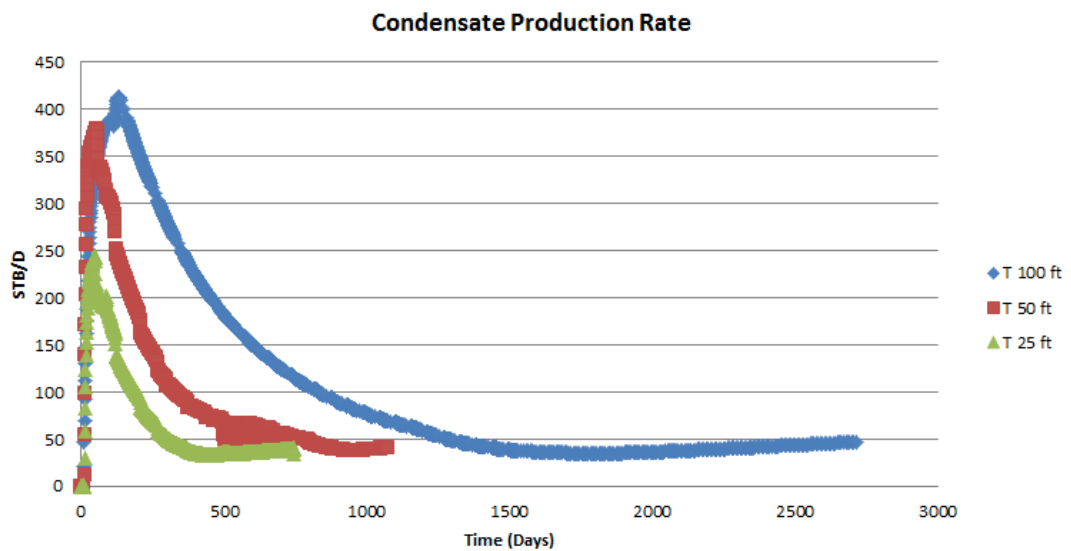


**Figure B.2:** Condensate production rate in case of thickness variation in Scenario 1

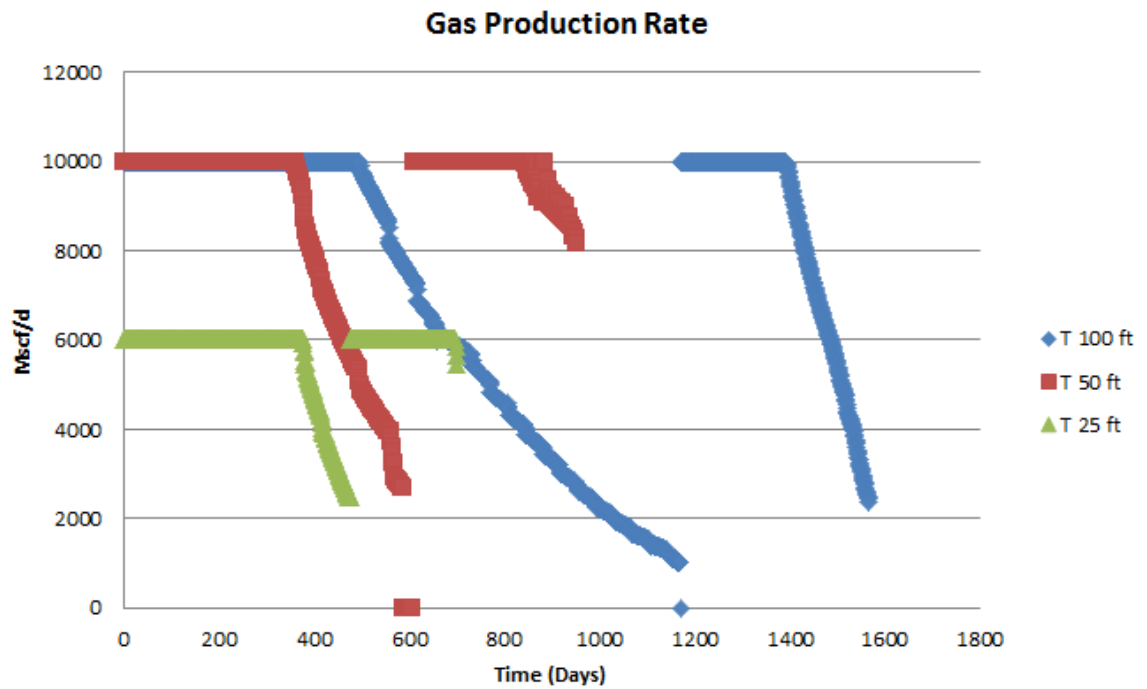


**Figure B.3:** Gas production rate in case of thickness variation in Scenario 2

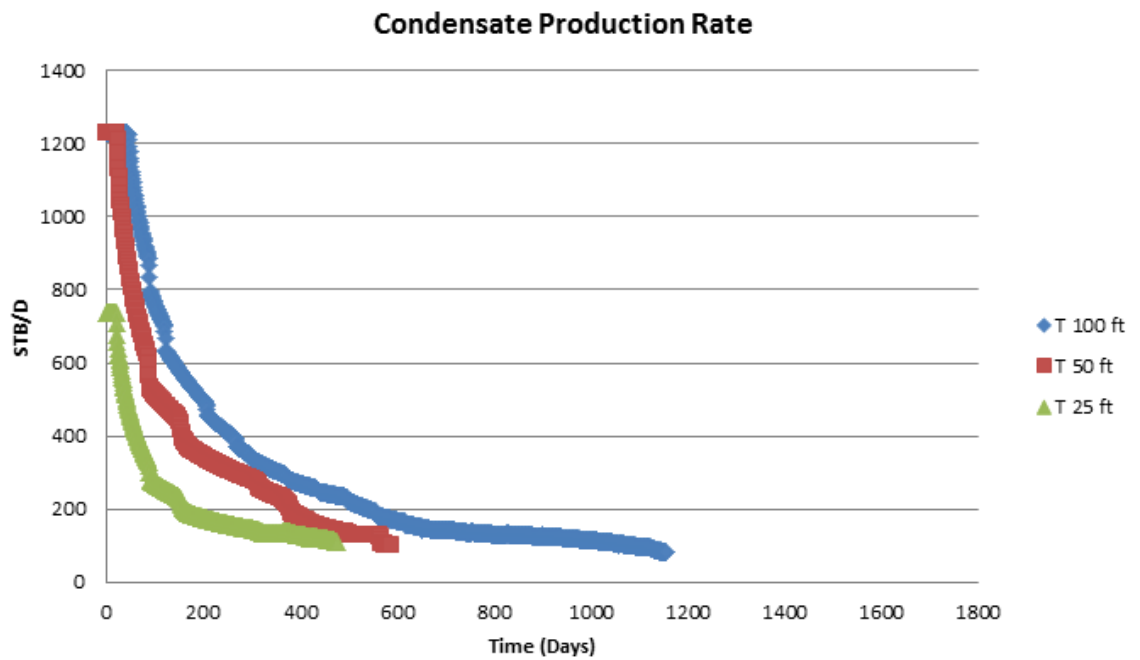


**Figure B.4:** Condensate production rate in case of thickness variation in Scenario 2

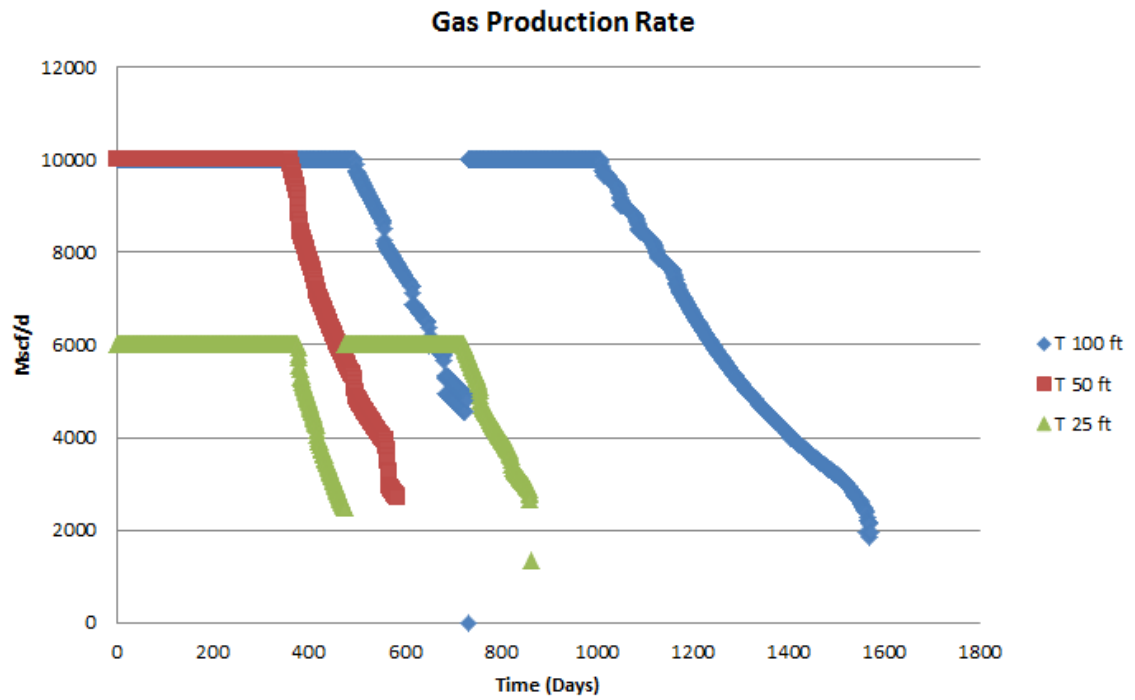


**Figure B.5:** Gas production rate in case of thickness variation in Scenario 3

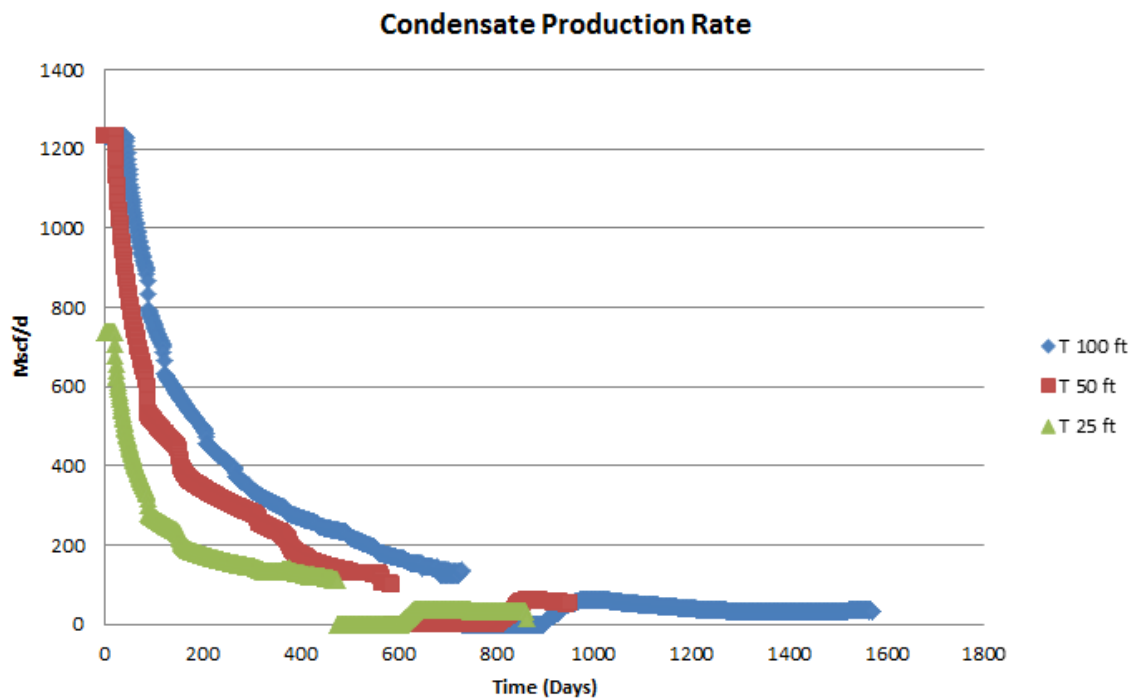


**Figure B.6:** Condensate production rate in case of thickness variation in Scenario 3



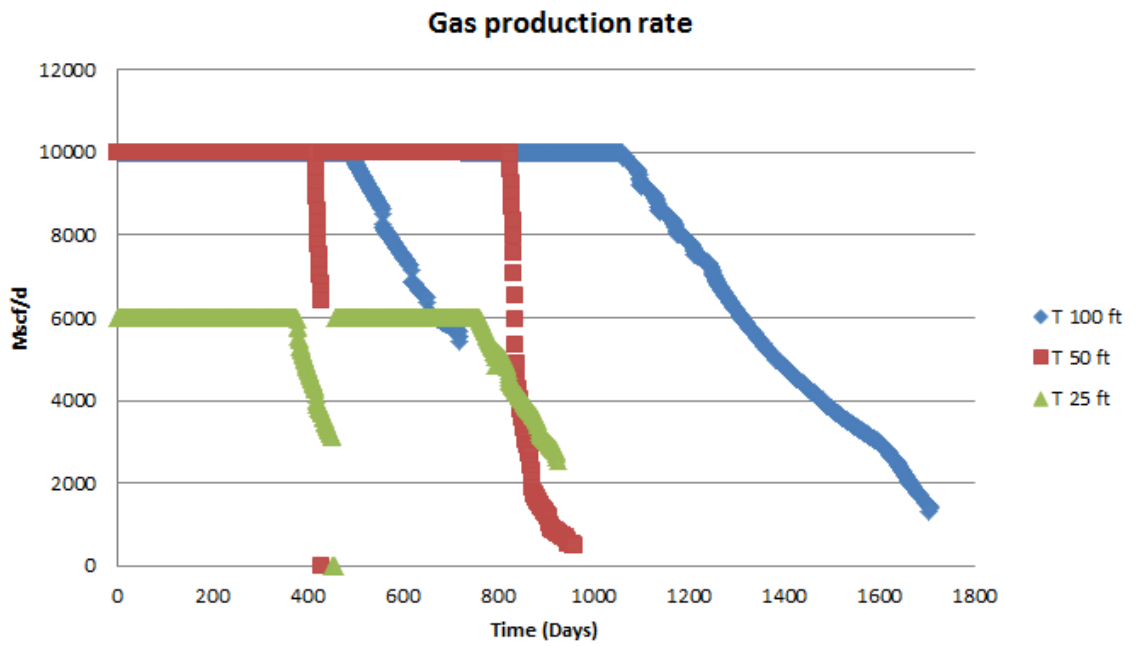


Figure B.7: Gas production rate in case of thickness variation in Scenario 4

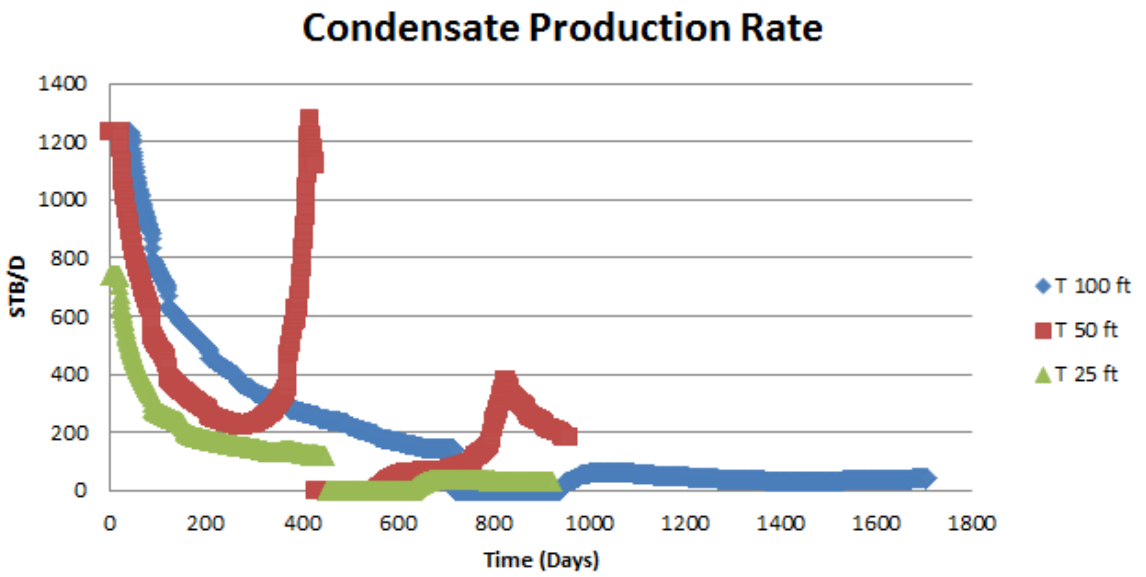
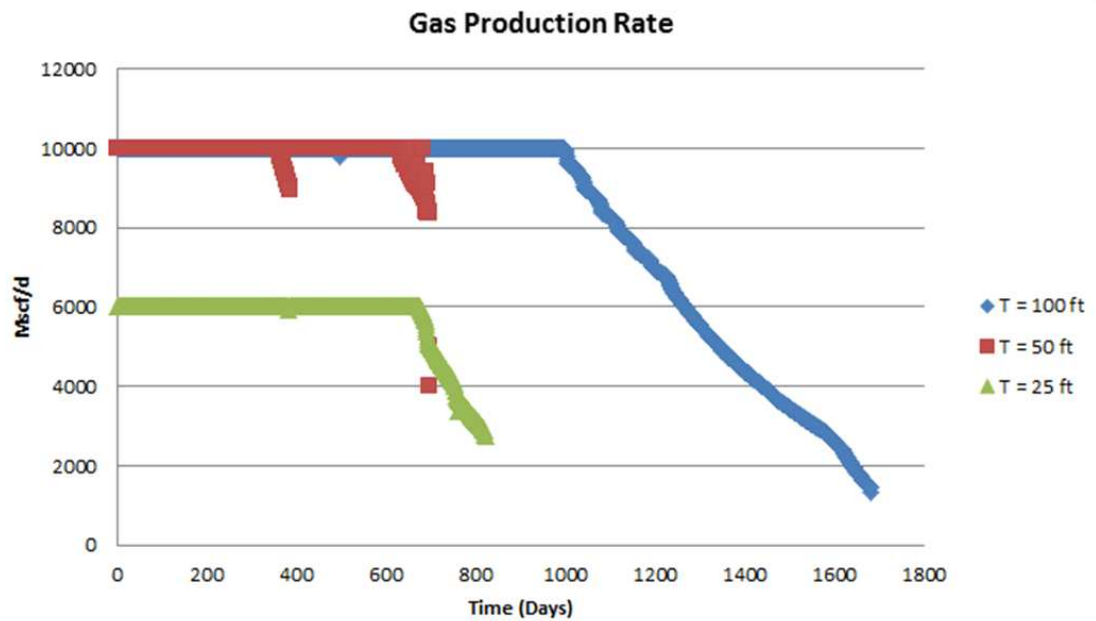
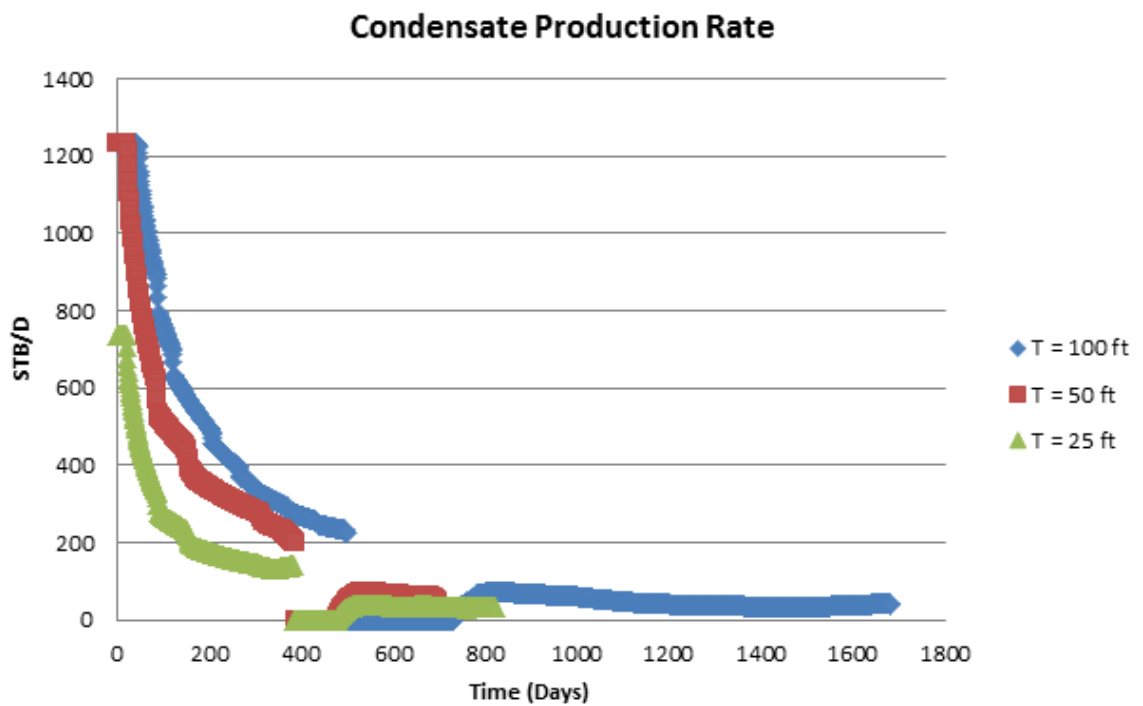


Figure B.8: Condensate production rate in case of thickness variation in Scenario 4



**Figure B.9:** Gas production rate in case of thickness variation in Scenario 5



**Figure B.10:** Condensate production rate in case of thickness variation in Scenario 5

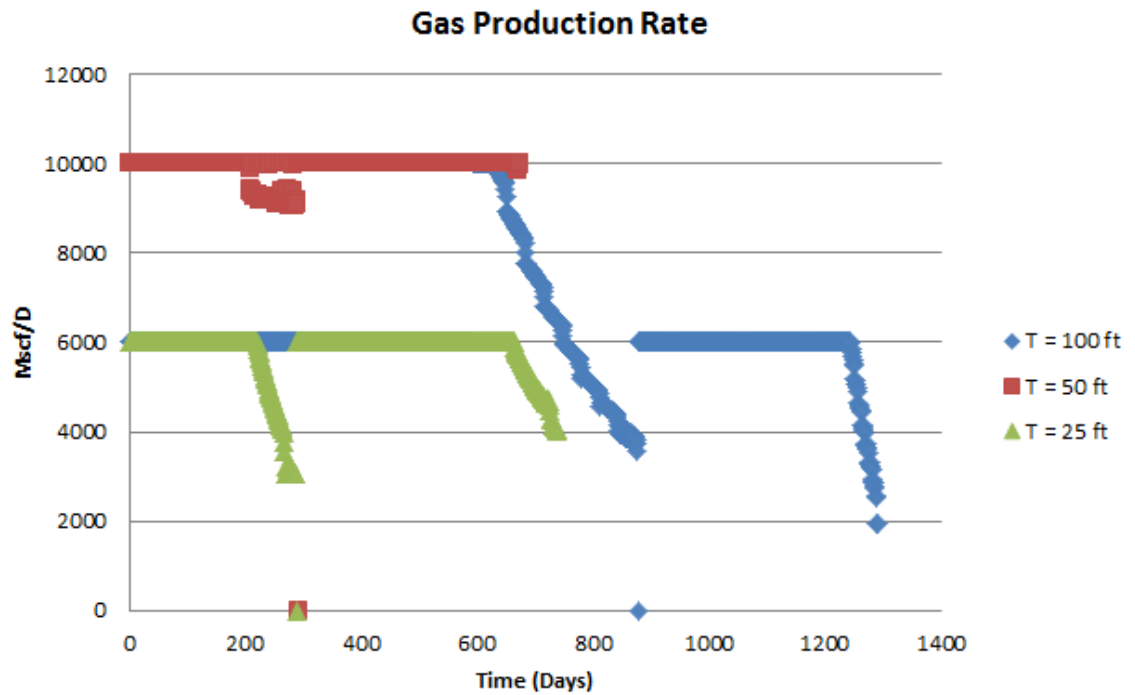


**Figure B.11:** Gas production rate in case of thickness variation in Scenario 6

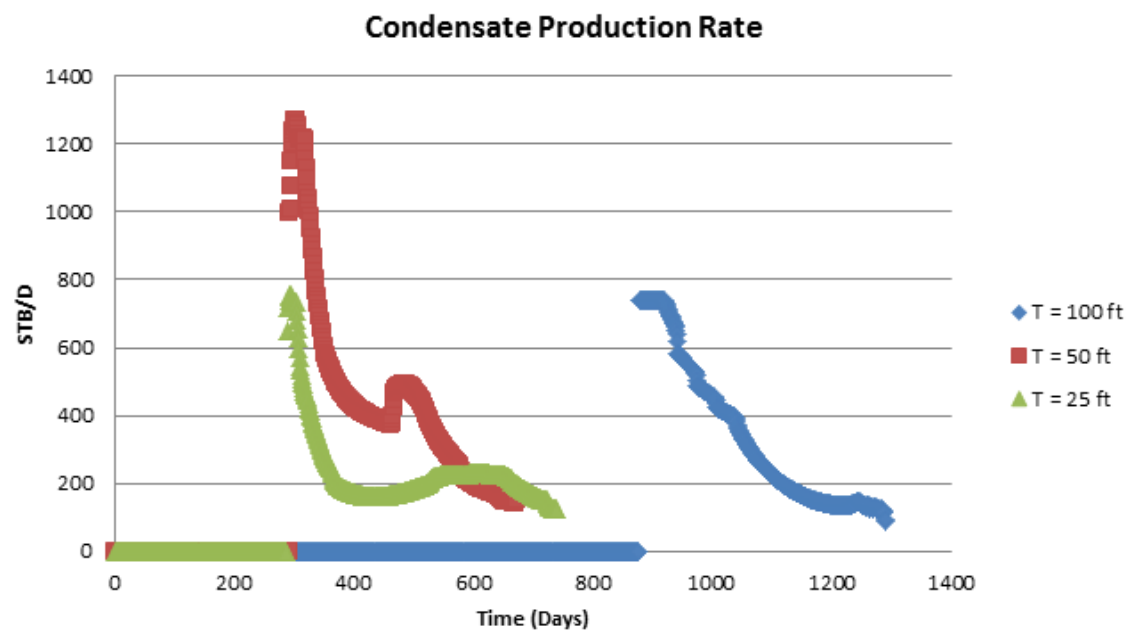


**Figure B.12:** Condensate production rate in case of thickness variation in Scenario 6

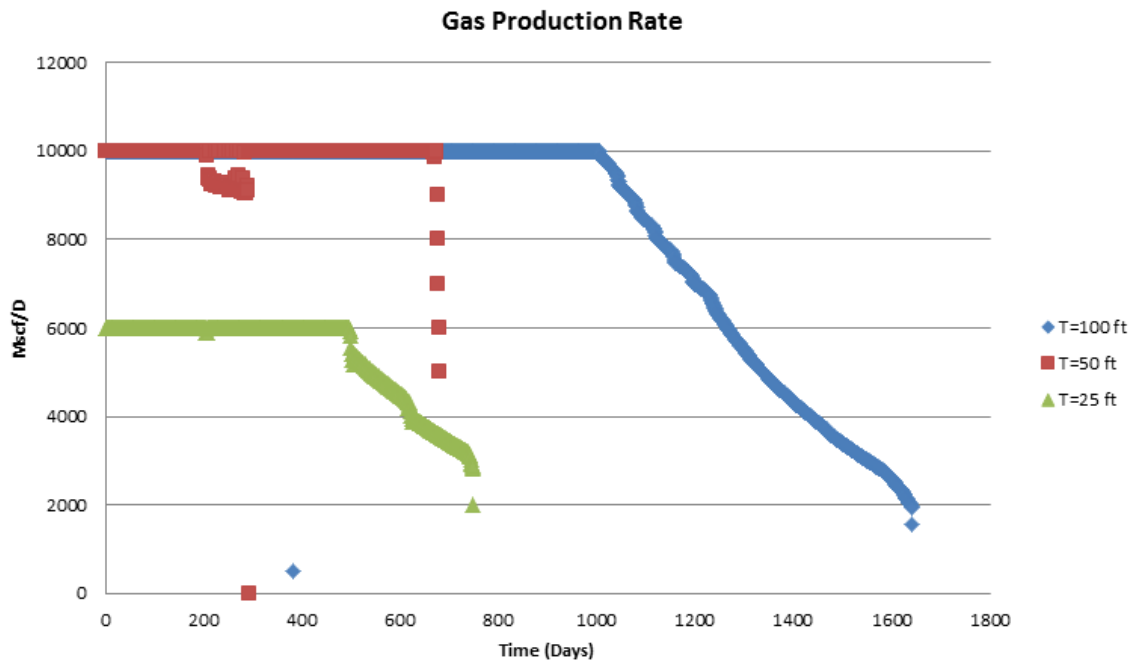


Figure B.13: Gas production rate in case of thickness variation in Scenario 7

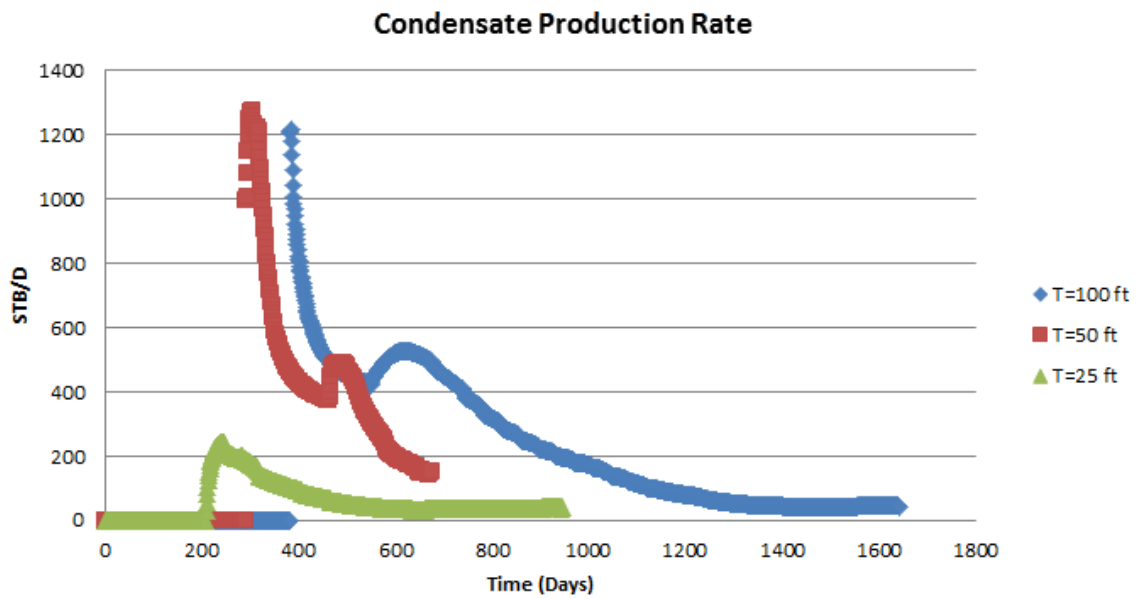
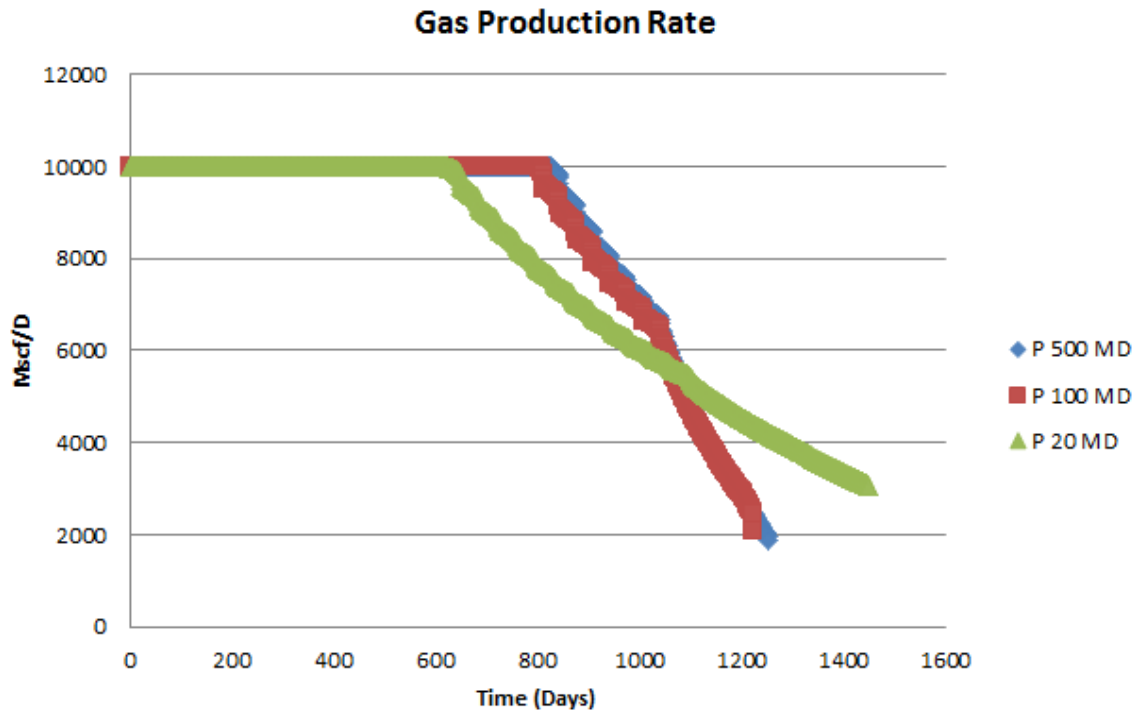
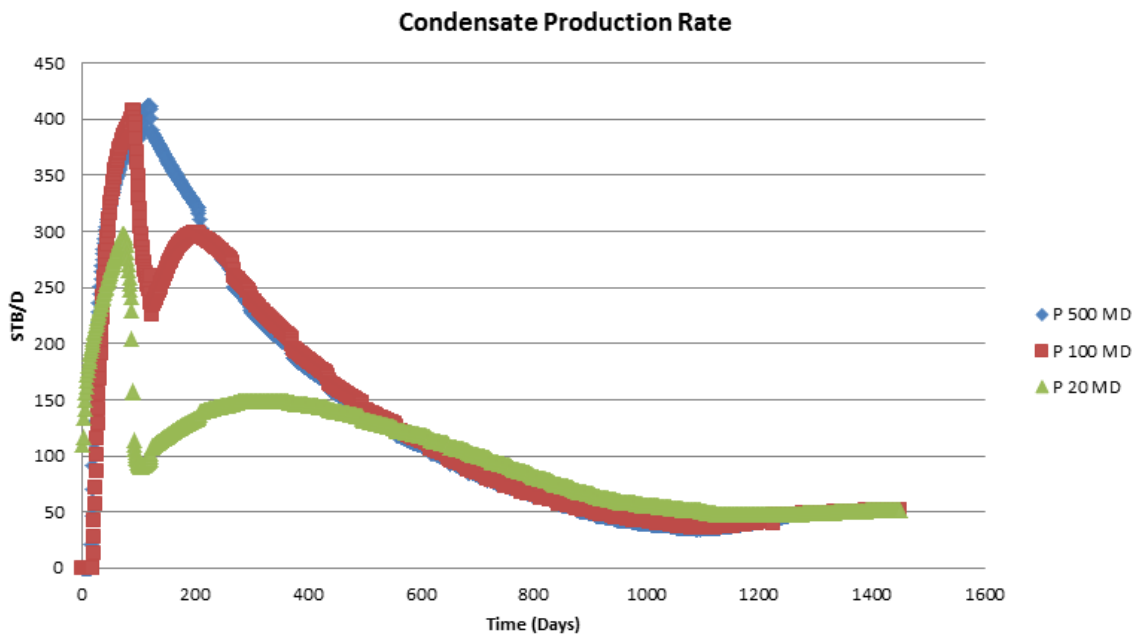


Figure B.14: Condensate production rate in case of thickness variation in Scenario 7



**Figure B.15:** Gas production rate in case of permeability variation in Scenario 1



**Figure B.16:** Condensate production rate in case of permeability variation in Scenario 1

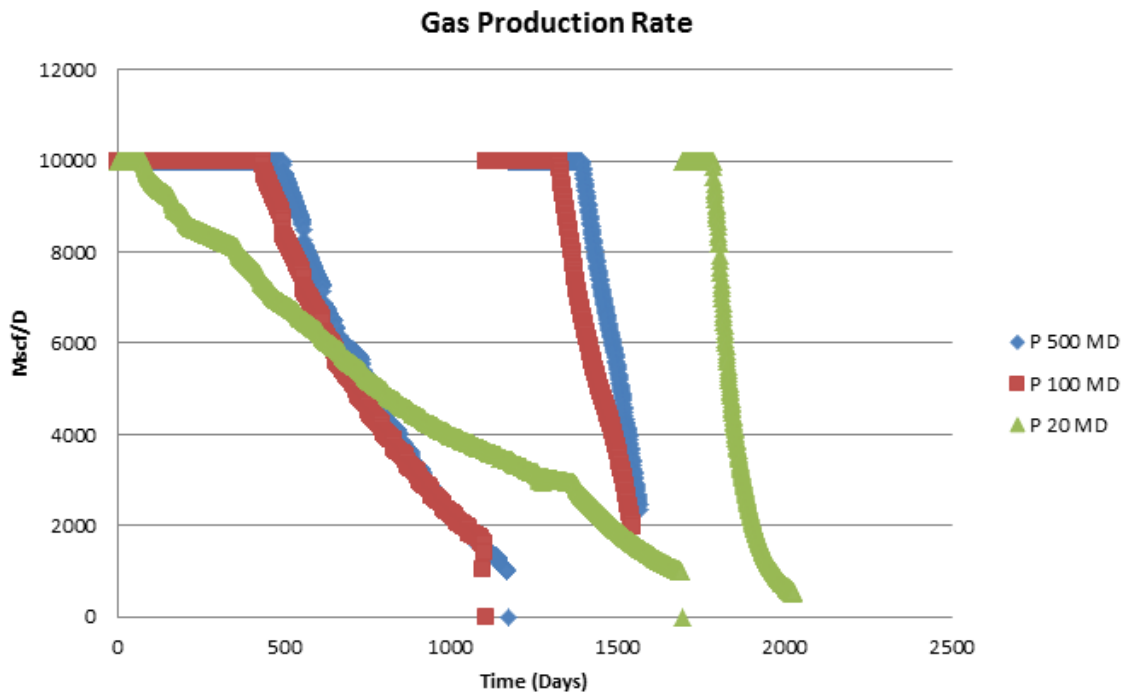


**Figure B.17:** Gas Production Rate in case of permeability variation in Scenario 2

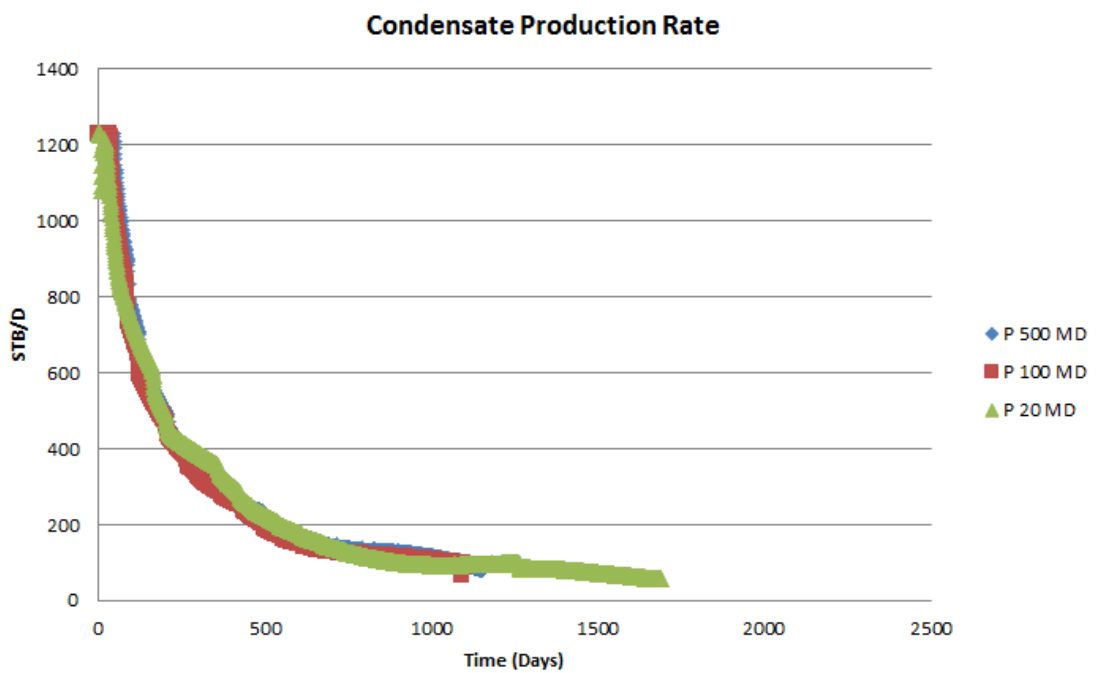


**Figure B.18:** Condensate production rate in case of permeability variation in Scenario 2

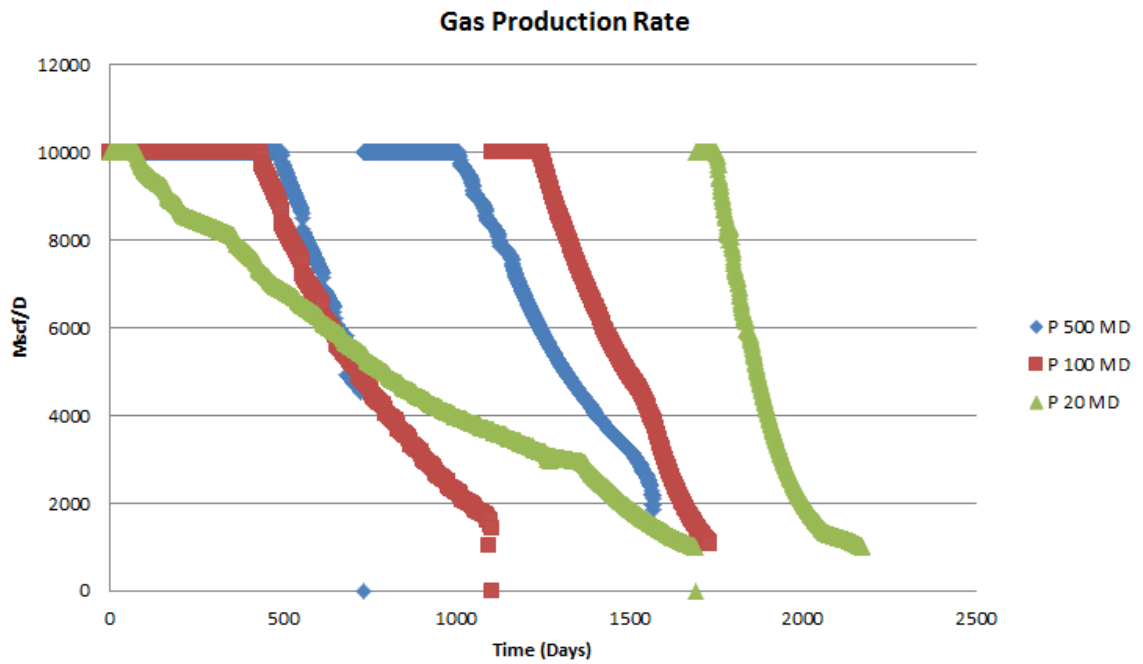


**Figure B.19:** Gas production rate in case of permeability variation in Scenario 3

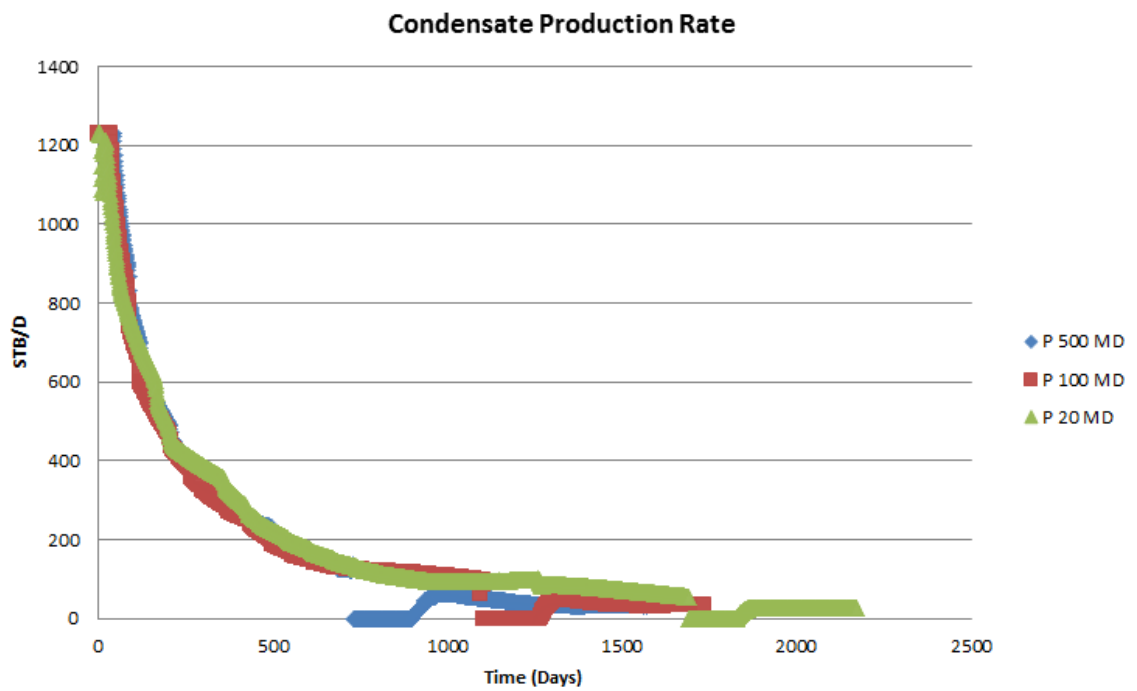


**Figure B.20:** Condensate production rate in case of permeability variation in Scenario 3

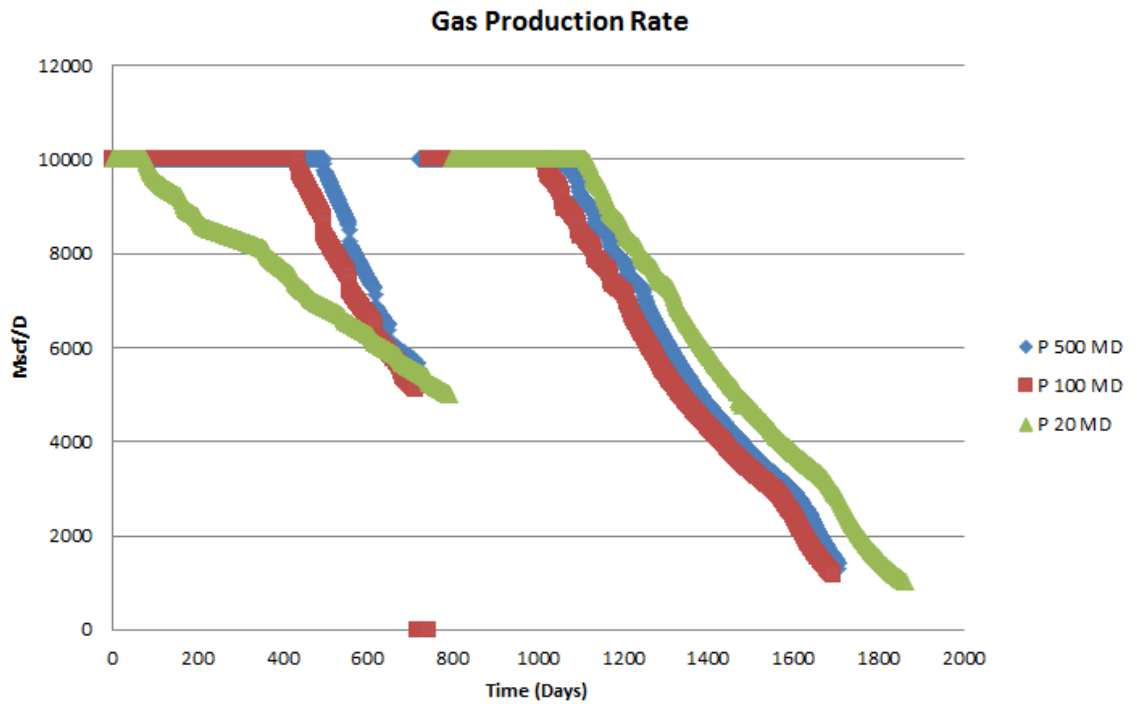


**Figure B.21:** Gas production rate in case of permeability variation in Scenario 4

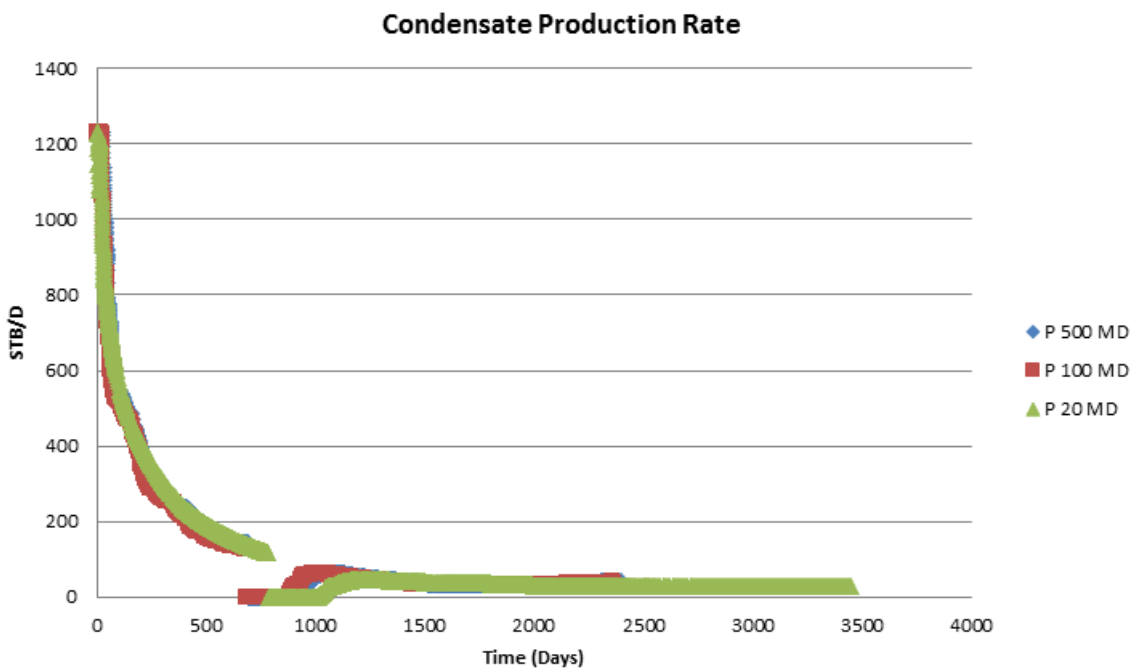


**Figure B.22:** Condensate production rate in case of permeability variation in Scenario 4



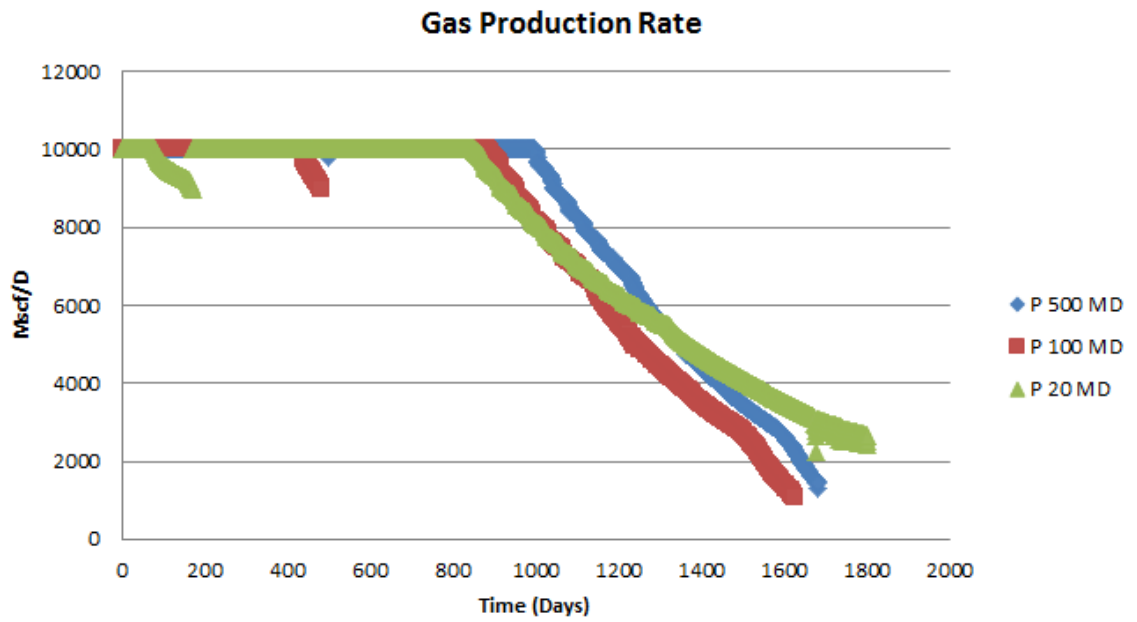


**Figure B.23:** Gas production rate in case of permeability variation in Scenario 5

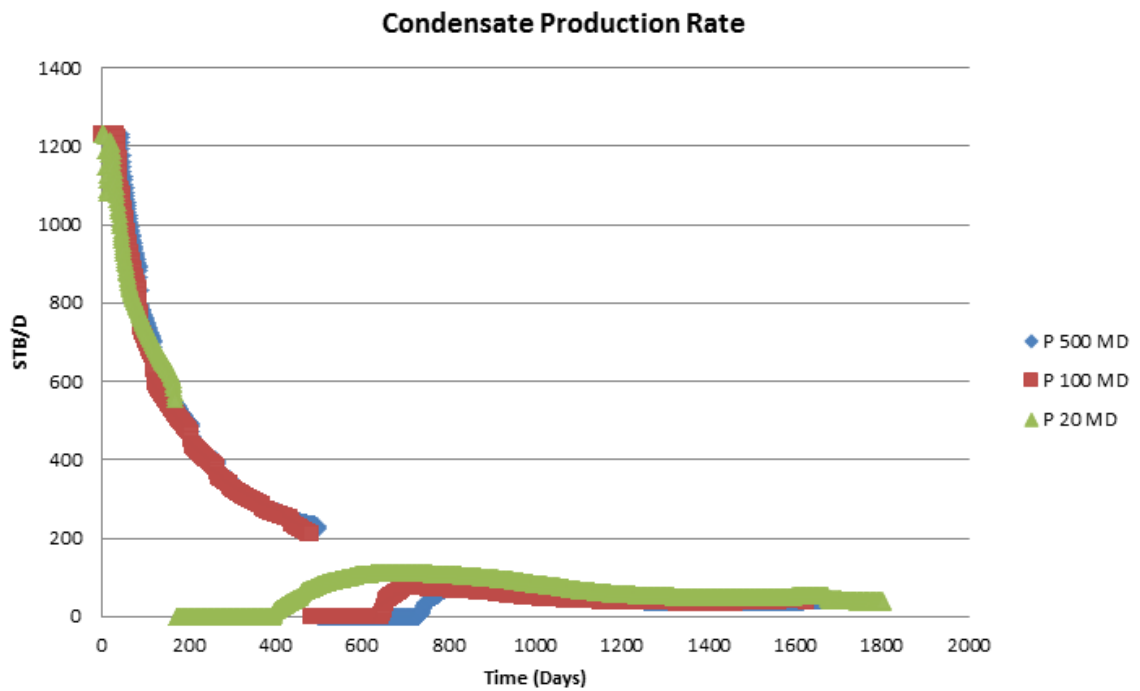


**Figure B.24:** Condensate production rate in case of permeability variation in Scenario 5

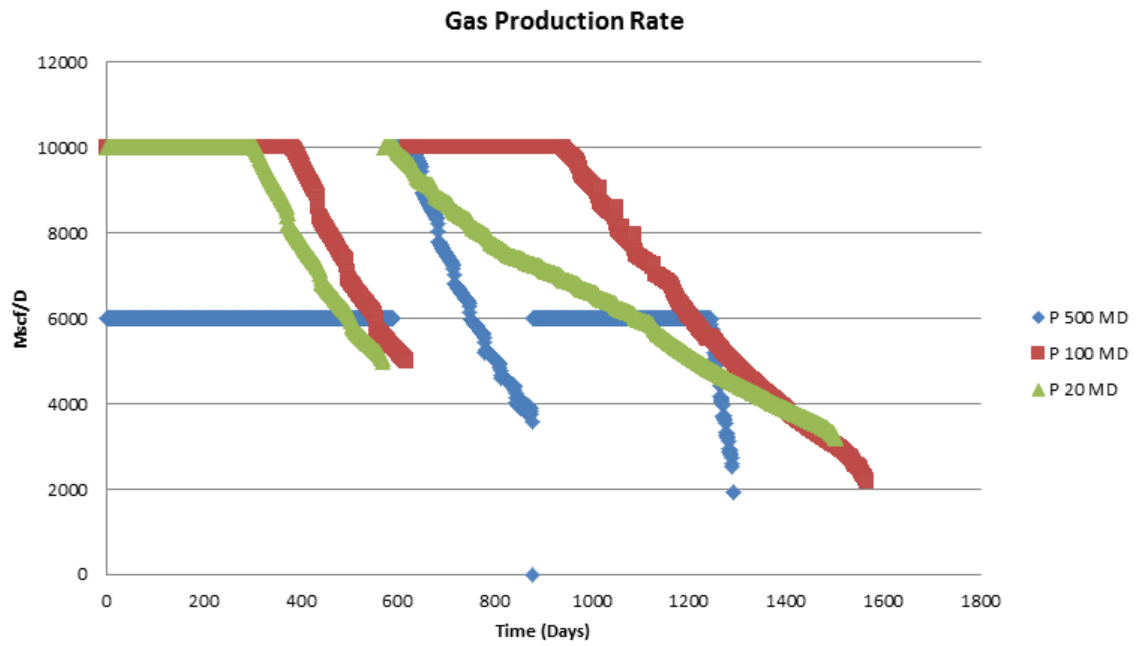


**Figure B.25:** Gas production rate in case of permeability variation in Scenario 6

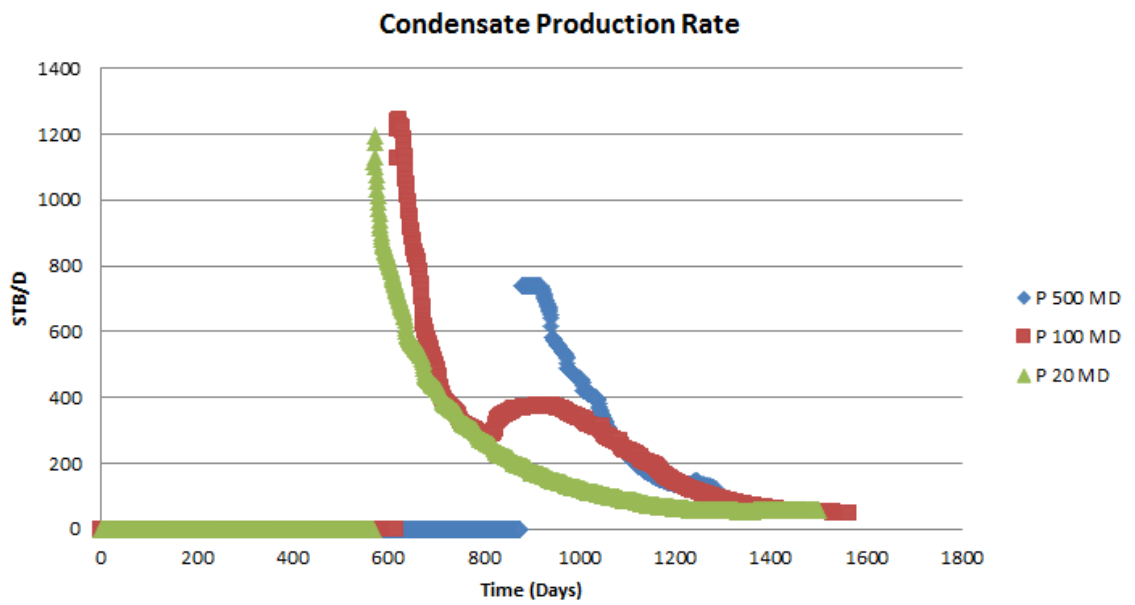


**Figure B.26:** Condensate production rate in case of permeability variation in Scenario 6

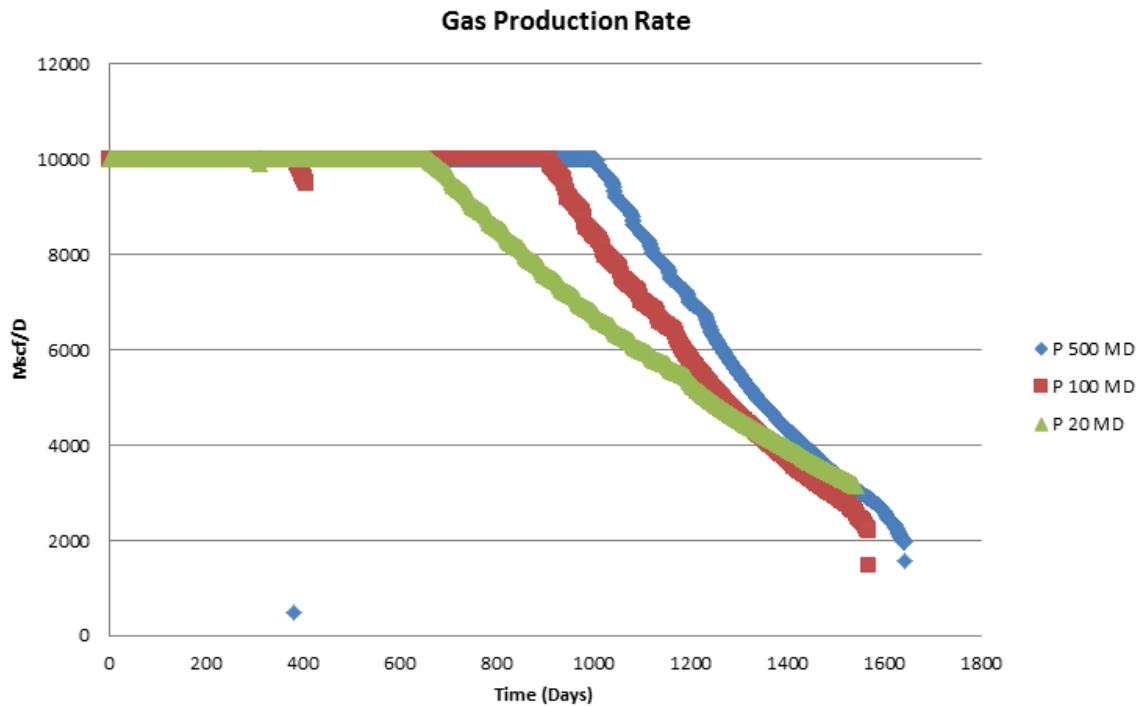


**Figure B.27:** Gas production rate in case of permeability variation in Scenario 7

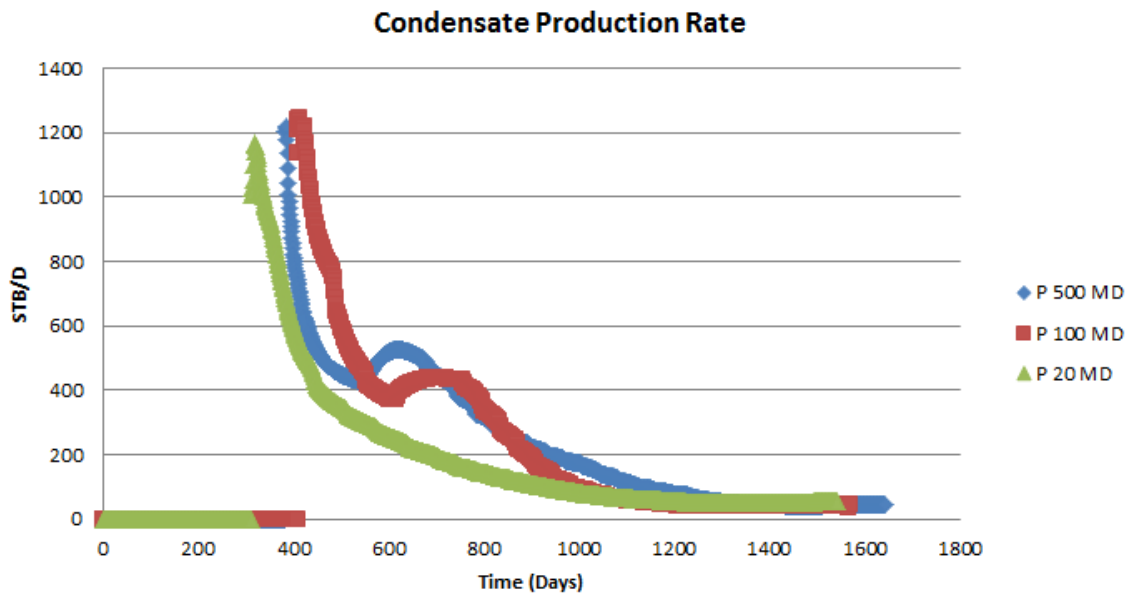


**Figure B.28:** Condensate production rate in case of permeability variation in Scenario 7

## B-2) Vertical Flow Performance (VFP)

The vertical flow performance curves are generated by production and system performance analysis software (PROSPER) in order to put the proper pressure traverse calculations in the simulation cases.

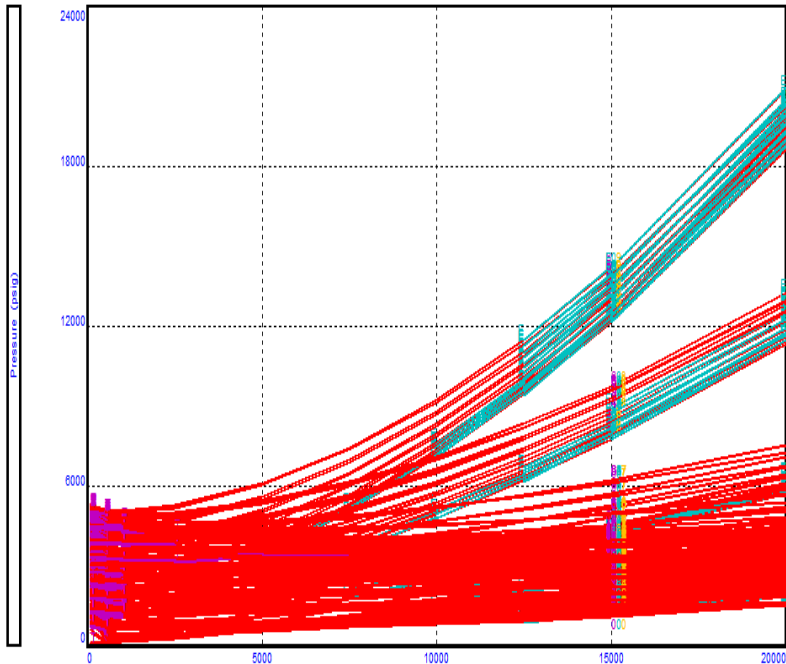
### VFP NO.1

Well name : PROD

Fluid : Concentration of each composition

VLP (TUBING) CURVES (PROD 05/09/13 12:02:49)

X:6775  
Y:8430

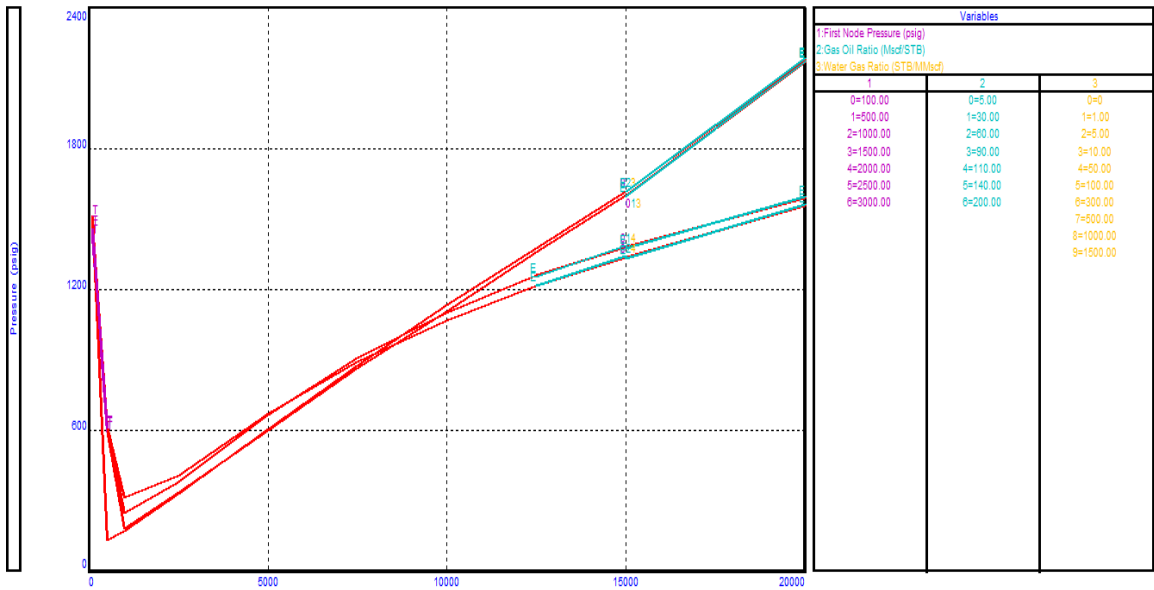


Variables		
1	2	3
0=100.00	0=5.00	0=0
1=500.00	1=30.00	1=1.00
2=1000.00	2=80.00	2=5.00
3=1500.00	3=90.00	3=10.00
4=2000.00	4=110.00	4=50.00
5=2500.00	5=140.00	5=100.00
6=3000.00	6=200.00	6=300.00
		7=500.00
		8=1000.00
		9=1500.00

Gas Rate (Mscf/day)	
PVT Method Eq. of State	Bottom Measured Depth 6000.0 (feet)
Fluid Condensate	Bottom True Vertical Depth 6000.0 (feet)
Flow Type Tubing	Surface Equipment Correlation Fancher Brown
Well Type Producer	Vertical Lift Correlation Duns and Ros Original
Artificial Lift	First Node 1 Xmas Tree 0 (feet)
Lift Type	Last Node 4 Tubing 6000.0 (feet)
Predicting Pressure and Temperature (offshore)	
Temperature Model Rough Approximation	
Company	
Field	
Location	
Well PROD	

VLP (TUBING) CURVES (PROD 05/07/13 22:09:44)

X:6025  
Y:1503



Gas Rate (Mscf/day)	
PVT Method Eq. of State	Bottom Measured Depth 8000.0 (feet)
Fluid Condensate	Bottom True Vertical Depth 8000.0 (feet)
Flow Type Tubing	Surface Equipment Correlation Fancher Brown
Well Type Producer	Vertical Lift Correlation Duns and Ros Original
Artificial Lift	First Node 1 Xmas Tree 0 (feet)
Lift Type	Last Node 4 Tubing 8000.0 (feet)
Predicting Pressure and Temperature (offshore)	
Temperature Model Rough Approximation	
Company	
Field	
Location	
Well PROD	

## Vitae

Pimsiri Sirikhuang was born on November 4<sup>th</sup>, 1981 in Phrae, Thailand. She received her Bachelor of Engineering in Mechanical Engineering from the Faculty of Engineering, King Mongkut's Institute of Technology Latkrabang in 2005. After her graduation she had got the scholarship for the technical exchange internship for 3 months in Thessaloniki, Greece. Soon after coming back from Greece, she was employed by Canadoil Pipe in the position of Mechanical Engineer and had been working with them for 2 years. In 2007, she has started to work with Chevron in the position of Completion Engineer while pursuing her Master's Degree Program in Petroleum Engineering of the Department of Mining and Petroleum Engineering, Chulalongkorn University since 2009 (Chevron's scholarship). In 2013, she has transferred to work with Chevron Canada Resources in the position of Completion Advisor for shale gas exploration and development until present.